SAPIENZA
UNIVERSITÀ DI ROMA

PhD COURSE IN BIOCHEMISTRY
XXXIII CYCLE

ENDOCANNABINOIDS MODULATE NEUROGLIAL PHENOTYPE AND PROTEOTOXIC STRESS

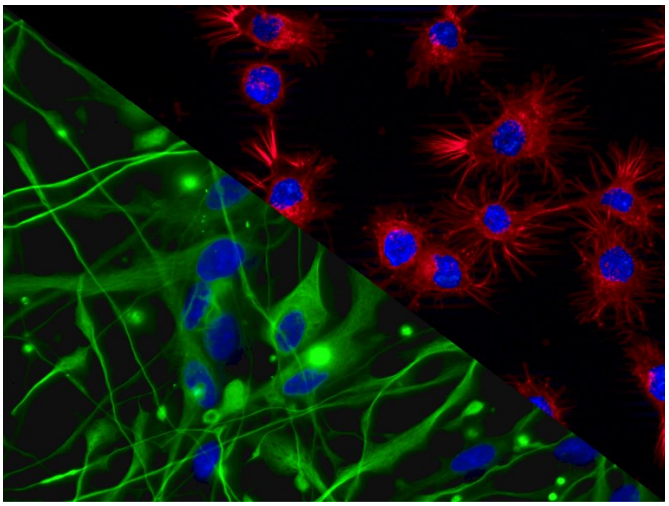

PhD student
MADDALENA GRIECO

Tutor
Prof. Maria d'Erme

Coordinator
Prof. Stefano Gianni

December 2020

ACKNOWLEDGMENTS

I would like to thank Prof. Maria d'Erme for guiding me during my PhD and for teaching me that tenacity and critical thinking are the basis of a good researcher.

I would like to thank Prof. Luciana Mosca for supporting and encouraging me along with all the wonderful S30 Lab group.

A special thanks goes to Dr. Anna Maggiore, for being a formidable friend and colleague with whom to share pain and joys of work and life. She was an indispensable support to achieve this goal.

I would like to thank Prof. Patrizia Mancini, Prof. Rita Businaro, Prof. Tiziana Bisogno, Dr. Maria Giovanna De Caris and Dr. Elisa Maggi for their fundamental collaboration to this project.

I would like to thank Prof. Marcel Leist and his lab for the hospitality and the support given to me during the ten months spent in Konstanz.

I would like to thank Prof. Fabien Gosselet and Prof. Filomena Fezza for the careful supervision of my thesis and for their valuable advice.

Furthermore, I would like to thank Prof. Francesco Malatesta for teaching us that the knowledge sharing represents a precious treasure to achieve whatever goals.

I would like also to thank all Professors of the Department of Biochemical Sciences, and all my colleagues for their valuable contribution to my scientific education.

Last but not least, I would like to thank Domenico and my whole family for always believing in me!

SUMMARY

ABSTRACT

Neuronal survival in neurodegenerative diseases and brain damage is closely related to the cell populations of the environment and in particular to glial cells. Astrocytes, microglia and oligodendrocytes oversee brain homeostasis providing the intrinsic brain defence system. Damage to brain cells triggers a condition generally referred to as reactive gliosis, which includes astrogliosis and activation of microglia. Neuroglia is also thoroughly involved in pathogenesis of many chronic neurological disorders and in neurodegeneration. Endocannabinoids modulating the behaviour of microglia and astrocytes might act as possible targets for therapeutic intervention. Recent studies have indicated that endocannabinoid levels and metabolic enzymes change during the progression of Alzheimer's disease (AD) and that the inhibition of fatty acid amide hydrolase (FAAH), the main catabolic enzyme of anandamide (AEA), has beneficial effects in mice with AD. The aim of this study was to determine whether URB597, a FAAH inhibitor, targets microglia polarization by altering the cytoskeleton reorganization induced by amyloid-β peptide (Aβ) in BV-2 microglial cells. Evaluation of actin cytoskeleton showed that Aβ treatment increased the surface area of BV-2 cells, which acquired a flat and polygonal morphology. Although URB597 did not affect cell morphology only, it partially rescued the control phenotype in BV-2 cells incubated with the combined treatment. Rho family proteins have a critical role in the plasticity of the actin cytoskeleton, influencing morphological changes, migration and phagocytic activity of cells. We observed an increase of Rho protein activation in Aβ samples and a decrease in samples treated with URB597 alone or in combination with Aβ compared to controls, while an increase of Cdc42 protein activation was observed in all samples with respect

to control. Aβ induced the migration of BV-2 cells up to 2 h after stimulation. We also found that by reducing Rho protein activity, URB597 was able to reduce the migration rate. URB597 also increased the number of BV-2 cells performing phagocytosis. Taken together, these data suggest that an increase of anandamide (AEA), due to FAAH inhibition, may induce cytoskeleton reorganization, regulating phagocytosis and cell migration processes, and promote microglial polarization towards an anti-inflammatory phenotype.

As most research worldwide has focused on neurons, there is a dearth of protocols to generate glial cells and to produce co-culture systems for biomedical research. The aim of this project has also been the generation of co-culture with neurons, astrocytes and microglia cells and the subsequent characterization of the resulting model, evaluating interspecies differences through the generation of co-cultures with murine microglia. We focused our interest on the repair functions during brain injury and on the interactions between microglia and astrocytes. The protective effect of astrocytes and microglia against neuronal cells in the presence of inflammatory and pro-apoptotic processes was investigated. Human astrocytes and human microglia cells were activated with TNF-α, IL-1β and IFN-γ to evaluate the inflammatory response. The results showed an increase of inflammatory cytokines gene expression such as IL-6 and IL-8 in both cell lines examined. The astrocytes activation by TNF-α, or by conditioned medium (CM) of activated microglia cells was confirmed by NF-kB nuclearization. Therefore, the arise of inflammatory process in astrocyte cells is driven not only by TNF-α induction, but also by a synergic effect due to microglia activation. Neuroinflammation, oxidative stress, and progressive degeneration of specific brain regions is also driven by proteasomal impairment, promoting protein accumulations. Since LUHMES neurons are quite susceptible cells to

proteotoxic stress and amino acid starvation, we investigated whether murine microglia and human astrocytes exerted a protective effect also when the cell lines were treated with URB597. The obtained data demonstrated that the astrocytes through the glutathione (GSH) release, were able to attenuate neuronal proteotoxic stress in LUHMES cells. URB597 contributed to GSH anti-oxidant effects modulating GSH metabolism. The overall data demonstrated that neuroglial cells play a pivotal role on neuronal protection from noxious stimuli.

1. INTRODUCTION

Numerous studies indicate that inflammation-mediated neurodegeneration processes and disturbed neuron-microglia interactions may mediate the pathogenesis of several neurodegenerative diseases [1,2]. The two most important endogenous cells in the Central Nervous System (CNS) that promote inflammation are astrocytes and mononuclear phagocytes, which include microglia and perivascular macrophages. Astrocytes are the most important abundant glial cells in the CNS. They derive from the neuroectoderm and are essential in the synapse formation and function, in ion and neurotransmitter concentrations, contributing to the integrity of the blood–brain-barrier (BBB) and in brain homeostasis and neuronal survival [3]. Astrocytes show an important role in neuroinflammation with the production of anti-inflammatory cytokines, such as transforming growth factor β (TGFβ), able to contrast microglia activation during an inflammatory process [4,5]. Two different phenotypes have been identified in the CNS, A1 and A2. Neuroinflammation stimulate A1 astrocytes to release neurotoxins that induce death of neurons. On the other hand A2 astrocytes promote neuronal survival and tissue repair [6]. This terminology parallels the M1 and M2 macrophage nomenclature, which has also been applied to microglia in the CNS [7]. Microglia are the resting macrophages of the CNS generated by the embryonic yolk sac. They migrate into the developing neural tube and after they extend to the brain parenchyma [8].Several markers and receptors in microglia are similar to monocytes and macrophages of peripheral tissue. The M1 phenotype is induced by toxins, lipopolysaccharides (LPS), interferon gamma (IFN-γ) and pro-inflammatory cytokines. On the contrary M2 phenotype release anti-inflammatory cytokines such as IL-4 and IL-10

counteracting neuroinflammation and neuron damages [9]. Under neuroinflammatory conditions, neurons or astrocytes produce endocannabinoids (eCB) as a means of recruiting microglia [10]. Neuroglial cells involved in the inflammation process express functional cannabinoid receptors and produce and degrade eCB, suggesting that the endocannabinoid signaling system has a regulatory function in the inflammatory response. Inflammation are on the bases of several diseases as diabetes [11], cardiovascular diseases and neurodegenerative diseases [12], and eCB exhibit pleiotropic effect on the complex development of these diseases. Several studies have indicated that eCB levels and metabolic enzymes change during neurodegenerative process and that the inhibition of the major N-Arachidonoylethanolamine (AEA)-hydrolyzing enzyme, fatty acid amide hydrolase (FAAH), has a possible neuroprotective role towards oxidative stress, inflammation and excitotoxicity [13].

2. ENDOCANNABINOID SYSTEM

Over the past millennia, *Cannabis sativa* was considered healers in early civilizations for the therapeutic effects of its psychotropic compounds obtained from desiccated flowers. The most important natural compounds derive from cannabis plant flowers are Δ9-tetrahydrocannabinol (THC) and the non-euphoric cannabidiol (CBD) [14,15]. More recent study suggest the therapeutic effects of these plants [16], but the first cannabis-derived compounds for neurological disorder were approved only in the 20th century, with the commercialization of nabiximolz (Sativex®) [17]. In animals, the THC and a less degree the CBD, produce similar effects to those of marijuana, such as catalepsy, hypo-locomotion, analgesia and hypothermia in mice and static ataxia in dogs [18,19]. There is no evidence that allows us to associate medical beneficial effects to THC alone. The CDB shows a safer therapeutic window and it is more amenable to clinical development, even for paediatric populations [20,21]. The first evidence for the existence of a specific binding site for THC took place in the 1988, when Devane et al. (1988), during experiments using radio-marked CP55940, identified the cannabinoid receptor 1 (CB1), a G protein-coupled receptor (GPCR) that is expressed most abundantly in the brain [22]. Cannabinoid receptor 2 (CB2) was identified only in the 1990 through homology cloning. It is also a GPCR and is highly expressed in the immune system. CB1 and CB2 receptors exhibit 68% structure homology [23,24]. CB1 is expressed in both presynaptic and postsynaptic neurons. CB1 on the presynaptic membrane can inhibit voltage-gated Ca^{2+} channels and vesicular release of GABA or glutamate by a retrograde modulation [25]. In the postsynaptic neurons, CB1 mediate slow self-inhibition of neocortical interneurons and change expression of precursors

of appetite- controlling peptides in the arcuate nucleus of the hypothalamus [26]. CB1 is also located in the external membrane of mitochondria, where it inhibits electron transport and the respiratory chain, thereby affecting brain metabolism and memory formation [27,28]. In astrocytes, CB1 is involved in the regulation of synaptic plasticity in the hippocampus and in leptin signalling in the hypothalamus [29]. Activation of CB1 also stimulates proliferation of adult progenitor stem cells and their differentiation into neurons or astrocytes, a role that could be relevant to neurodegenerative disorders [30]. CB2 receptor is considered an immune-modulator receptor. CB2 is highly expressed in microglia and it shown a close correlation with neurodegenerative pathology like Alzheimer disease (AD), Multiple sclerosis (MS) and Amyotrophic lateral sclerosis (ALS) [31,32]. Some evidence suggests an important role of CB2 in the modulation of inflammatory cytokines. Indeed, CB2 is able to reduce pro-inflammatory cytokines release from microglia cells in AD [33]. Today we know that there are several other receptors related to the endocannabinoid system (ECS) such as metabotropic receptors GPR55, GPR119, GPR18 and transient receptor potential vanilloid receptor (TRPV). TRPV1 receptor is present in GABAergic and glutamatergic terminals and neuronal somata in the hippocampus and cerebellum [34,35]. Some study suggests an involvement of TRPV1 in the generation of Ca^{2+} influx and depolarization in spinal or sensory neurons, but the demonstration is difficult. TRPV1 is implicated in short- term and long- term synaptic plasticity , in the regulation of mood, fear, memory, food intake, visual development and locomotion [36]. TRPV1 is also important in the reduction of inflammatory cytokines from activated microglia [37]. PPARα and PPARγ are expressed in neurons, astrocytes and microglia in the brain, where they have anti-inflammatory and neuroprotective effects during acute and chronic neuroinflammatory insults, such as brain trauma, ischaemia,

AD and MS [38]. PPARα also reduces food intake [39], whereas PPARγ is involved in neuronal differentiation [40]. The role of GPR55 is not so clear today. It is able to stimulates excitatory hippocampal neurons [41,42], whereas the expression in microglia suggests an involvement of this receptor in the inflammation processes [43].

The identification of CB1 and CB2 allowed the sudden characterization of two endogenous ligands that have high affinity for these two receptors, which are the lipids anandamide (ethanolamide of arachidonic acid - AEA) and 2-arachidonoylglycerol (2-AG) [44-47]. AEA can bind both receptor subtypes as a partial agonist [48,49]. 2-AG is also able to activate both receptor subtypes, however, behaving as a full agonist [45]. AEA is able to target also TRPV1 and PPARγ and inhibits Ca^{2+} channels and transient receptor potential cation channel subfamily M member 8 (TRPM8) channels, whereas 2-AG activates TRPV1 channels and $GABA_A$ receptors [50]. Many enzymes are involved in the endocannabinoids' synthesis and degradation. N-acylphosphatidylethanolamine (NAPE)-specific phospholipase d-like hydrolase (NAPE-PLD) catalyses the synthesis of AEA and other N-acylethanolamines, and fatty acid amide hydrolase (FAAH) catalyses the hydrolysis of AEA (and other N-acylethanolamines and fatty acid primary amides). Diacylglycerol lipase α and β (DAGLα, DAGβ) catalyse the biosynthesis of 2-AG and other monoacylglycerols and monoacylglycerol lipase (MAGL) catalyses the hydrolysis of 2-AG (and that of other monoacylglycerols) [51-54] (Fig. 1).

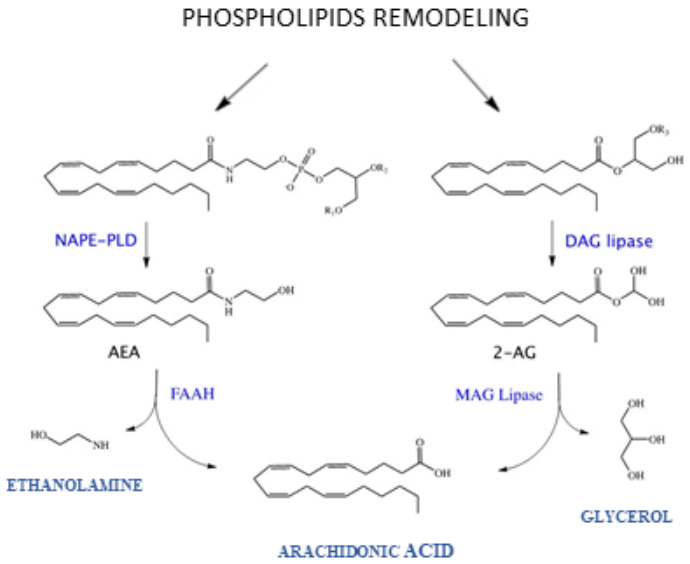

Figure 1: Endocannabinoids metabolism

AEA and 2-AG can be metabolized via oxidation by cyclooxygenase 2 (COX-2) and the end products like prostaglandin ethanolamides and prostaglandin glycerol esters, are able to activate other receptors than cannabinoid and prostanoid receptors [55]. AEA and 2-AG can also be inactivated by other hydrolases, but these enzymes also metabolize other lipids, so targeting them would create other problems [56,57]. Although 2-AG is an excellent CB1 agonist, the hyperactivation of the receptor leads to its consequent desensitization. Furthermore, chronic administration of MAGL inhibitors produces an effect opposite to that obtained from the CB1 receptor [58,59]. At the same time 2-AG is a precursor of arachidonic acid and pro-inflammatory proteinoids [60,61]. Therefore, inhibition of the two main enzymes involved in endocannabinoid synthesis, like NAPE-PLD and DAGL, does not show selectivity and effectively in the reduction of eCB levels, this because there is a compensation from other mediators [62]. Several pathways

and enzymes are involved in the synthesis of AEA, 2-AG and other N-acylethanolamines and monoacylglycerols. In nerve cells, eCB are formed by the Ca^{2+}-dependent activation of phospholipases C or D which catalyse the formation of 2-AG and AEA respectively from membrane phospholipids. The synthesis of endocannabinoids is favoured by all the processes that lead to an increase in [Ca^{2+}] such as, for example, the activation of the phosphoinositide pathway with synthesis of IP3 and release of Ca^{2+} from the endoplasmic reticulum (ER) or opening of the Ca^{2+} VOC channels following membrane depolarization. 2-AG and AEA are fat-soluble molecules that diffuse across the cell membrane and interact with cannabinoid receptors on surrounding cells (Fig. 2).

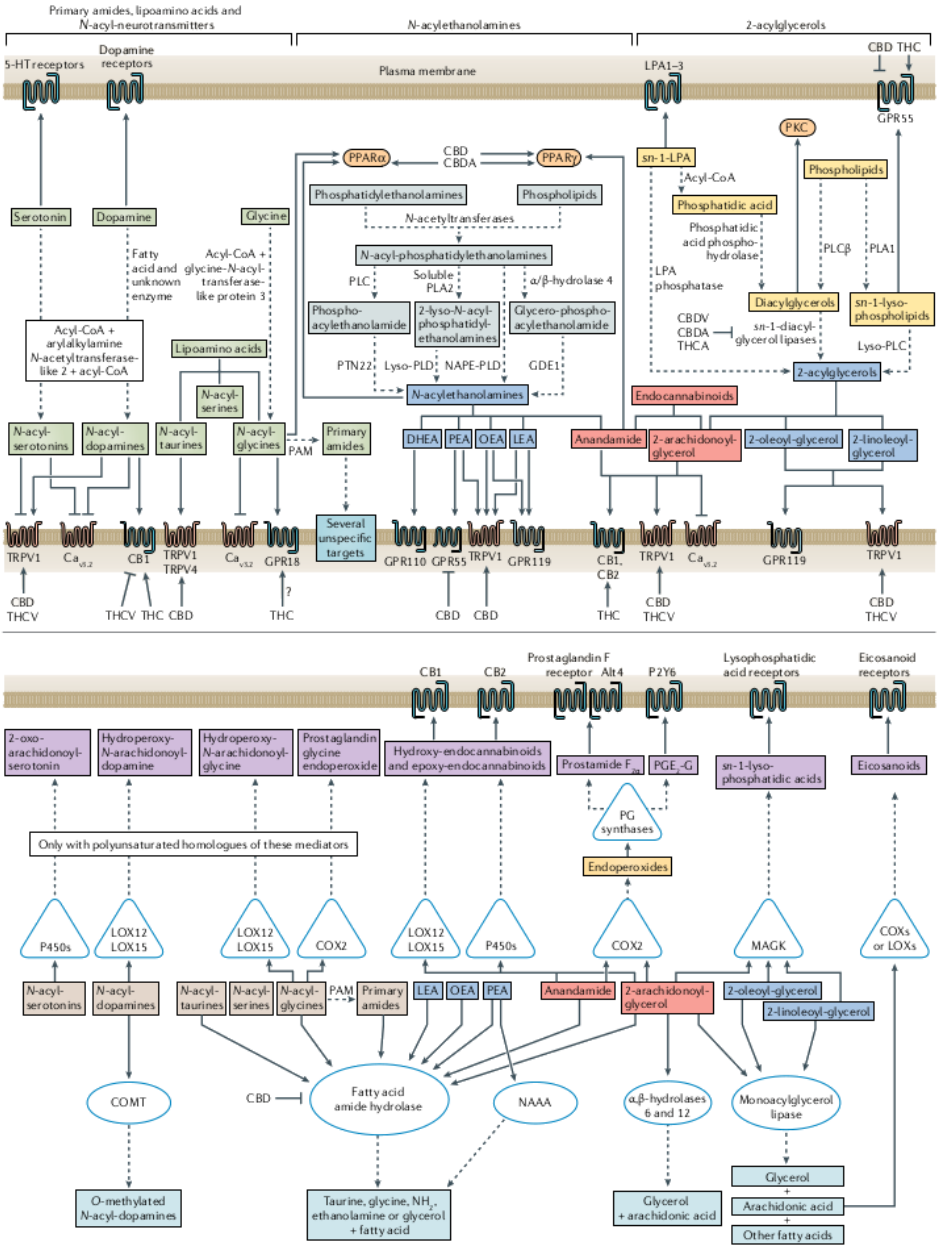

Figure 2: Endocannabinoid system *(From Cristino et al. Nat Rev Neurol. 2020)*

Retrograde signaling is the principal mode by which endocannabinoids mediate short- and long-term forms of plasticity at both excitatory and inhibitory synapses. However, growing evidence suggests that endocannabinoids can also signal in a non-retrograde manner [63] (Fig. 3)

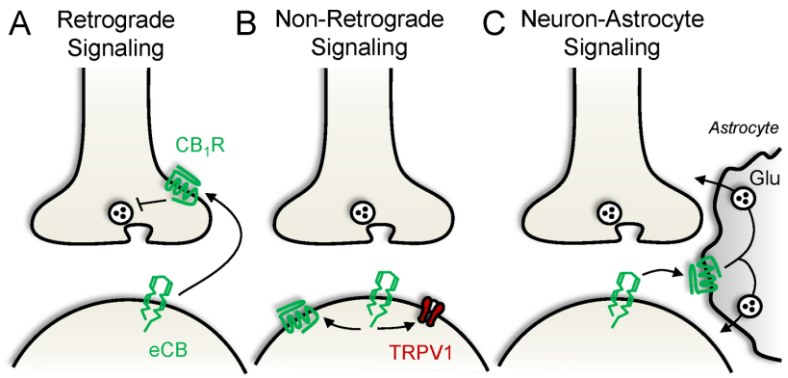

Figure 3: Endocannabinoid signaling at the synapse *(From Castillo P.E. et al. Neuron 2012)*

Retrograde activation of the receptor underlies short-term and long-term forms of synaptic plasticity, including depolarization-induced and metabotropic receptor-mediated suppression of excitatory and inhibitory neurotransmission, long- term depression of excitation or inhibition, and long-term potentiation [64]. Retrograde signal of endocannabinoids which regulates the release of GABA at the level of the inhibitory terminations in some neurons of the hippocampus and cerebellum. This effect is absent after treatment with an endocannabinoid antagonist. The molecular mechanism underlying this response is the Ca^{2+}-dependent activation of the PLC which leads to the synthesis of 2-AG. 2-AG back scatters in the synaptic space and interacts with CBRs present on the synaptic membrane. CBRs are believed to be associated

with a Go protein which through βγ dimer to cause the closure of N-channels of Ca^{2+} [65] (Fig. 4).

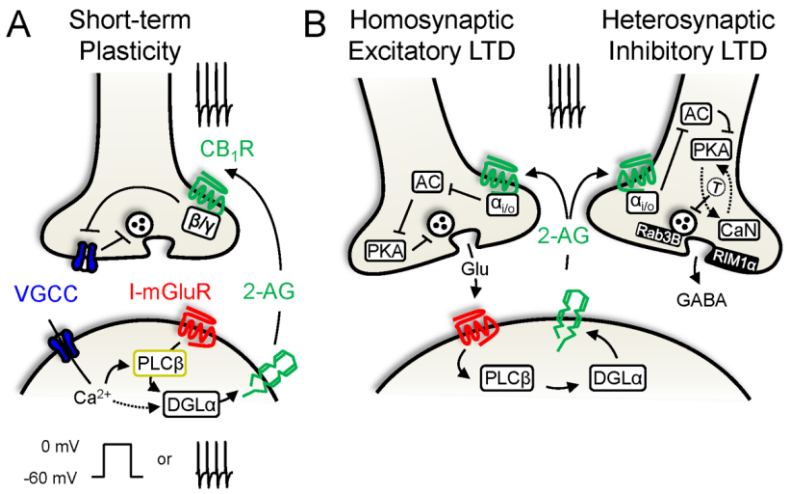

Figure 4: Molecular mechanisms underlying endocannabinoid-mediated short (A)- and long-term synaptic plasticity (B) *(From Castillo P.E. et al. Neuron 2012)*

2.1. FAAH enzyme

The role of FAAH enzyme was first reported in 1993[66], but a similar enzyme was identified in 1960s [67]. FAAH is a protein of 65kDa and 579 amino acids, purified for the first time in 1996 by Cravatt's group from rat liver membranes [68] (Fig. 5). Subsequently through sequence analysis it was found that it is a protein belonging to the amidase family. FAAH is the only member characterized in mammals predominantly in microsomal and mitochondrial fractions [69,70]. It is a membrane-bound serine hydrolase, responsible for the hydrolysis of a family of naturally occurring fatty acid amides, abundantly expressed in the CNS and peripheral tissues, such as kidney, liver, lung, testicle, small intestine and prostate [71]. Enzymes of this family are found in

bacteria, archaea and eukaryotes and hydrolyse different substrates represented by a series of physiologically active lipids, including AEA. The human, porcine, mouse, and rat FAAH enzymes are 73% identical at the amino acid level overall and 90% identical in the amidase signature sequence, amino acids 215–257 [72,73].

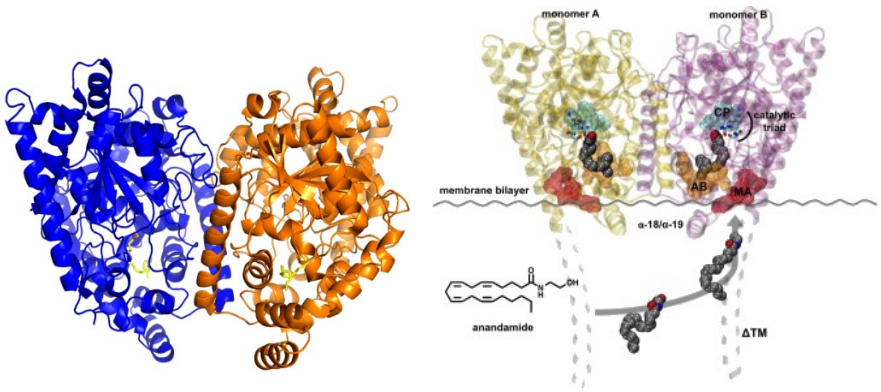

Figure 5: Fatty acid amide hydrolase (FAAH) *(From Palermo et al. Med Chem. 2015)*

The reaction consists in the hydrolysis of amide bonds, present in these substrates. This family of enzymes is characterized by a highly conserved consensus sequence rich in Serine and Glycine residues of approximately 50 amino acids. Cluster analysis of 21 amidases revealed a highly conserved central region rich in glycine, serine and alanine residues. This region has been defined as the signature consensus sequence of amidase of 56 amino acids with GGSSGG that is the longest block of strictly conserved residues in different enzymes. In mammalian, consensus sequence corresponds to amino acids 215-257. Other 17 stable positions were identified throughout the sequence. To date, over 45 proteins containing the amidase identification sequence have been identified, including in addition to FAAH, many prokaryotic and fungal

enzymes, one avian enzyme and three putative members of C Elegans [74] (Fig. 6).

Figure 6: Amidase signature sequences *(FromPatricelli et al. Biochemistry. 1999)*

FAAH is able to hydrolyse AEA and, more less, (2-AG), N-oleoylethanolamine, N-palmitoylethanolamine, and N-oleoyltaurine. FAAH degrades AEA through a hydrolysis mechanism that involves an unusual catalytic triad: Ser 241 - Ser 217- Lys 142, which replaces the typical Ser-His-Asp motif of serine hydrolases [66,75] (Fig. 7).

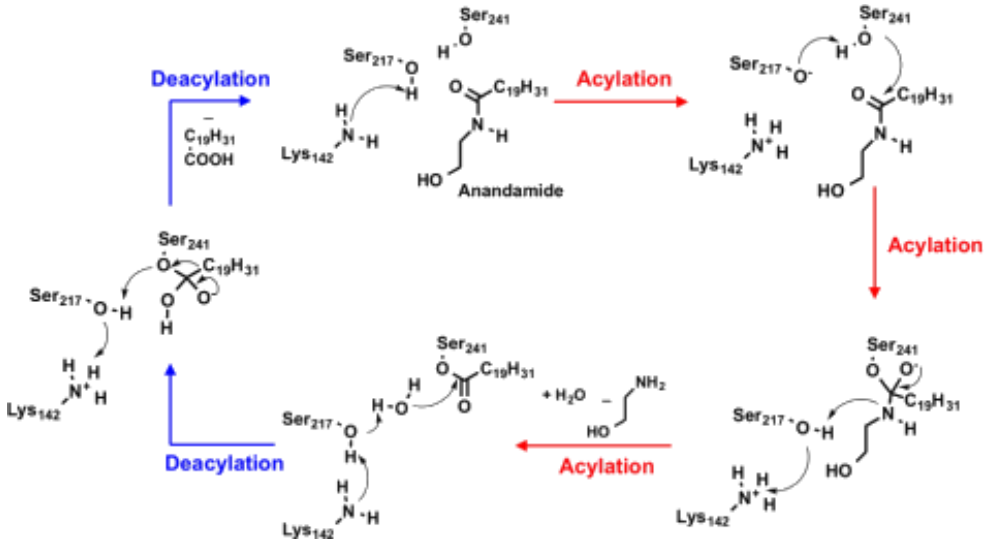

Figure 7: Hydrolysis mechanism of FAAH enzyme *(From Palermo et al. Med Chem. 2015)*

Other members of the same FAAH family are soluble enzymes that hydrolyse hydrophilic substrates such as acetamide, malonamide, and glutamine. Compared to these enzymes, two distinguishing features of FAAH are its integration into membranes and its strong affinity for hydrophobic substrates. For this reason, the pharmacological inhibition of FAAH allows for the modulation of endogenous levels of cannabinoids, so it is a promising target for treatment of pain, inflammation and many other diseases [76].

2.2. The endocannabinoid system and its therapeutic exploitation

New pharmacological approaches for treatment of neurological disorders were identified in the ECS modulation. Many studies suggest how an increase of eCB levels and an enhancement of CB1/CB2 receptors activity can improve neuropathological condition [77-79]. However, an up-regulation of ECS has been associated with controlling or contributing to pathological effects [80]. Many compounds have been identified to regulate eCB degradation and biosynthesis acting as indirect agonist or indirect antagonist. Drugs that alkylate serine, cysteine and histidine residues or BTNP, an inhibitor of Ca^{2+}-independent PLA2, are able to inhibit the formation of AEA in cortical neurones [81], while RHC80267 [1,6- bis-(cyclohexyloximino carbonylamino)-hexane] and tetrahydrolipstatin (THL), have been shown to inhibit DAGL-α, reducing the production of 2-AG. O-3640 and O-3841 compounds have been developed as inhibitors of 2-AG biosynthesis with hight selectivity for DAGL-α, but they are not suitable for systemic use in vivo [82]. EMT inhibitors have been identified and they represented a perfect case study to evaluate the influence of ECS in different pathological conditions of both the central and peripheral nervous system. AM404, VDM-11, OMDM-1 and-2, UCM707 and AM1172 represent the most important compounds of this

class that includes long chain fatty acid derivatives such as amides or retroamides of arachidonic and oleic acid with amines containing an aromatic constituent [83,84]. Several studies have focused their attention of the possibility to counteract endocannabinoid inactivation. In particular, serine hydrolase inhibitors have showed therapeutic value in the treatment of several disorders. Belonging to this class we find fluorophosphonates, trifluoromethyl ketones, the a-keto heterocycles OL-135 and a-KH 7, and the carbamates URB597, BMS-1, SA-47 and SA-72 [85]. Another important class of compounds act on the modulation of CB1/CB2 receptors. The most important are SR141716A, a selective CB1 receptor antagonist, AM251, inverse agonist of the CB1 receptor, AM630, inverse agonist of the CB2 receptor [86,87], AM6545, a neutral antagonist CB1 receptor, URB447 [88,89], a CB1 antagonist/CB2 agonist, and last but not least, WIN55,212-2 [90], a non-selective cannabinoid receptor agonist [91]. In autoimmune encephalomyelitis (EAE) mice SR141716A inhibited the expression of CB1 receptor, whereas increased the expression of CB2 receptor in brains, spinal cords and spleens. At the same time this compound increased IFN-γ, IL-17 and inflammatory cytokines such as IL-1β, IL-6 and tumor necrosis factor-alfa (TNF-α) in brains and spinal cords [92]. In hypoxia-ischemia (HI) neonatal rats was observed that URB447 is able to reduce neurodegeneration after brain injury. A comparable effect was observed with SR141716A, whereas the WIN-55,212-2 reduced the effect of URB447 [93]. WIN-55,212-2 and URB597 have showed neuroprotective effect in neurological disorders. Su et al. (2017) have demonstrated how these two compounds can improve neuroinflammation in rats with chronic cerebral hypoperfusion (CCH) reducing the number of activated microglia and astrocytes in frontal cortex and hippocampus CA1 region. Moreover, the combined treatment can reduce the release of pro-

inflammatory cytokines and contain the translocation of NFkB. Antioxidant and anti-apoptotic properties of these two compounds was observed against the adverse effects of ischemia [94]. eCB are also able to prevent BBB integrity by attenuation of LPS-induced modifications in the diameter and permeability of vessels and margination of leukocytes. suggesting that ECS could be considered to develop a new strategic approach to protect BBB in different neurodegenerative disorders [95].

2.3. URB597: a selective FAAH inhibitor

Main actor of this work is URB597, also known as KDS-4103. URB597 (cyclohexylcarbamic acid 3'-carbamoylbiphenyl-3-yl ester) is a crystalline white solid with a molecular weight of 338.4 (Fig. 8). The compound has two hydrogen bond donors and five hydrogen bond acceptors [96,97].

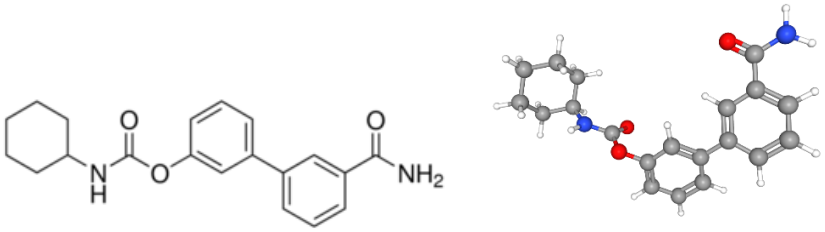

Figure 8: URB597 molecular structure

URB597 has a high degree of membrane permeability, evaluated in CaCo II TC7 cells, with an apparent permeability coefficient of 45.3 x 10^{-6} cm/sec [98]. URB597, an aryl ester of archilcarbamic acid, is able to block the hydrolysis enzyme FAAH activity [99,100]. It is a covalent irreversible inhibitor, hydrolysed by the enzyme itself and the enzyme is inhibited by

carbamylation of the nucleophilic residue Ser241 [101,102]. Russo et al. (2007) observed that a repeated oral administration of the URB597 (1–50 mg/kg, once daily, for 4 days) in mouse chronic constriction injury (CCI) model produced antipyralgia and pain relief [103]. Moreover, URB597 increased activity of serotonergic neurons in the dorsal raphe nucleus and noradrenergic neurons in the nucleus locus ceruleus in C57BL/6 [104]. In the lipopolysaccharide (LPS) mouse model of inflammatory pain, URB597 attenuated the development of LPS-induced paw edema and reversed LPS-induced hyperalgesia, reducing levels of the proinflammatory cytokines IL-1β and TNF-α [105].

2.4. Endocannabinoid system in neurodegenerative disorders

Numerous studies have well analysed the important role of the ECS in neurodegenerative diseases [13,106]. In animal models was observed a dysregulation of endocannabinoid mediators, which contribute to disease in different ways depending on the location and timing of their production and on the progression of the disease [50]. eCB play a key role in peripheral and brain immune function and its agonism is typically associated with a modulation of pro- and anti-inflammatory activities, like the release of inflammatory mediators, including nitric oxide, IL-2 and TNF-α, the inhibition of the activation of the cell-mediated immune processes, and the inhibition of proliferation and chemotaxis [107-109].

Animal models of Parkinson disease (PD), pathology characterised by an impairment of dopaminergic system, showed a biphasic dys-regulation of CB1, such as hypoactivity in pre-symptomatic and early PD and hyperactivity at later stages [110]. PET and MRI analysis showed an increased level of CB1 in patients with PD, as well CB2 receptor [111,112]. In 6-OHDA- treated rat models, the activation of CB2 reduces dopamine depletion and counteracted

MPTP-induced neurotoxic and neuroinflammatory events in mice [113,114]. Another study, showed how an up-regulation of CB2 in LPS-treated rats, is able to reduce expression of inflammatory markers [115]. An impairment of ECS was demonstrated in patients with PD and in 6-OHDA-treated and reserpine-treated rats, where abnormal eCB levels in cerebrospinal fluid (CSF) were observed. A treatment with levodopa has demonstrated a revert of the pathological condition [116-118]. MAGL inhibitors mediate neuroprotection through CB2 activation, while FAAH inhibition improve motor behaviour via CB1/CB2 receptors, but no neuroprotective effects in MPTP-treated mice [119,120].

Huntington disease (HD) is another neurodegenerative disease that shows involvement of the ECS. HD is caused by death of dopaminergic neurons in the globus pallidus, due to expansion of CAG triplet repeats in the gene that encodes the huntingtin protein. This condition leads to progressive locomotor impairment and mental impairments. R6/1, R6/2 and HD94 mice are used like experimental models to study HD. The induction of the pathology through treatments with neurotoxins injected into the globus pallidus has showed a loss of CB1 receptors and the same condition was observed post-mortem in patents with HD [121-123]. In HD, a protection of medium spiny neuron populations by endocannabinoids might involve a retrograde inhibition of glutamate excitotoxicity at excitatory terminals [124,125]. CB1 and CB2 agonists are considered important targets to prevent motor impairment and loss of medium spiny neurons [126]. A reduction of AEA and 2-AG and in the striatum of R6/2 mice model was observed [127], while in R6/1 2-AG was increased and AEA levels were decreased [128]. Battista et al. (2007) found a dramatically decreased (down to less than 10%) of the FAAH activity in

peripheral lymphocytes of HD patients compared to those of healthy subjects [129].

Alterations in CB1 and CB2 receptors were reported also in Multiple sclerosis (MS). Experimental autoimmune encephalomyelitis (EAE) or chronic relapsing EAE (CREAE) and Theiler's Murine Encephalitis Virus-Induced Demyelinating Disease (TMEV-IDD) are clinically relevant murine models of multiple sclerosis (MS). Several studies showed beneficial effects due to the activation of CB1 and CB2 receptors. In CREAE mice, CB1 agonists ameliorated tremor and spasticity [130,131], while in TMEV-IDD mice an improvement of clinical diagnosis via immunomodulatory and anti-inflammatory mechanisms after treatments with CB1 and CB2 agonists was observed [132]. AEA and 2-AG were found increased in brain and spinal cord of EAE and TMEV-IDD mice, but blood tests on patients with MS have showed an increase of endocannabinoids with a consequent reduction of AEA in CSF [133,134].

A down regulation of CB1 receptors was observed in Amyotrophic lateral sclerosis (ALS) experimental models. The causes of this pathology are still unknown, although in 1993 Rosen et al. found that mutations in the gene of Cu/Zn superoxide dismutase (also known as the SOD1 enzyme) were associated with some cases of familial ALS (~ 20%). This enzyme has an antioxidant function, as it reduces the level of superoxide ion (O^{2-}) a toxic free radical produced during cellular oxidative metabolism capable of altering proteins, membranes and DNA [135]. In SOD1 mice, characterised by an overexpression of SOD1, was observed an upregulation of CB2 receptors in the spinal cord [136], as well in post-mortem primary motor cortex and spinal cord sample from patients with ALS [137]. In SOD1 mice, AEA and 2-AG in the lumbar spinal cord were increased [138] and a genetic knockout of FAAH

showed a damping of symptoms, while treatment with MAGL inhibitors have showed also an increased survival [139,140].

2.5. Alzheimer disease (AD) and Endocannabinoid system

With the increasing life span of the general population, Alzheimer's disease (AD), which is an age-related neurodegenerative disorder, is becoming the major worldwide cause of dementia. With a prevalence of 46.8 million people in the world AD is one of the most important global health issues. This number will double by 2040 [141]. AD is a chronic neurodegenerative condition clinically characterized by progressive memory impairment and cognitive deficits. Other cognitive deficits include changes in attention and problem-solving abilities, impaired judgment, decision-making and orientation. As dementia progresses, language dysfunction and personality changes frequently appear [142]. Mild cognitive impairment (MCI) is a hallmark of AD. For this reason, MCI profiles may prove to be a promising link to identify AD in its earliest stages and therefore provide an opportunity to apply preventive measures to slow down the disease (Fig. 9).

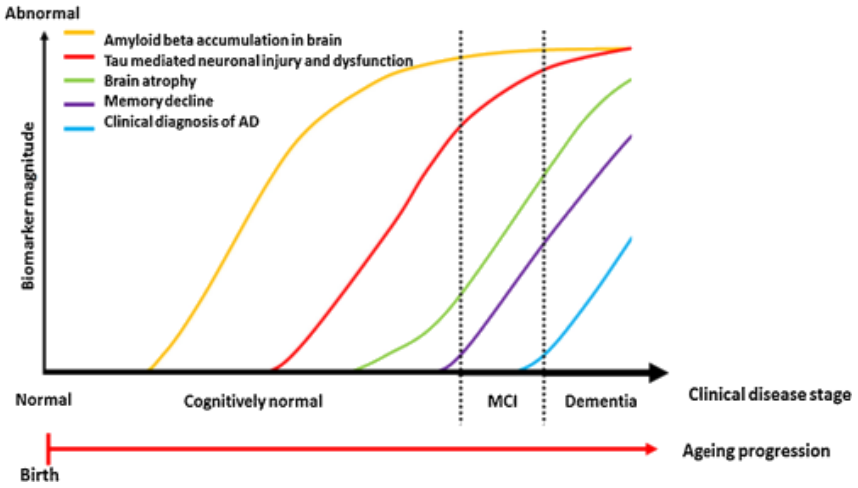

Figure 9. This diagram illustrates the progression from normal cognitive aging to mild cognitive impairment (MCI) and Alzheimer's disease (AD) as indicated by related sector changes (From *Lee et al. Mutat Res. 2015)*

AD can be classified into two forms: 1) sporadic AD, which accounts for the majority of cases, with less apparent or no familial aggregation and usually later onset age (> 60 years, SAD) and 2) the rarer, familial early-onset form, with Mendelian inheritance of predominantly early-onset (< 60 years, FAD), in which there are mutations of genes encoding, for example, amyloid beta precursor protein (APP) and presenilin-1 and -2 [143]. The macroscopic level of patients' brain shows a cortical diffuse atrophy, a loss of volume and a loss weight of the brain. On a microscopic level it is possible to observe the presence of extracellular senile plaques mainly composed of amyloid-beta peptide (Aβ) and intraneuronal neurofibrillary tangles (NFT) containing hyperphosphorylated tau protein [144,145]. Aβ is derived from Amyloid Precursor Protein (APP) that is an integral membrane protein expressed in many tissues and concentrated in the synapses of neurons. It is implicated in synapse formation, neural plasticity, antimicrobial activity, iron export and

intracellular calcium concentration functions through a kinase-dependent mechanism [146-149]. The gene encoding for APP is located on the long arm of chromosome 21 [150]. It generates a transcript that can undergo different processes of alternative splicing leading to the formation of different isoforms of the protein. In the cytoplasm APP cleavage occurs via two distinct ways, non-amyloidogenic and amyloidogenic pathways, through proteolytic processing by three enzymes BACE (β-secretase), α-secretase and γ secretase (Fig. 10). In the non-amyloidogenic pathway APP is hydrolysed by α secretase on the transmembrane segment [151,152], generating a different soluble APP variant (sAPPα) and a shorter C-terminal fragment, C83, which is subsequently hydrolysed by γ secretase producing the peptide P3, a non-toxic fragment of Aβ [153]. In the amyloidogenic pathway APP is hydrolysed by BACE, releasing a soluble APP fragment (sAPPβ) and a shorter C-terminal fragment, C99, which is subsequently hydrolysed by γ secretase generating an intracellular peptide called AICD (APP intracellular C-terminal domain) and Aβ. Besides the N-terminal variations due to BACE, Aβ can also have different C-terminal endings depending on the γ-cleavage site (Aβ40 or Aβ42). The most abundant Aβ species produced in the brain and found in the CSF is Aβ1–40, whereas levels of the more readily aggregating Aβ1–42 generally make up only 5 to 10% [154].

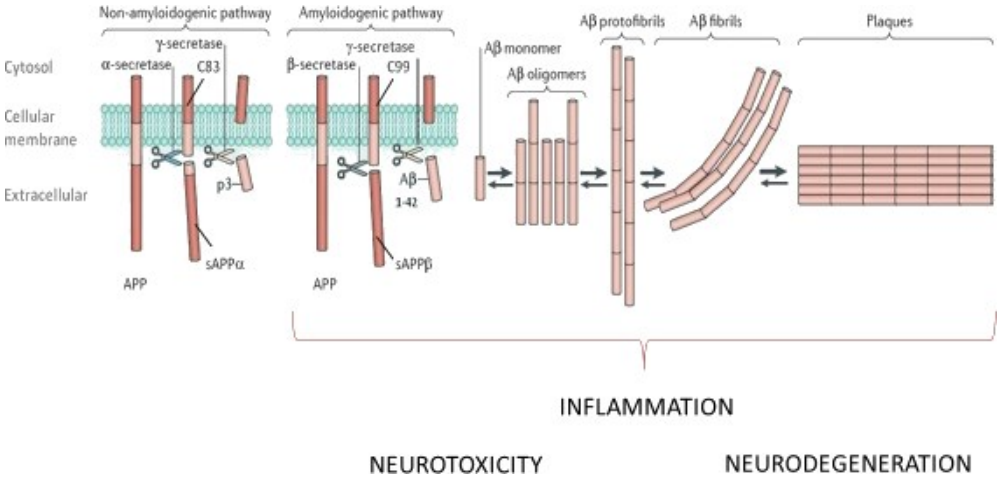

Figure 10: APP protein proteolysis *(Modified from Heppner et al. Nat Rev Neurosci 2015)*

Therapeutic approaches

The molecular basis of the pathogenesis of AD is not yet clear and efficacious drug therapy to counteract the clinical course of the disease still does not exist. The pharmacological approach currently adopted tries to modulate the neurotransmitter imbalances to counteract the neuronal death. Treating AD is the biggest unmet medical need in neurology. The main therapies currently adopted aim to improve symptoms, firsts of all inhibitors of acetylcholinesterase enzyme (AChE) (donepezil, galantamine and rivastigmine) and N-methyl-D-aspartate (NMDA) receptor antagonist (memantine). AChE inhibitors enhance cholinergic neurotransmission by preventing conversion of acetylcholine in choline and acetate, increasing acetylcholine in the inter-synaptic spaces and enhancing post-synaptic activation [155]. There is no significant difference in efficacy between the three drugs that are well tolerated by patients [156]. This class of drugs promotes a moderate improvement of cognitive functions in patients with moderate AD,

while the therapeutic efficacy on the most acute forms remains in doubt. Memantine, the last drug approved by the FDA, is a non-competitive NMDA antagonist. It is able to reduce the excitatory neurotoxicity effect of glutamate and it showed modest efficacy and safety profile in moderate and severe AD when used as monotherapy [157]. In combination with AChE inhibitors suggests benefits when compared to a non-combination treatment [158]. Some evidence suggests that anti-inflammatory drugs are able to delay neurodegeneration. Indeed, numerous mediators of inflammation are often associated with Aβ aggregation and increasing of toxicity [159]. To date, no drugs used in therapy seems to improve the prognosis of the disease. Actually, the current therapeutic strategies are aimed exclusively at relieving the symptoms and slowing down the course. For this reason, enormous efforts have been made to discover new molecules with the potential to change the course of the disease (Fig. 11).

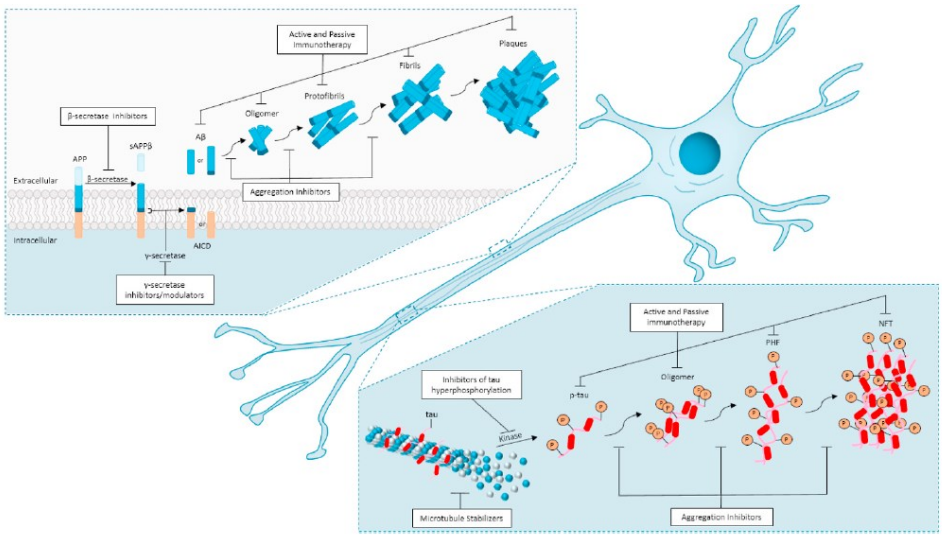

Figure 11: New therapeutic targets for treatment of Alzheimer's disease *(Vaz et al. Eur J Pharmacol 2020)*

The new targeting of research follows essentially the two pathological features of AD: the amyloid plaques (Aß) and the NFT (tau-protein). Therefore, the future therapies of AD will divide into two main strategies: anti-amyloid therapy and anti-tau therapy. Three approaches have been studied as anti-amyloid therapy: reduction of Aß production, prevention of Aß aggregation and promotion of Aß clearance. To reduce Aβ production BACE1 inhibitors were tested (verubecestat, lanabecestat, atabecestat, umibecestat and elenbecestat). All these drugs showed effective reduction of Aß levels in cerebrospinal CSF of AD patients, but in some cases, a cognitive exacerbated was observed [160,161]. Anti-aggregation agents represent a new strategy in disease-modifying therapy. Studies are currently focused on two molecules, scyllo-inositol and tramiprosate, but they showed severe adverse effects without a significant difference in cognitive scores [162,163]. One promising concept for preventing and treating AD is based upon stimulating the immune system to remove Aβ from the brain, promoting its clearance [164]. These therapeutic approaches involve use of specific anti-Aβ antibodies to induce the immune system to develop its own antibodies or direct injection of exogenous antibodies (active and passive immunization) [165]. On the other hand, the anti-tau therapies include the prevention of tau hyperphosphorylation and aggregation and the promotion of tau clearance (Tideglusib, Lithium). Several protein kinases are involved in tau phosphorylation, such as glycogen synthase kinase 3-beta (GSK-3β). These drugs showed a reduction in CSF levels of p-tau, but at the same time a slowing of cognitive decline [166]. Another therapeutic approach is the inhibition of tau aggregation constitutes (Methylthioninium chloride) [167,168]. These new approaches represent the most promising strategy to slow AD progression.

Modulation of the endocannabinoid system as new therapeutic approach for Alzheimer's disease

The ECS can be activated by different stimuli and may induce multiple responses, such as the anti-excitotoxic and antioxidant defense, as well as neuromodulatory and immunomodulatory actions, which help to restore cerebral homeostasis in different pathological conditions [62]. Alterations of ECS were observed in AD. Studies post-mortem on brains of patients with AD have shown the increased of expression of CB1/CB2 receptors in the microglia located close to the amyloid plaques [169]. Furthermore, the expression of FAAH, the enzyme responsible for the degradation of AEA, is increased in the senile plaques [170]. Oxidative stress, inflammation and excitotoxicity are typical feature observed in the pathogenesis of AD and the ECS display a possible neuroprotective role against these effects [171]. Gliosis and degeneration of neurons in the hippocampus due to Aβ aggregation were associated with an increase of 2-AG, suggesting that the ECS might activate in response to neuronal damage, representing a physiological neuroprotective response of the organism [172]. Tg2576 transgenic mice, which overexpress a mutant form of APP, and in APP/PS1 mice, which express the same mutant APP and mutant presenilin 1, did not show an alteration of CB1 levels. An alteration in CB1 levels was only observed in presymptomatic Tg2576 mice [173,174]. CB2 agonists ameliorated memory and cognitive impairments in Tg2576 mice and in APP/PS1 mice [175], while amnesia induced by Aß is counteracted by CB1 antagonism [176]. An upregulation of CB2 was observed in microglia of APP/PS1 mice treated with intracerebral injection of Aß, suggesting a protective effect against inflammation by CB2 activation [177]. In AD disease in vitro and in vivo

models, CB2 activation reduced levels of pro-inflammatory mediators produced by reactive astrocytes and microglial cells, decreasing Aβ levels [178,179]. In AD mice models hippocampal levels of 2-AG are increased in the early stage of disease, while AEA levels resulted decreased in later stage [180]. These observations were confirmed in human AD [181]. In a study on post-mortem brains from patients with AD, AEA levels in the midfrontal and temporal cortex were reduced, while the expression and activity of FAAH enzyme were found increased in neuritic plaque-associated astrocytes and microglia [170,182].

3. AIM OF WORK

Recent reports pointed out on the possible role of the ECS in inflammatory processes of the brain and, specifically, on the one associated to AD [170,183,184]. Studies in transgenic model of the familiar form of AD showed a cognitive recovery by a modulation of the ECS [185]. Double transgenic TASTPM mice, overexpressing the APP and the presenilin-1 genes respectively, exposed to a mild stress procedure, showed a down-modulation of eCB and CB1 levels in brain limbic areas [186]. At the same time a chronic unpredictable stress (CUS) protocol was widely used in presence of the CB1 receptor agonist HU-210, to study the impact of stress exposure in several animal models. These data showed that HU-210 completely blocked the deficits in reversal learning and perseveratory behaviour seen following CUS [187]. Kofalvi et al. (2016) demonstrated as the levels of AEA were reduced in the hippocampus of AD mouse genetic model [182]. In the neurodegenerative processes an important role is played by the proteasome. A dysfunction of the proteasome could induce an accumulation of aggregated proteins and oxidative stress, conditions closely related to the increase of the inflammation [188,189].

Therefore, this projects thesis is aimed to:

I. Study the immune-modulatory effects and the cytoskeletal reorganization induced by URB597 in BV-2 cells treated with amyloid-β peptide (Aβ)

II. Study the cross-talk between microglia and astrocytes cells in a co-culture system to characterize the inflammatory processes. These experiments were performed at the University of Konstanz (Germany) in Marcel Leist's laboratory.

III. Study the protective effect of the co-culture system of human astrocyte stem cells and murine microglia against proteotoxic stress induced in LUHMES neurons and to analyse the potential neuroprotective effect of URB597 against proteasome dysfunction. These experiments were performed at the University of Konstanz (Germany) in the Marcel Leist's laboratory.

4. MATERIALS AND METHODS

4.1. Materials and chemicals

URB597 [3-(3-carbamoylphenyl) phenyl] N-cyclohexylcarbamate was from Selleck Chemicals (Selleck Chemicals, Houston, TX, USA). β-amyloid peptide ($A\beta_{25-35}$) fragment was synthesized by conventional solid phase [190]. Tissue culture medium and serum were from Gibco BRL (Life Technologies Inc., Grand Island, NY, USA). 3-(4,5-dimethylthiazol-2-yl)-2,5 diphenyltetrazolium bromide (MTT), 4', 6-diamidino-2-phenylindole (DAPI) and TRITC-phalloidin were purchased from Sigma-Aldrich (St. Louis, MO). *Bradford* Protein *Assays was from Bio-Rad* (BioRad, Segrate Milano, IT). Fluorescein isothiocyanate (FITC)-dextran was from Sigma-Aldrich (Sigma-Aldrich, St. Louis, MO). The primary antibody mouse monoclonal IgG β-Actine antibody was from Millipore (Merck-Millipore Darmstadt, DE), mouse monoclonal IgG anti-GAPDH was from Abcam (CA, United States), Anti-Rabbit IgG (H+L)-HRP Conjugate and Goat Anti-Mouse IgG (H+L)-HRP Conjugate were from BioRad (BioRad, Segrate Milano, IT), goat anti-rabbit TRITC secondary antibody was from Jackson ImmunoResearch (Jackson ImmunoResearch Europe Ltd, Cambridge House, St. Thomas' Place, UK) and goat anti-rabbit Alexa Fluor 488 secondary antibodies were from Biotium (Biotium, Inc, Landing Parkway, Fremont, CA, USA). Pull-Down and Detection Kits were from Thermo Scientific Pierce, Rockford (Thermo Scientific Pierce, Rockford, IL). The miRNeasy Micro kit was obtained from QIAGEN (Hilden, Germany), NanoDrop One/One C was from Thermo Fisher Scientific (Waltham, MA, USA). The High-Capacity cDNA Reverse Transcription kit and Power SYBR® Green Master Mix was purchased from

Applied Biosystems (Foster City, CA, USA). MG-132 and URB597 [3-(3-carbamoylphenyl) phenyl] N-cyclohexylcarbamate was purchased from Selleckchem Chemicals (Selleck Chemicals, Houston, TX, USA). Dibutyryl-cAMP (cAMP), fibronectin, Hoechst bisbenzimide H-33342, resazurin sodium salt, tetracycline, L-cysteine Adenosine triphosphate (ATP), Nicotinamide adenine dinucleotide phosphate (NADPH) and reduced glutathione (GSH) were purchased from Sigma (Steinheim, Germany). Recombinant human fibroblast growth factor (FGF), recombinant human glial cell-derived neurotrophic factor (GDNF) and epidermal growth factor (EGF) were purchased from R&D Systems (Minneapolis, USA). Leukaemia inhibitory factor (LIF) was purchased from Merckmillipore (Germany). Tween-20 and sodium dodecyl sulphate (SDS) were purchased from Roth (Karlsruhe, Germany). All cell culture reagents were purchased from Gibco/Fisher Scientific (Hampton, New Hampshire, USA) unless otherwise specified.

4.2. SPERIMENTAL MODELS

Microglia

Microglia are the resting macrophages of the CNS generated by the embryonic yolk sac. They migrate into the developing neural tube and after they extend to the brain parenchyma [8]. Microglia rapidly respond to brain injury and disease by altering their morphology and phenotype to adopt an activated state [191]. Activation of microglia takes place upon exposure to different stimuli in the CNS, including trauma to brain or spinal cord, ischemia, infection, air pollutants, neurotoxic agents, dysregulated cellular functions or the accumulation of Aβ [192]. A BBB damage can expose microglia to multiple pro-inflammatory agents and immunogenic molecules, such as

lipopolysaccharide (LPS) and bacterial DNA, that induce microglial activation triggering surface toll-like receptors (TLRs), with a consequence morphological modification [193,194]. Numerous markers and receptors in microglia are similar to monocytes and macrophages of peripheral tissue. The M1 phenotype is induced by toxins, LPS, IFN-γ and pro-inflammatory cytokines. On the contrary M2 phenotype release anti-inflammatory cytokines such as IL-4 and IL-10 to bring down neuroinflammation and neuron damages [9,195] (Fig. 12).

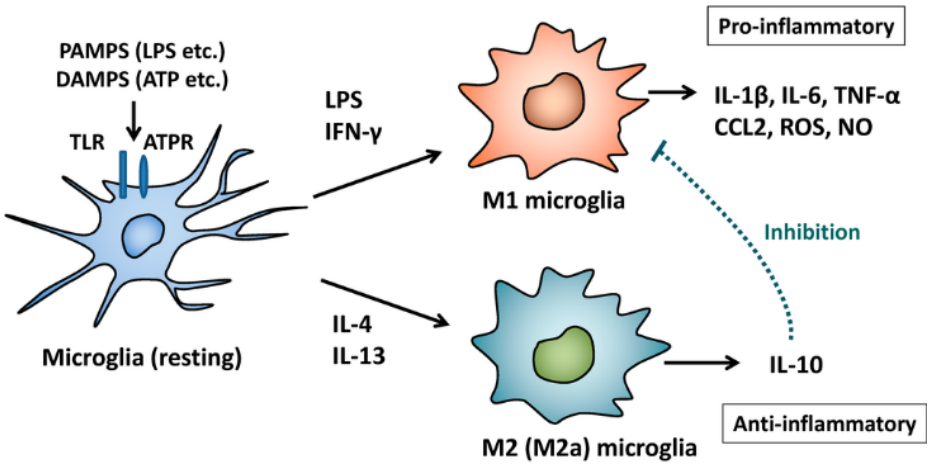

Figure 12: Microglia activation *(Modified by Nakagawa e Chiba, 2014)*

More recent studies have shown that microglia are never quiescent, but are in a state of motility, which allows them to probe the environment to identify alterations in cerebral homeostasis [196]. In physiological conditions, microglia use their ramifications as sentinels of the surrounding microenvironment, modulating their length and direction, without significant changes in the

cellular soma. In neuropathological conditions or in the presence of infectious agents, microglia undergo a rapid activation, adopting an amoeboid phenotype characterized by a large cell body. Davalos et al. (2005) showed that the induction of brain's damage induces microglia cells to extend their ramifications towards the site of insult [192]. Depending on the source of the signal, microglia give a specific response, through different receptors and signaling pathways, which include phagocytosis, increased migration, proliferation and release of bioactive molecules [197]. Although, activation of microglia has a neuroprotective function. Hyperactivation of these cells can cause neurotoxicity through the release of inflammatory cytokines and chemokines [191]. In AD's patients, the areas of amyloid plaques in the brains are surrounded by activated microglia, which suggests that the cytokines and cytotoxic molecules might be released from microglia [198]. Microglia express neurotransmitter receptors to communicate with neurons [199], to detect damaged neurons and to support them in secreting neurotrophic factors for neuronal regeneration [200]. The function of microglia differs during aging. This assumption is based on the facts that aged microglia secret more IL-6 and TNF-α, they are less responsive to stimulation and they have reduced levels of Glutathione [201].

Astrocytes

Astrocytes are the most important abundant glial cells in the CNS. They derive from the neuroectoderm and are essential in the synapse formation and function, in ion and neurotransmitter concentrations, contributing to the integrity of BBB and in brain homeostasis and neuronal survival [3,202]. Astrocytes are in contact with different brain cells as well as the vasculature, thereby coupling neurons and other brain cells to blood supply through

astrocytic end feet. Astrocytes show an important role in neuroinflammation with the production of anti-inflammatory cytokines, such as TGFβ, able to contrast microglia activation during an inflammatory process [4,203]. Two different phenotypes have been identified in the CNS, A1 and A2. Neuroinflammation stimulates A1 astrocytes to release neurotoxins that induce death of neurons. On the other hand A2 astrocytes promote neuronal survival and tissue repair [6]. Moreover, astrocytes themselves are connected through gap junctions (connexins), forming highly regulated networks of complex cell interactions [5]. During neurotransmission, the levels of extracellular potassium increase, which would disturb the depolarization of neurons. Astrocytes release glutamate that binds to receptors at the postsynaptic membrane leading to postsynaptic neuron depolarization. A rapid and efficient removal of remaining glutamate from the synaptic interspace is indispensable for terminating glutamate signaling and preventing excitotoxicity of glutamate. Astrocytes can also store glutamate in vesicles by the expression of vesicular glutamate transporters (vGLUT). As mentioned above, astrocytes play a crucial role also in the formation and maintenance of the BBB, by directly interacting with brain capillary endothelial cells [204,205]. They are one of the main inductors of the BBB phenotype [206]. Interactions between astrocytes and capillary endothelial cells during disease may affect the BBB integrity, as for example in PD and AD [207,208]. In AD brain endothelial cell-derived extracellular vesicles (EVs), are able to transfer Aβ to astrocytes and pericytes and then across the BBB into the brain. These EVs from astrocytes seems to be altered in AD [209].

LUHMES cells as neuronal model system

LUHMES (Lund human mesencephalic) cells are a subclone of the originally generated MESC2.10 cell line [210], obtained by preparation of precursor cells from embryonic ventral mesencephalic tissue and immortalized with a LINX v-myc retroviral vector system [211]. The mesencephalon, or midbrain, is considered as part of the brainstem and is associated with multiple brain functions, such as vision, motor control, alertness and reward [212]. The LINX v-myc retroviral vector consists of a tetracycline-controlled transactivator (tTA), a minimal CMV promotor (Tet-O), the oncogene v-myc and a gene that confers a neomycin resistance (neo) In this system, tTA strongly activates transcription of v-myc from Tet-O in the absence of tetracycline (Fig. 13). This allows the cells to continuously proliferate in a medium containing fibroblast growth factors (bFGF). To start the differentiation process, the cells are incubated with medium containing non-toxic concentrations of tetracycline, dibutyryl cyclic adenosine 3',5'-monophosphate (db-cAMP) and glial cell line-derived neurotrophic factor (GDNF). The role of tetracycline is that to suppress the transcription activation by tTA. In this way the production of v-myc is blocked and the cells readily start to transform into post-mitotic neurons. LUHMES cells are an interesting model system to investigate the processes of neurodegenerative diseases as well as to test compounds interfering with this process in vitro [263-267].

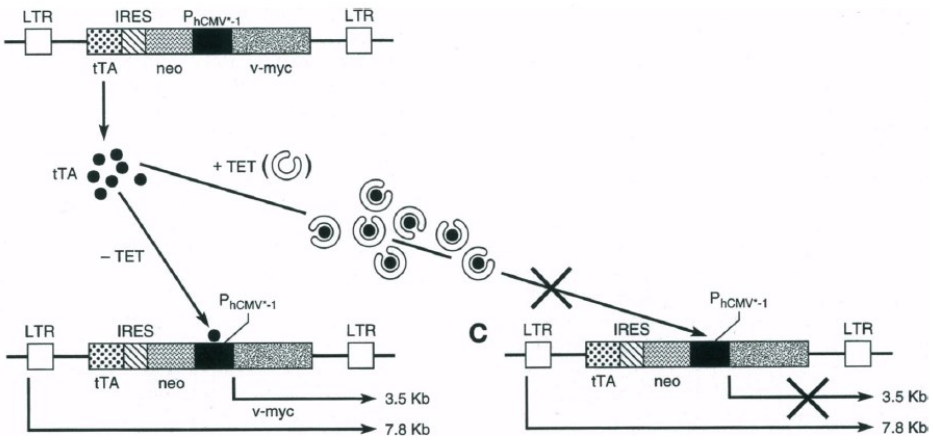

Figure 13: Structure of LINX v-myc retroviral vector system *(Modified from Hoshimaru 1996 Proc Natl Acad Sci U S A. 1996).*

4.3. Preparation of Aβ$_{25–35}$ and URB597 Stock Solution

Aβ$_{25–35}$ was dissolved in sterile phosphate buffered saline, pH 7.4 (PBS) at a concentration of 1 mM. To induce the aggregation, the solution was incubated in a sonicator bath on ice for 30 min. After treatment the solution was stored at -20°C until use. URB597 was dissolved in dimethyl sulfoxide (DMSO) at a final concentration of 1 mM.

4.4. Fatty acid amide hydrolase assay

FAAH enzymatic activity was studied by using membranes prepared from BV-2 cells treated with vehicle or Aβ$_{25–35}$ 30 μM for 4 h and 24 h, or pre-treated with 5 μM URB597 for 4 h and incubated with 30 μM Aβ$_{25-35}$ for 24 h. Membrane preparations were then incubated with [14C]-AEA (85.0 mCi/mmol,ARC St. Louis, MO, USA) properly diluted with AEA (Cayman

Chemicals, Ann Arbor, MI, USA) in 50 mM Tris–HCl, pH = 9, for 30 min at 37°C. [14C]-Ethanolamine produced from [14C]-AEA hydrolysis was measured by scintillation counting of the aqueous phase after the extraction of the incubation mixture with two volumes of CHCl3/CH3OH (1:1, v/v) and the activity was expressed as percentage of the maximum effect observed in absence of treatments.

4.5. Cell cultures and treatments

Project I

Mouse microglia cell line (BV-2), kindly provided by Dr. Mangino, Sapienza University of Rome, were seeded in DMEM/F-12 medium containing 5% fetal bovine serum, 4 mM L-glutamine and 1% of penicillin-streptomycin (Gibco BRL Life Technologies Inc., Grand Island, NY, USA), at 37 ◦C in a humidified atmosphere with 5% CO2. Cells were plated at an appropriate density according to each experimental setting and after 24 h treated with $A\beta_{25–35}$ 30 μM in presence or absence of URB597 5 μM. The cells were pre-treated with URB597 for 4h before adding the $A\beta_{25–35.}$

Project II and III

LUHMES cells (Lund human mesencephalic cells) were generated as described in detail [213]. Proliferating LUHMES cells were cultivated in PLO/fibronectin coated T75 flasks (Sarstedt, Germany) in 12 ml proliferation medium composed of advanced DMEM/F12 supplemented with 2 mM glutamine (Sigma-Aldrich, St. Louis, MO), 1x N2 supplement and 40 μg/ml FGF. Cells were passaged at a confluence approximately of 80%. Before being detached, the medium was removed and the cells were washed with 10 ml

phosphate buffered saline (PBS) (Merck-Millipore Darmstadt, DE). After they were incubated for 3 min at 37°C in 2 ml 0,05% trypsin-ethylenediaminetetraacetic acid (EDTA) solution. Afterwards, 13 ml of advanced DMEM-F12 without supplements were added to the trypsinized cells and centrifuge at 1200 rpm for 5 min. Supernatant was aspired and cells were resuspended in 5 ml of advanced DMEM-F12. Cells number was obtained using a Neubauer chamber. Cells were seeded at a confluence of 40 000 cells/cm^2 for two days of proliferation and at a confluence of 15 000 cells/cm^2 for three days of proliferation. Cells were cultivated at 37°C in a humidified atmosphere with 5% CO2. To start the differentiation process, proliferating LUHMES were seeded at a confluence of 87 000 cells/cm^2 in differentiation medium (indicated as d0 in the Fig.14). The differentiation medium is composed by advanced DMEM-F12 F12 supplemented with 2 mM glutamine, 1 mM cAMP, 2 ng/ml GDNF and 2,25 µM tetracycline. LUHMES cells were differentiated for two days before the seeding in the appropriate plates at a confluence of 145 000 cells/cm^2. They were treated on day 6, according to each experimental setting.

Human astrocytes were differentiated from human stem cells H9 [214] according to Palm et al. 2015 [215] until they reached the neural stem cell (NSC) state. At this state, NSC were cultivated for 49 days in NSC-medium consisting of DMEM-F12 supplemented by 0,5x N2, 1x B27 with Vitamin A, 2 mM glutamine, 20 µg/ml FGF, 20 µg/ml EGF and 1,5µl/ml LIF and frozen in liquid nitrogen. For further differentiation towards astrocytes, NSC were thawed and seeded on Matrigel-coated (1:20 dilution in cold DMEM/F-12) plates in astrocyte differentiation medium for at least 35 days until start of experiments. Astrocytes differentiation medium is composed by DMEM/F12, 2 mM L-glutamine, 0.5x N2, 0,5x B27 and 1% FBS. Therefore, astrocytes

were detached with Accutase (Corning, USA) for 5 min at 37 °C, added of DMEM/F-12 and centrifuged at 500 x g for 5 min. After supernatant was aspirated, pellet was resuspended in LUHMES differentiation medium and counted using a Neubauer chamber. Astrocytes monoculture or in co-culture with microglia or BV-2, were seeded at a confluence of 30 000 cells/cm^2, while astrocytes in co-culture with LUHMES cells were seeded at a confluence equal to 10% of LUHMES cells, that is 145 000 cells/cm^2 as mentioned above. Cells were cultivated at 37°C in a humidified atmosphere with 5% CO2.

Human monocytes were generated from an iPSC line (STBCi026-A, StemBANCC) that stably express green fluorescent protein (GFP) under a constitutive promotor by lentiviral transfection. iPS cells were differentiated in macrophage progenitors as described in detail [216,217]. iPSC cells were detached with Accutase (Corning, USA) for 5 min at 37°C. Afterwards, mTESR (StemCell Technology, Canada) was added to the cell suspension and centrifugate for 5min at 300 x g. To promote the Embryoid Body (EB) formation, $4*10^6$ cells per well were seeded in an Aggrewell 800 plate (StemCell Technology, Canada) in mTESR medium containing 10 µM Rock inhibitor Y27632 (Tocris, United Kingdom). The cells were cultured for four days with a 66% medium change every 24 h. Subsequently, to induce the mesoderm formation were added to the medium 50 ng/ml BMP4 (Peprotech, USA), 50 ng/ml VEGF (R&D Systems, USA) and 20 ng/ml SCF (R&D Systems, USA) at 24 h after replanting. After four days, the EBs formed were transferred in cell culture dishes in XVIVO medium (Lonza, Switzerland) supplied with M-CSF (Miltenyi, Germany) and 25 ng/ml IL-34 (Miltenyi, Germany). After seven days the 50% of the medium was renewed and only after 14 days the EBs were reseeded. When the cell culture was confluent and the pre-macrophages was ongoing, the medium was change twice per week.

To induce the differentiation of the pre-macrophages in microglia-like cells, the cells were cultivated for seven days in XVIVO medium supplied with 1x GlutaMAXTM (Gibco, USA), 1x Penicillin-Streptomycin (Gibco, USA), 100 ng/ml IL-34 (R&D Systems, USA) and 10 ng/ml GM-CSF (R&D Systems, USA). Microglia monoculture were seeded at a confluence of 30 000 cells/cm^2. The same confluence was used for the co-culture with the astrocytes. Cells were cultivated at 37°C in a humidified atmosphere with 5% CO2.

BV-2 cells, a mouse microglia cell line (kindly provided by E. Blasi, Perugia) [218] were seeded in DMEM/F-12 medium containing 10% fetal bovine serum, 4 mM L-glutamine and 1x Penicillin-Streptomycin (Gibco, USA), at 37 °C in a humidified atmosphere with 5% CO2. The cells were passaged with the same procedure used for LUHMES cells and plated at an appropriate density according to each experimental setting. BV-2 monoculture or in co-culture with astrocytes were seeded at a confluence of 30 000 cells/cm^2 while BV-2 in co-culture with LUHMES were seeded at a confluence equal to 10% of LUHMES cells, that is 145 000 cells/cm^2 as mentioned above.

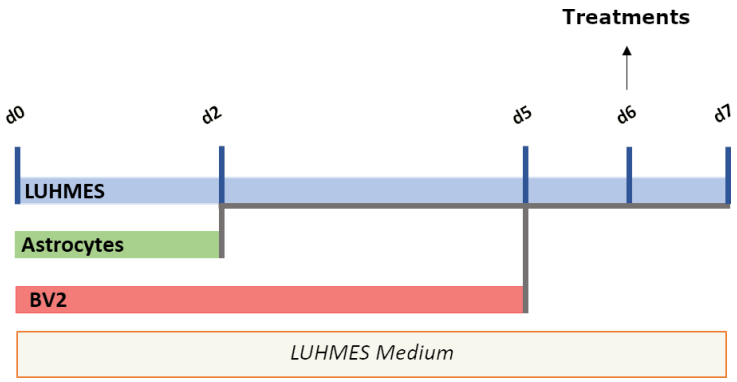

Figure 14: Co-culture were generated by mixing LUHMES d2 and astrocytes. The BV-2 cells were added on d5.

Human microglia conditioned medium

Conditioned medium (CM) was obtained from human microglia seeded with a confluence of 30 000 cells/cm^2 in a 6 wells plate. Cells were treated with 10 ng/ml TNF-α and 100ng/ml LPS for 24 h. After the incubation, the medium was centrifugated and cell debris. Then, the CM was transferred to the mono and co-culture astrocytes.

4.6. Cell viability assays

MTT assay

Cell viability was evaluated with MTT cell metabolic activity assay. Cells were seeded in 96-wells plates at a density of 3000 cells for each well. After treatments, 20 µL of a 5 mg/mL solution of MTT in PBS was added to the culture medium at a final concentration of 0,5 mg/mL and cells were incubated at 37°C for 2h. The supernatant was removed from each well and the formazan crystals were solubilised in 100 µL of DMSO. The optical density (OD) was measured at 570 nm with a reference at 690 nm using a microplate reader (Thermo Scientific Appliskan Multimode Microplate Reader).

Resazurin

Cells were seeded in a 96 wells plate at an appropriate density according to the experimental setting. Metabolic activity was determined by resazurin assay. Briefly, resazurin solution was added to the cell medium to obtain a final concentration of 10µg/ml. After 60 min of incubation at 37°C, the fluorescence signal was measured at an excitation wavelength of 530 nm, using a 590-nm long-pass filter to record the emission. The normalization of

the fluorescence values was calculated considering the untreated wells as 100% [219].

LDH release

Cells were seeded in a 96 wells plate at an appropriate density according to the experimental setting. LDH activity was detected separately in the supernatant and in the cell homogenate. The medium was transferred into a separate plate and the cells were lysed in PBS/0,1% Triton X-100 for at least 2h or ON. After that, 20 µL of sample, derived from the supernatant and from the lysate, were transferred in a new plate and added of 180 µL of reaction buffer containing 100 µM NADH and 600 µM sodium pyruvate in potassium-phosphate buffer (KPP-buffer, pH 7,4). Absorption at 340 nm was measured at 37 °C in 1 min intervals over a period of 15 min. The slope of the absorption intensity was calculated. The ratio of LDH supernatant/LDH total was calculated using the slopes of supernatant and homogenate. LDH release was expressed in percent [220].

ATP assay

Cells were seeded in a 96 wells plate at an appropriate density according to the experimental setting. For the detection of ATP levels, a commercially available ATP assay reaction mixture CellTiter-Glo (Promega, USA), containing luci-ferin and luciferase, was used. 100 µl sample and 50 µl of assay-mix were added to a black 96-well plate. Standards were pre-pared by serial dilutions of ATP disodium salt hydrate (Sigma, Steinheim, Germany) to obtain final concentrations ranging from1000 nM to 7.8 nM. Determination of

protein concentration was per-formed by using a BCA protein assay kit (Pierce/Thermo Fisher Scientific, Rockford, IL, USA).

4.7. Immunocytochemistry

Project I

Cell were grown on 12 mm of glass coverslips in a 24-wells plates at a density of $15x10^3$ cells and fixed after treatments with 4% paraformaldehyde for 30 min. Then, each glass coverslips were incubated with 0.1 M glycine in PBS for 20 minutes and with 0.1% Triton X-100 in PBS for additional 5 minutes to allow permeabilization. To analyze cytoskeletal actin organization, cells were incubated with rhodamine-conjugated phalloidin (TRITC-phalloidin) for 45 minutes. For detection of M1/M2 polarization markers, cells were incubated with primary antibodies raised against polyclonal anti-rabbit IgG anti-Iba1 (dil.1:100 - AB-83747, Immunological Sciences, IT), polyclonal anti-rabbit IgG anti-iNOS (dil. 1:100 - D6B65, Cell Signaling Technology, USA) or polyclonal anti-rabbit IgG anti-Arg-1 (dil.1:50 - D4E3M, Cell Signaling Technology, USA) and subsequently with anti-rabbit Alexa Fluor 488. Finally the cells were marked with DAPI to highlight the nucleus. The fluorescence signal was analyzed using an Axio Observer inverted microscope, equipped with the ApoTome System (Carl Zeiss Inc., Ober Kochen, Germany). Cell area was quantified with ImageJ software.

Project II

Cell were grown on 13 mm of glass coverslips (Menzel, Braunschweig, Germany) in a 24-wells plates at an appropriate density according to each experimental setting and fixed after treatments with 4% paraformaldehyde for

30 min at RT or ON at 4°C. After that, each glass coverslips were washed with PBS and then permeabilized with PBS/0.06% Triton X-100 for 10 min at RT. Each glass coverslips were blocked in PBS/0,01% Triton X-100/5% FBS for 30 min at RT. For proteins detection cells were incubated with primary antibodies raised against NF-kB diluted 1:200 in blocking buffer (Biosciences, USA) and GFAP diluted 1:600 in blocking buffer (Cell Signaling, USA) and subsequently with the appropriate secondary antibody (Alexa Fluor) and Hoechst-33342 (1 μg/ml) for 30 min. Coverslips were mounted on glass slides with Fluorsave reagent (Calbiochem/Millipore/Darmstadt/Germany). The fluorescence signal was analyzed using an Olympus IX81 inverted epifluorescence microscope (Hamburg, Germany). For image processing, Image J open-source software was used.

4.8. Migration assays

To evaluate the migration capacity of the cells following treatments, we performed a Scratch assay. Cells were seeded at 1x106 cells on 35 mm plates and grown until confluence. A cell-free area was introduced by scraping the monolayer with a sterile tip. After intensive wash, the remaining cells were incubated with URB597 or Aβ25–35 or URB597 and Aβ25–35 at different time points. After incubation, images were taken using an Axio Observer inverted microscope (Zeiss). Migration was quantified by measuring the recovered scratched area, by Axio Vision software (Zeiss).

4.9. Fluorescein isothiocyanate (FITC)-dextran uptake assay

The phagocytic capacity was evaluated by measuring the internalization of the dextran conjugated with FITC into the cells after treatments. Cells were plated on 12 mm of glass coverslips in a 24-wells plates

at a density of $17x10^3$ cells/well. After treatments, the cells were incubated with dextran conjugated with FITC in culture medium for 1 hour at 37°C, or at 4°C for the negative control. The cells were stained with DAPI to detect nucleus and we took a picture on the microscope. Those cells that were found positive for FITC, detected by the fluorescence, were considered as cells that had successfully engulfed dextran. The quantitative analysis of the fluorescence intensity of the dextran and the number of dextran-positive cells was carried out using the ImageJ software.

4.10. Western Blotting

Cells were lysed in 100 μL/10^6 cells of RIPA buffer (50 mM Tris-HCl pH 7.4, 150 mM NaCl, 5 mM NaF, 0,5% NaDOC, 0,1% SDS, 1 mM Na_3VO_4, 1 mM PMSF, 1% NP-40 and proteases inhibitors). Lysed samples were incubated on ice for 30 min and centrifuged at 14000 rpm for 15 min at 4°C. Supernatants was collected and the proteins amount was quantified using a Bradford Assay. 20 ug of proteins for each sample, added with Laemmli buffer (240 mM Tris-HCl, pH 6.8, 40% glycerol, 5% β-mercaptoetanolo, 8% SDS, 0,04% di *Bromophenol blue*), were boiled for 3 min at 80°C and loaded on 4–20% Criterion™ TGX Stain-Free™ Protein Gel (BioRad). Proteins were transferred onto PVDF membranes (BioRad) using Turbo Blot system (BioRad). Membranes were blocked with 5% Milk (w/v) in Tris-*buffered* saline (TBS)-Tween (0.5% (v/v)) for 1 h. Primary antibodies were incubated at 4°C overnight. Primary antibodies used: mouse monoclonal IgG anti-Rho (dil. 1:1000 - sc418, Santa Cruz Biotechnology, Inc., Santa Cruz, CA, USA), mouse monoclonal IgG anti-Cdc42 (dil. 1:1000 – sc8401, Santa Cruz Biotechnology, Inc., Santa Cruz, CA, USA), mouse monoclonal IgG anti-NRF2 (dil. 1:1000 - sc-365949, Santa Cruz Biotechnology, Inc., Santa Cruz,

CA, USA), polyclonal anti-rabbit IgG anti-ATF4 (1:1000 - A6455, Molecular probes by life technologie). Following the washing steps with TBS-Tween (0.1%), appropriate peroxidase-conjugated secondary antibodies were incubated for 1 h at RT. The proteins bands intensity with Crescendo (Millipore) using ChemiDoc (MolecularImager ® ChemiDoc^{TM}mod. MP System – BioRadLaboratories) and densitometric analyses were performed with ImageLab software (Biorad) and normalized to to the corresponding β-Actine and GAPDH controls.

4.11. Pull down assay for activated Rho GTPases

Pull down assay was performed using "Active Rho Pull-Down and Detection Kit" (Thermo scientific – n°16116, 16119). Briefly, cells were plated at an appropriate density in order to have at least 500 µg of total protein to add to the column for each sample. The cells were scraped, collected in a tube and gently rinsed once in ice-cold TBS, 1 mM PMSF, proteases inhibitors cocktail and 1 mM Na3VO4. 106 cells were lysed in 100 mL of Lysis/Binding/Wash Buffer (25 mM Tris HCl, pH 7.2, 150 mM NaCl, 5 mM MgCl2, 1% NP-40, 5% glycerol, proteases inhibitors cocktail, 1 mM PMSF and 1 mM Na3VO4). Subsequently the lysates were incubated on ice for 15 min and centrifuged at 16000 × g for 15 min at 4 °C. To ensure the pull-down procedure, GTPγS and GDP regarding as positive and negative control, were incubated with 500 µg of total protein, respectively. The samples were left at 30 °C for 15 min under constant stirring and the reaction was ended by mixing the sample with MgCl2 at a final concentration of 60 mM on ice. The supernatant of each sample was passed through a column and incubated with 100 µL Glutathione Resin (50% slurry containing 0.05% sodium azide) and 400 µg of GST-Rhotekin-RBD (5-6 mg/mL) at 4 °C for 1 hour with gentle rocking. The columns were washed

three times with Lysis/Binding/Wash Buffer. Each washing step included an intermediate centrifuge at 6000 x g for 10-30 seconds. The bound proteins were eluted with 2X SDS Sample Buffer (125 mM Tris HCl, pH 6.8, 2% glycerol, 4% sodium dodecyl sulfate (SDS) (w/v), 0.05% bromophenol blue and 5% □-mercaptoethanol). The samples were electrophoresed and analyzed by western blot with a rabbit IgG anti-Rho antibody (dil. 1:670 – 16116, Thermo Scientific Pierce, Rockford, IL). The same procedure was performed to Cdc42 pull down assay, using a mouse monoclonal IgG1 anti-Cdc42 antibody (dil. 1:167 – 16119, Thermo Scientific Pierce, Rockford, IL).

4.12. Determination of total glutathione

Cells were seeded in a 96 wells plate at an appropriate density according to the experimental setting. To determine the glutathione level, cells were lysed in 100 µL of 1% sulphosalicylic acid (w/v). The total glutathione was detected by a DTNB (5,5′-dithiobis(2-nitrobenzoic acid)) reduction assay. 40 µl of sample was mixed with 60 µl of assay mixture containing 300 µM DTNB, 1 U/ml glutathione reductase, 400 µM NADPH and 1 mM EDTA in 100mM sodium phosphate buffer, pH 7.5 (all purchased from Sigma, Steinheim, Germany). DTNB reduction was measured photometrically at 405 nm in 5-min intervals over 30 min. GSH standard curves were performed by serial dilutions ranging from 1000 to 7.8 nM, respectively. Determination of protein concentration was per-formed by using a BCA protein assay kit (Pierce/Thermo FisherScientific, Rockford, IL, USA).

4.13. Real-time quantitative PCR analysis

Project I

Total RNA was extracted from control and treated BV-2 cells using the miRNeasy Micro kit (Qiagen, Hilden, Germany) and quantified using NanoDrop One/OneC (Thermo Fisher Scientific, Waltham, MA, USA). cDNA was generated using the High-Capacity cDNA Reverse Transcription kit (Applied Biosystem, Foster City, CA, USA). Quantitative real-time PCR (qPCR) was performed for each sample in triplicate on an Applied Biosystems 7900HT Fast real-rime PCR System (Applied Biosystem, Cheshire, UK) through the program SDS2.1.1 (Applied Biosystem, Foster City, CA, USA) using the Power SYBR® Green PCR Master Mix (Applied Biosystem, Foster City, CA, USA). The primers for real-time PCR amplification were designed with UCSC GENOME BROWSER (http://genome,cse.ucsc.edu/;university of California, Santa Cruz) (table). The primer pair sequences were matched by BLASTn to the genome sequence to identify the primer locations with respect to the exons. A comparative threshold cycle (CT) method was used to analyze the real-time PCR data. The amount of target, normalized to the endogenous reference of *18S* rDNA *primers* (ΔCT) and relative to the calibrator of untreated control (ΔΔCT), was calculated by the equation $2^{-\Delta\Delta CT}$ as previously described [221].

Project II and III

Total RNA was extracted from control (CTR) and treated cells using PureLink RNA Mini Kit (Thermo Fisher Scientific) and quantified using NanoDrop 1000 Spectrophotometer (Thermo Fisher Scientific). cDNA was generated using iScript™ Reverse Transcription Supermix (Bio-Rad, US) for

5 min at 25 °C, 20 min at 46°C and the reverse-transcriptase was inactivated for 1 min at 95 °C. All RT-PCRs were based on the SsoFast EvaGreen detection system, were run in a CFX96 Cycler (Biorad, München, Germany) and analysed with Biorad iCycler software. A comparative threshold cycle (CT) method was used to analyze the RT PCR data. The amount of target, normalized to the endogenous reference of *PGK* and *RPL13A* rDNA *primers* (ΔCT) and relative to the calibrator of untreated CTR (ΔΔCT), was calculated by the equation $2^{-\Delta\Delta CT}$ as previously described [221].

5. PROJECT I
Results

To study the immune-modulatory effects and the cytoskeletal reorganization induced by URB597 in BV-2 cells treated with amyloid-β peptide (Aβ).

5.1. Aβ$_{25-35}$ does not affect the activity of the FAAH enzyme

The FAAH enzyme has been identified as the main hydrolase responsible for the degradation of AEA in vivo as well as other eCBs [222]. Genetic and pharmacological studies on the ECS have identified FAAH enzyme as a promising therapeutic target for the treatment of a wide range of inflammatory disorders [76]. To this purpose we treated BV-2 cells with Aβ$_{25–35}$ that induces neurotoxicity and neuroinflammation comparable to full-length Aβ$_{1-42}$ peptide [223], for 4 h and 24 h and determined FAAH activity. As shown by Fig.15, Aβ$_{25–35}$ did not exert any effect on FAAH activity both at 4 h and 24 h.

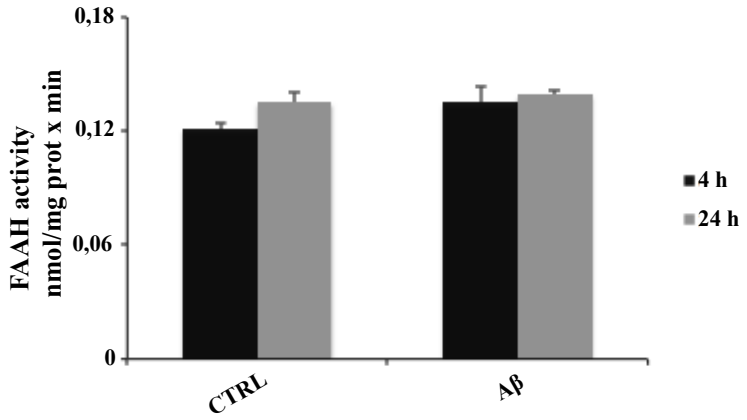

Figure 15: FAAH activity in $A\beta_{25-35}$-stimulated BV-2 cells for 4 h and 24 h. Data are reported as mean ± SD of three independent experiments. Statistical significance was determined using ANOVA analysis by Tukey's test.

5.2. $A\beta_{25-35}$ induces upregulation of the Iba1 microglia marker

A selective marker of microglial activation is Iba1. It is upregulated during the activation of these cells following nerve injury, central nervous system ischemia, inflammatory conditions and several other brain diseases [224-227]. The Iba1 protein (ionized calcium binding adapter molecule 1) also known as AIF-1 (Inflammatory Allograft Factor 1), is one of the most important selective microglia markers, which is peculiarly expressed also in macrophages [228,229]. It is expressed uniformly in the cytoplasm and along the branched processes of these cells. Iba1 takes part in cytoskeleton reorganization, binding actin molecules and leading to the formation of microfilaments [230]. We observed an upregulation of Iba1 in BV-2 cells treated with 30 μM $A\beta_{25-35}$ for 24 h, confirming microglial activation (Fig. 16).

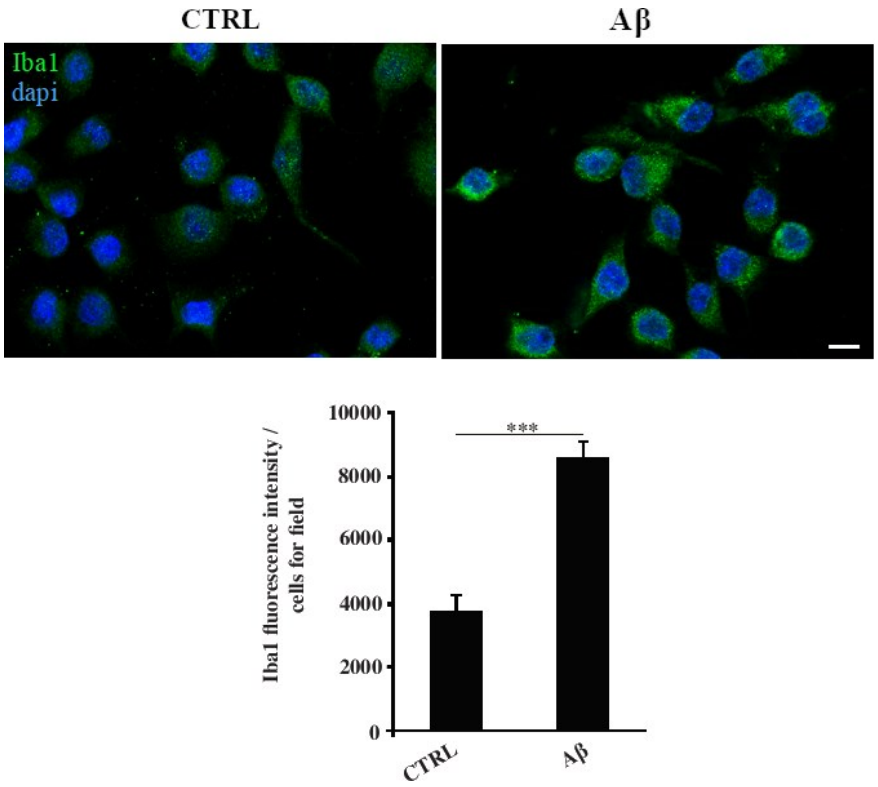

Figure 16: Immunofluorescence analysis of Iba1 of BV-2 cells treated with 30 μM $A\beta_{25-35}$ for 24 h. Quantization of the intensity of the fluorescence signal was performed using the ImageJ software. The results are expressed as the mean ± SD of three independent experiments. Statistical significance was determined using ANOVA analysis by Tukey's test. *** P <0.001 vs CTRL. Bar 20 μm.

5.3. URB597 does not exhibit cytotoxic effects in BV-2 cells

In order to evaluate the possible URB597 cytotoxicity on BV-2 cells and to define the optimal concentration for the purpose of analysis, cell viability experiments by MTT assay were performed. The results showed in Fig. 17 indicated that cell viability was not affected by URB597 at 1 μM, 5μM and 10 μM when BV-2 cells were treated for 24 h and 48 h. On the contrary, a cytotoxic effect was observed at 5 μM and 10 μM of URB597 at 72 h compared

to the control cells. In agreement with literature data we choose a concentration of 5 μM URB597 [96].

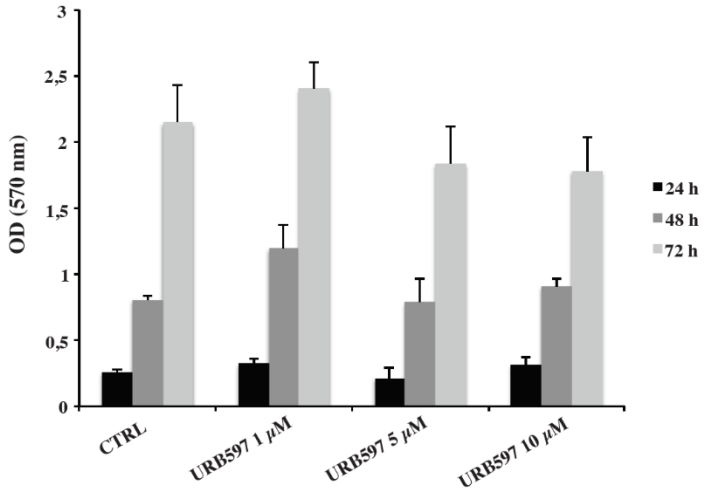

Figure 17: MTT assay on BV-2 cells treated with URB597 at concentration of 1 μM, 5 μM, and 10 μM for 24 h, 48 h and 72 h. The data are reported as mean optical density ± SD of three independent experiments. Statistical significance was determined using ANOVA analysis by Tukey's test.

Moreover, to confirm the modulation of FAAH enzyme activity due to URB597 compound, we performed an enzymatic assay on BV-2 cells in the combined treatment with $A\beta_{25–35}$. BV-2 cells were pre-treated with 5 μM URB597 for 4 h and incubated with 30 μM $A\beta_{25-35}$ for 24 h (Fig. 18).

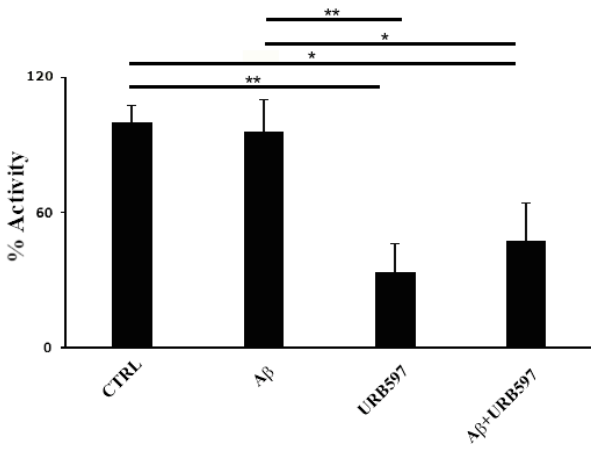

Figure 18: FAAH activity in BV-2 cells were pre-treated with 5 μM URB597 for 4 h and incubated with 30 μM $A\beta_{25-35}$ for 24 h Data are reported as mean ± SD of three independent experiments. Statistical significance was determined using ANOVA analysis by Tukey's test. *p<0.05, **p< 0.01

5.4. URB597 on BV-2 cells viability

In order to determine the effect of $A\beta_{25–35}$ on BV-2 cells, in presence or absence of URB597, Trypan blue assay and MTT assay were performed. BV-2 cells were pre-treated with 5 μM URB597 for 4 h and incubated with 30 μM $A\beta_{25–35}$ for 24 h and 48 h. Untreated cells were regarded as control. Fig 19A shows a significant increase of cell death in presence of $A\beta_{25–35}$, whereas URB597 was able to counteract cell death. URB597 alone had no effect. In addition, we performed MTT assay using cells treated as above described. The data obtained showed that $A\beta_{25–35}$ induced a decrease in cell viability around 40% in both 24 h and 48 h. Treatment with URB597 alone did not interfere with the cell survival. On the contrary, FAAH inhibitor in combination with $A\beta_{25–35}$ did not prevent $A\beta_{25-35}$ challenge on the succinate dehydrogenase (Fig. 19B).

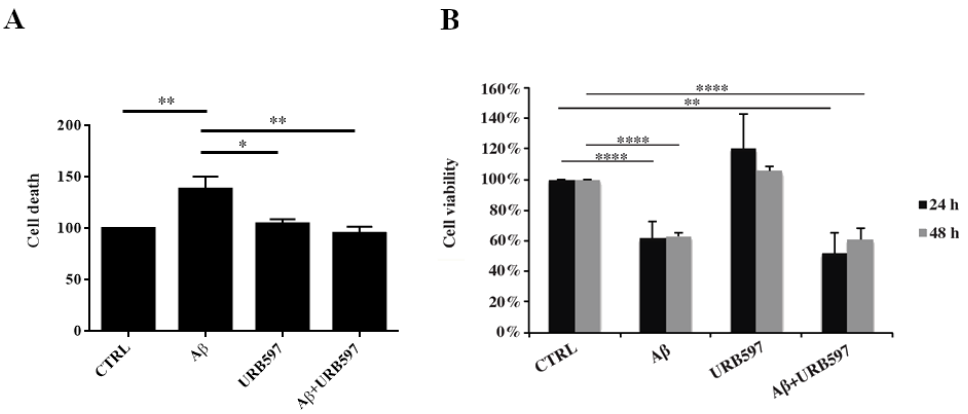

Figure 19: Effects of $A\beta_{25-35}$ in absence or presence of URB597 on BV-2 cells. **(A)** Trypan blue exclusion test. Cell count was determined in BV-2 cells exposed for 24 h to 30 μM $A\beta_{25-35}$ in presence or absence of 5 μM URB597 and expressed as death cell (cell death/cell death+alive cell). The data was reported as percentage versus CTRL or $A\beta_{25-35}$ respectively **(B)** Analysis of cell viability evaluated by MTT assay. MTT reduction was analyzed in the same samples at 24 h and 48 h to treated cells. Data was expressed as percentage versus CTRL or $A\beta_{25-35}$. The values are the mean ± SEM of triplicate determination from independent experiments. Statistical significance was determined using ANOVA analysis by Tukey's test. *p<0.05, **p< 0.01,****p< 0,0001

5.5. URB597 reverts morphological changes induced from $A\beta_{25-35}$

Microglia rapidly respond to brain injury and disease by altering their morphology and phenotype to adopt an activated state. In the activated state microglia from resting form shift to an ameboid form (M1/M2) [231]. Cells increase their surface area and acquired a flat morphology. To evaluate the effects of FAAH inhibition on the cell morphology, we performed immunofluorescence analysis using phalloidin staining of F-actin on BV-2 cells pre-treated with 5 μM URB597 for 4 h and incubated with 30 μM $A\beta_{25-35}$ (Fig. 20). The analysis was done at different time points (1 h, 3 h, 6 h 24 h).

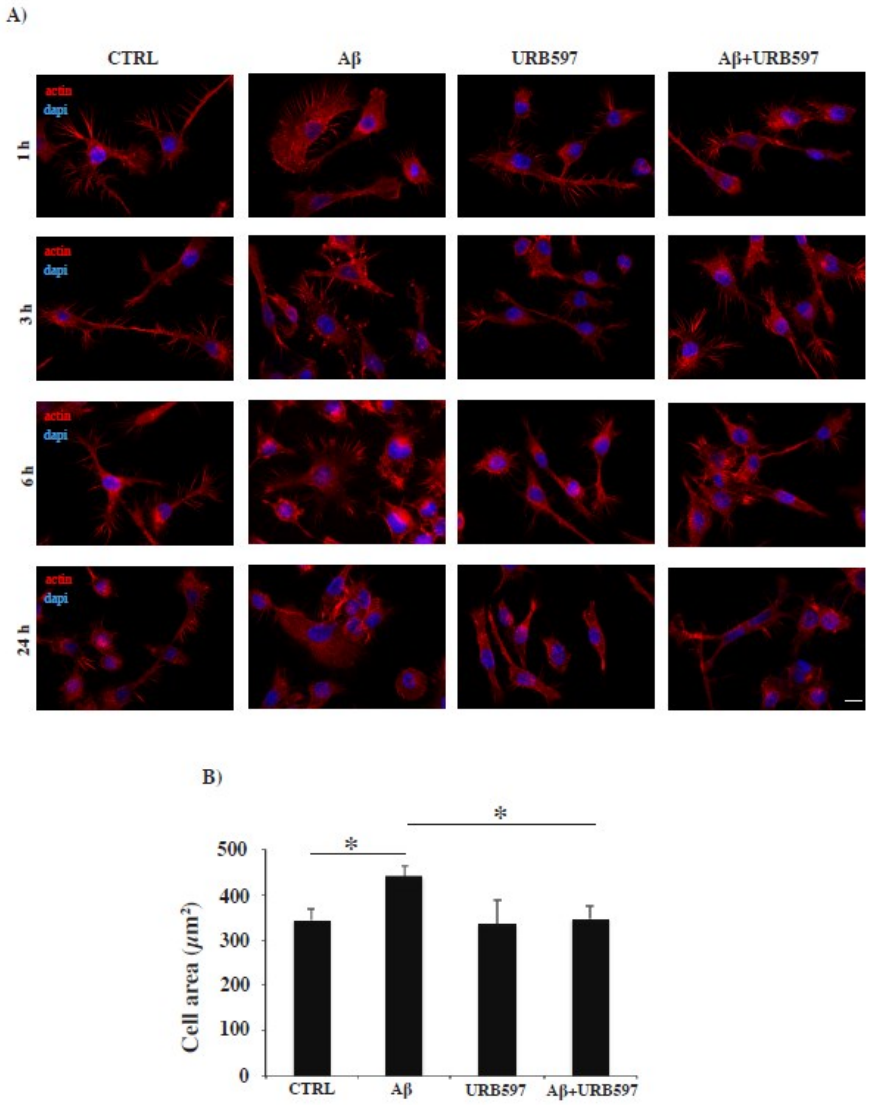

Figure 20: (A) Analysis of cell morphology by rhodamine-conjugated phalloidin (TRITC-phalloidin) staining to highlight actin and 4',6-diamidino-2-phenylindole (DAPI) to detect nucleus, after pre-treatment with 5 μM URB597 for 4 h and incubated with 30 μM $A\beta_{25-35}$ for 1 h, 3 h, 6 h, and 24 h. (B) Cell areas were quantified using Image J software. Data were reported as mean ± SD of at least three independent experiments. Statistical significance was determined using ANOVA analysis by Tukey's test. Bar: 20 μm. * $P < 0,05$ vs Aβ

The results showed that control cells were characterized by a very small cell body. They had long cell ramifications and actin was organized to form filopodi, used by the cell to explore the surrounding environment. In $A\beta_{25-35}$ samples, at all time points, the cells increased their surface area, acquiring a flat and polygonal morphology. Furthermore, it was evident that the cells retracted the branched processes typical of microglia in resting form. On the other hand, the cells treated with URB597 had a more rounded morphology, characterized by the shrinkage of the cellular body and the presence of cellular processes. Treatment with URB597 and $A\beta_{25-35}$ induced a phenotype similar to that obtained with only URB597 (Fig. 20A). The results were also confirmed by the quantitative analysis carried out by measuring the cellular area. To quantify these changes, cell area expressed in μm^2 was measured. The quantitative analysis confirmed that the treatment with URB597 alone presented area values similar to those of the control cells, while after stimulation with only $A\beta_{25-35}$, the cells underwent an enlargement of their soma. The cell area looked like 440 μm^2 compared to 340 μm^2 of the control sample. In the combined treatment URB597 reduced the area to values comparable to those of the control, indicating the capacity of URB597 to restore the amoeboid phenotype observed in the presence of $A\beta_{25-35}$ (Fig. 20B).

5.6. Effect of URB597 on Cellular Migration

One of the aspects of microglial cell activation is the acquisition of a migratory phenotype, which is essential for the cells to reach the insult site. As shown by Sacerdote et al. (2000), cannabinoids may modulate the migration of macrophages through their binding to CB2 receptors [232]. Here, to evaluate migration capacity induced by URB597, we performed a scratch assay. The cells were pre-treated with 5 μM URB597 for 4 h in the presence or absence of 30 μM $A\beta_{25-35}$ for 2 h, 4 h, 6 h and 24 h. Migration was quantized by measuring the width of the scratch (Fig. 21).

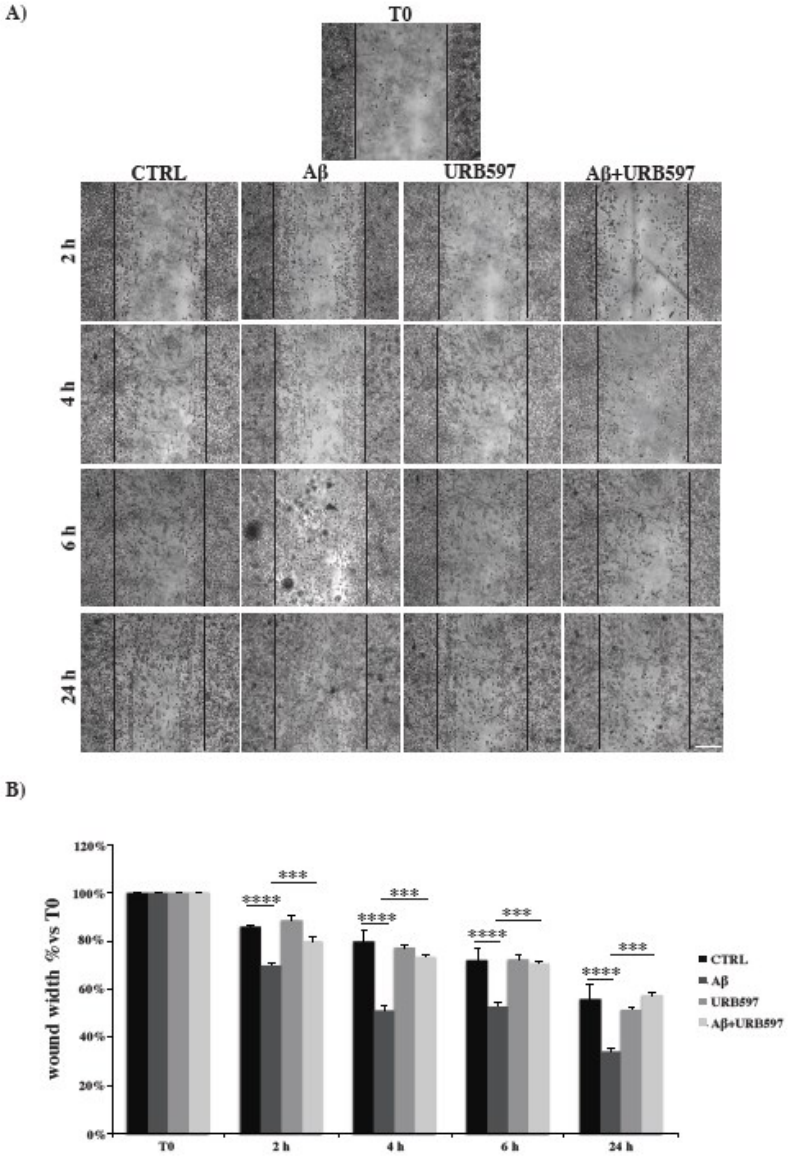

Figure 21: Analysis of cell migration determined by scratch assay. BV-2 were pre-treated with 5 μM URB597 for 4 h in the presence or absence of 30 μM $A\beta_{25-35}$ for 2 h, 4 h, 6 h and 24 h. T0 represents the control at time 0 and CTRL the control for each time point. The results were normalized on T0 sample and reported as a percentage. They represent the mean ± SD of three independent experiments. Statistical significance was determined using ANOVA analysis by Tukey's test. *** P< 0,001 vs Aβ. Bar 200 μm

As shown in Fig. 21, treatment with $A\beta_{25-35}$ induced migration already at 2h after stimulation, with a reduction of 20% in the width of the wound compared to the control cells. Treatment with URB597 did not induce migration and the width of the wound was similar to the control cells. The combined treatment with $A\beta_{25-35}$ and URB597 showed a migratory effect similar to that obtained with only URB597. The migratory effect was directly proportional at the different time points.

5.7. URB597 increases phagocytic capacity of microglia

Since the M2 phenotype is closely related to the cell phagocytic capacity, we evaluated the effect of URB597 on the phagocytosis process. BV-2 cells, pre-treated with 5 μM URB597 for 4 h and incubated with 30 μM $A\beta_{25-35}$ for 24 h, were incubated for 1h with FITC-dextran. The Fig. 22A showed the intensity of the fluorescent dextran in the different treatments. Stimulation with LPS represented the negative control of phagocytosis, while stimulation with IL-10 was used as a positive control. The sample treated with $A\beta_{25-35}$ showed a reduced ability to absorb dextran compared to the control and to the LPS sample. Moreover, in the sample treated only with URB597 the intensity value was comparable to that obtained by stimulating with IL-10. In the combined treatment with $A\beta_{25-35}$ and URB597, the inhibitor turned out to be capable of increasing the intensity value compared to the $A\beta_{25-35}$ sample. In the Fig. 22B the number of dextran-positive cells was quantified on the total cells and the results were reported as percentage. After stimulation with $A\beta_{25-35}$ as well as with LPS, the number of dextran-positive cells was reduced by approximately 80% compared to the control cells. On the other hand, treatment only with URB597 presented similar values compared to the control but lower

compared to the sample treated with IL-10. In the combined treatment with $A\beta_{25-35}$ and URB597, the inhibitor improved the number of dextran-positive cells with higher values of phagocytic cells compared with the sample treated with $A\beta_{25-35}$.

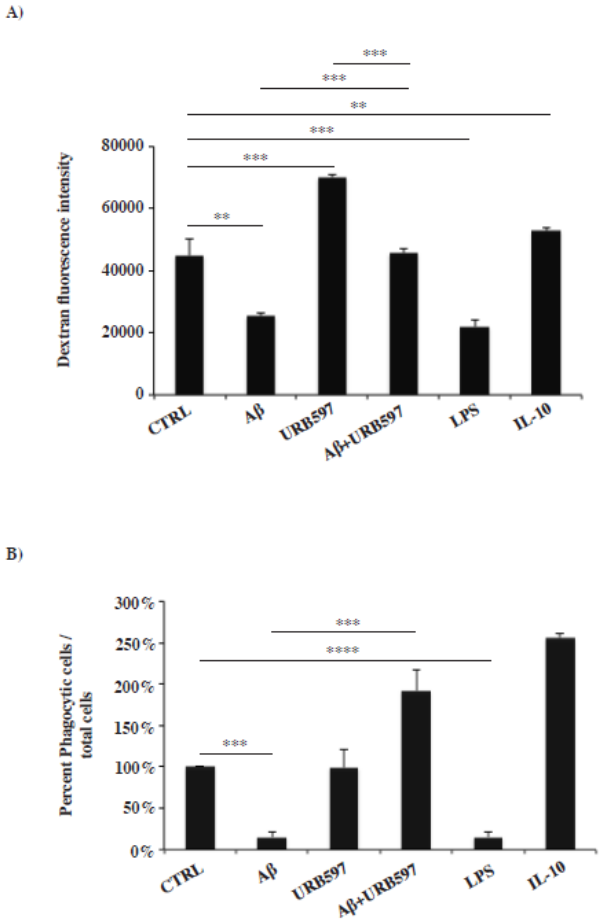

Figure 22: Analysis of the phagocytosis process using FITC-dextran on BV-2 cells pre-treated with 5 µM URB597 and incubated with30 µM $A\beta_{25-35}$ for 24 h. A) Quantization of the intensity of FITC-dextran. B) Quantization of the number of dextran-positive cells on the total cells. The data were normalized on CTRL and reported as a percentage. The results were expressed as the mean ± SD of three independent experiments. Statistical significance was determined using ANOVA analysis by Tukey's test. **p< 0.01, *** P <0.001 vs Aβ.

5.8. URB597 promotes the activation of Rho GTPase family

The cytoskeleton plasticity and the formation of actin-rich, with consequent morphological modifications are regulated by Rho GTPase protein family. Rho GTPase family represents a master regulator of cytoskeletal reorganization and plays an important role in membrane trafficking [233,234]. Rho GTPase family belong to the Ras superfamily of small guanine nucleotide-binding proteins. These proteins cycle between two conformational states: one bound to GTP ('active' state), the other bound to GDP ('inactive' state), and they hydrolyse GTP to GDP (Fig. 23) [235]. The inactivated state can be subsequently recognized by guanine nucleotide dissociation inhibitors (GDIs), which sequester Rho GTPases in the cytosol [236]. In this thesis we focused our attention on Rho and Cdc42 proteins as modulator of the cellular cytoskeleton.

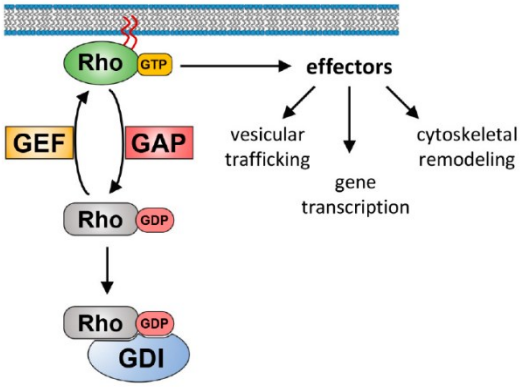

Figure 23: The Rho GTPase cycle *(From Olayioye et al. Cells 2019)*

Rho and Rac induce the assembly of contractile actin and myosin filaments (stress fibres) and actin-rich surface protrusions (lamellipodia). On the other hand, Cdc42 promotes the formation of actin-rich, finger-like membrane extensions (filopodia) [237]. To evaluate the influence of FAAH inhibitor on this class of proteins, we performed western blot analyses on total proteins extraction from BV-2 cells pre-treated with 5 μM URB597 for 4 h and incubated with 30 μM $A\beta_{25-35}$ for 24 h, with antibodies against RhoA and Cdc42 proteins. We observed a not significant slight increase of proteins levels in all the sample (Fig. 24).

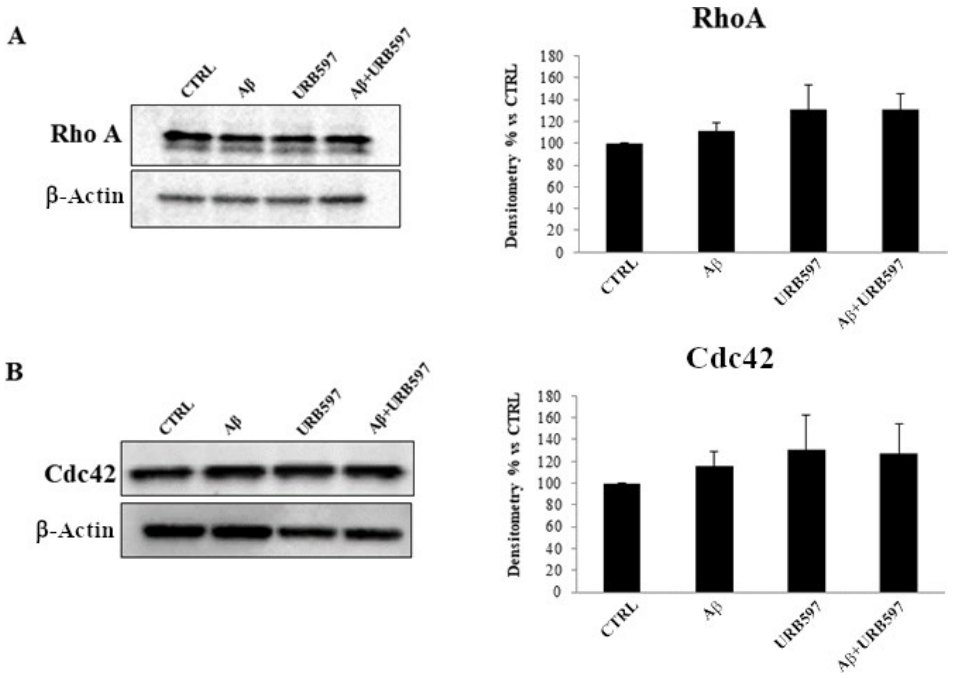

Figure 24: Expression levels of RhoA and Cdc42 proteins (A, B) analysed by western blot analysis in BV-2 cells pre-treated with 5 μM URB597 for 4 h and incubated with 30 μM $A\beta_{25-35}$ for 24 h. The data were normalized on the β-actin signal, reported as a percentage, normalizing on the control (CTRL). Data are expressed as the mean ± SD of three independent experiments. Statistical significance was determined using ANOVA analysis by Tukey's test.

Therefore, we performed an active pull-down assay for Rho, inducing the assembly of contractile actin, and Cdc42 proteins involved in promoting filopodia. This analysis allows the precipitation of active GTPases proteins only, through a specific binding protein. Our results showed a marked increase of Rho activity in the samples treated with $A\beta_{25-35}$ compared to the control cells, whereas a decrease was observed in the samples treated with URB597 in the presence or absence of $A\beta_{25-35}$ with respect to $A\beta_{25-35}$ samples (Fig. 25A). As shown in Fig. 25B, Cdc42 activity significantly increased in samples treated with URB597, considered both against control cells and $A\beta_{25-35}$ samples.

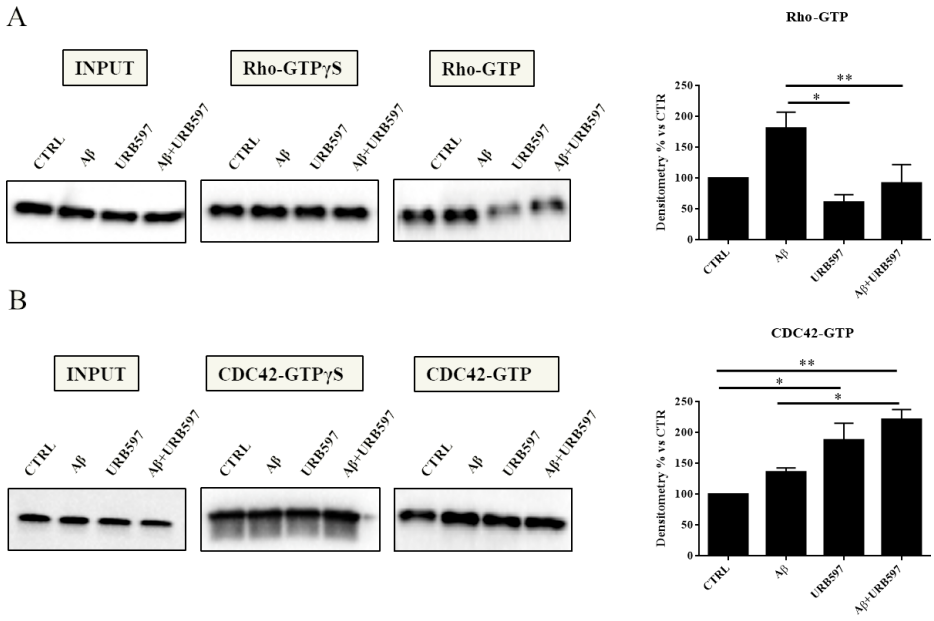

Figure 25: Pull down assay of Rho and Cdc42 proteins (A, B). BV-2 cells were pre-treated with 5 μM URB597 for 4 h and incubated with 30 μM $A\beta_{25-35}$ for 24 h. The pull-down assay with GTPγS was used as positive control. The results were reported as a percentage versus control (CTRL). Densitometric analyses were performed with ImageLab software (Biorad) and normalized to INPUT. The data are the ± SD average of three independent experiments. Statistical significance was determined using ANOVA analysis by Tukey's test. * P<0.05 VS CTRL and Aβ** P< 0,01 vs CTRL, *** P< 0,001 vs CTRL.

5.9. URB597 reduces mRNA expression of IL-1β and TNF-α and increases TGF-β and IL-10

Since the activation of Rho GTPases sustains the hypothesis of a cytoskeleton rearrangement driven by Aβ, leading to an increase of migration and phagocytosis, which were counteracted by URB597, we determined the level of inflammatory state in our BV-2 cell model. The expression of pro-inflammatory interleukins, such as IL-1β and TNF-α, as well as anti-inflammatory interleukins, such as TGF-β and IL-10, were analysed by qPCR. BV-2 cells were pre-treated with 5 μM URB597 for 4 h and incubated with 30 μM $A\beta_{25\text{-}35}$ for 1 h, 6 h and 24h. The results showed in Fig. 26 A and B demonstrated that IL-1β and TNF-α expressions increased within 1 h in BV-2 cells treated with $A\beta_{25–35}$ compared to the control. On the contrary a cytokines reduction was observed in the sample with the combined treatment compared to $A\beta_{25–35}$. Treatment with URB597 does not induce significant changes. As shown in Fig.26 C and D, URB597 alone or in combination with $A\beta_{25\text{-}35}$ seemed to upregulate TGF-β and IL-10 expression, respectively.

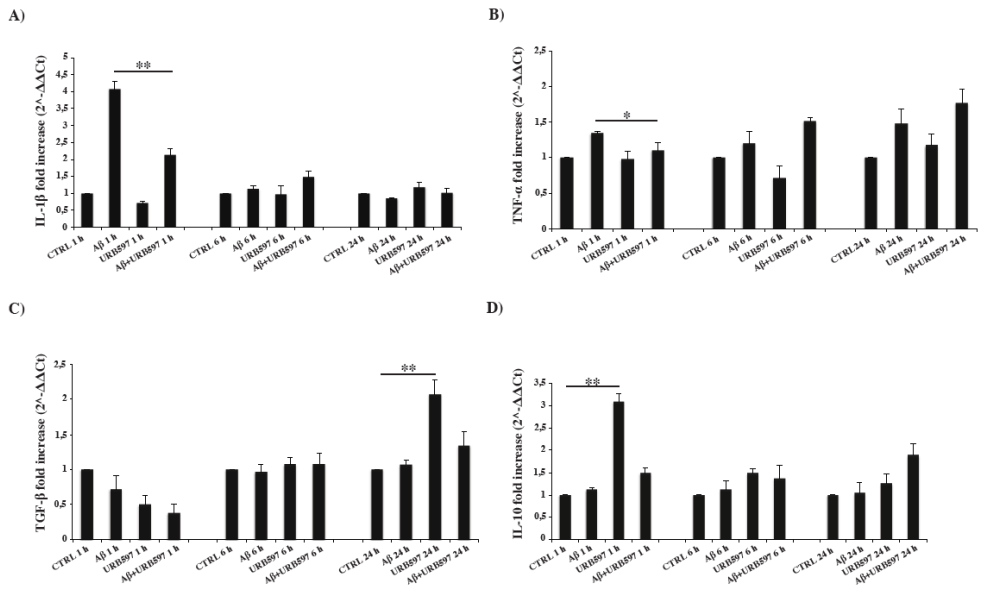

Figure 26: mRNA expression of different inflammatory cytokines, such as IL-1 β (A), TNF-α (B), TGF-β (C) and IL-10 (D), monitored by qPCR and normalized to 18S ribosome subunit. Data are shown as mean ± SD from three independent experiments performed in triplicate. Expression profiles were determined using the 2−ΔΔCT method. Statistical significance was determined using ANOVA analysis by Tukey's test. IL-1β** *P< 0,01 vs Aβ,* TNF-α * *P< 0,05 vs Aβ, TGF-β and IL-10* ** *P< 0,01 vs CTRL*

5.10. URB597 modulates iNOS and Arg-1 expression

The activation of microglia is a polarized process that can lead to a M1 activated phenotype, potentially neurotoxic, or to an M2 activated phenotype, potentially neuroprotective [195]. In order to evaluate the M1 or M2 states in the treated cells we performed an immunofluorescence analysis to evaluate the level of nitric oxide synthase (iNOS) and Arginase-1 (Arg-1), respectively markers of M1 and M2 microglia phenotypes (Fig. 27). BV-2 cells were pre-treated with 5 μM URB597 for 4 h and incubated with 30 μM $A\beta_{25-35}$ for 24h. LPS and IL-4 were considered as positive controls for iNOS and

Arg-1 markers, respectively. The stimulation of BV-2 cells with $A\beta_{25-35}$ induced a significant enhancement of the iNOS marker whereas a reduction of Arg-1 was observed compared to control. URB597 in combination with $A\beta_{25-35}$ induced a decrease of iNOS expression and an increase of Arg-1 with respect to $A\beta_{25-35}$. URB597 did not affect the expression of both markers.

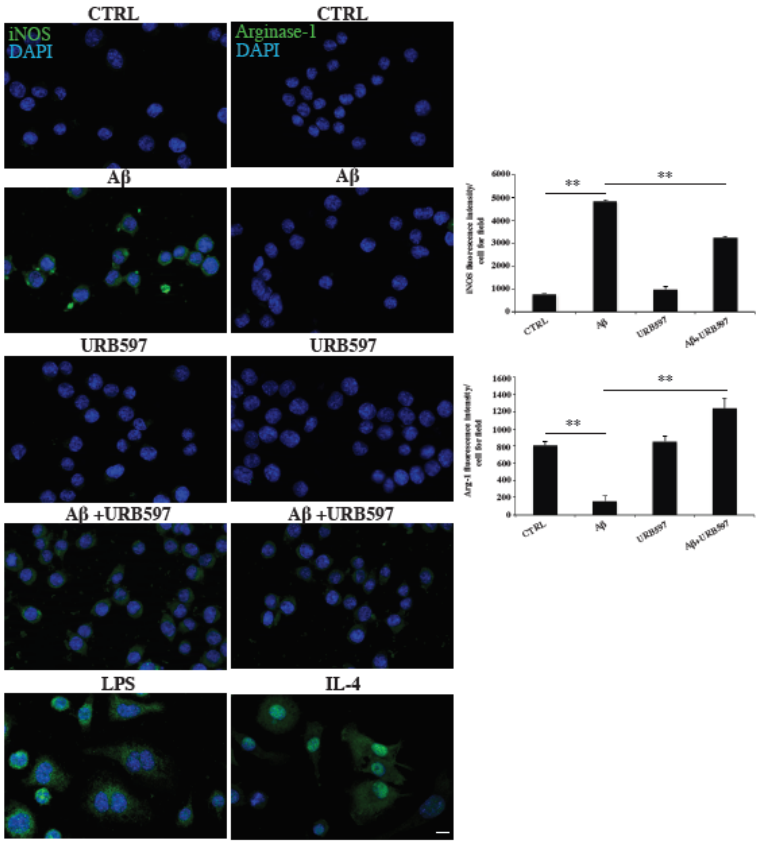

Figure 27: Immunofluorescence analysis on iNOS and Arg-1, M1/M2 markers respectively. BV-2 cells were pre-treated with URB597 5μM for 4 h and incubated with $A\beta_{25-35}$ 30 μM for 24 h. LPS and IL-4 were used as positive controls. Quantization of fluorescence signal intensity was analysed using ImageJ software. The results are expressed as the mean ± SD of three independent experiments. ** P <0.01 vs Aβ. Bar 20 μm.

DISCUSSION

Neuroinflammation might play a role in the pathophysiology of several neurodegenerative diseases by which microglia become chronically activated in response to pro-inflammatory insults through morphological changes. Abnormalities in cytoskeletal organization are a common feature of many neurodegenerative disorders, including AD [238,239]. Cytoskeleton modifications are essential for the innate primary immune response mediated by activation of microglia. Microglia takes part at the first defence responses of the brain in injury, repair and restore of the physiological homeostasis states. Microglia polarization and plasticity represent adaptative changes that allow them the capacity to probe the surrounding environment and identify possible harmful processes [240]. Microglia phenotype can be identified by upregulation of specific markers, such as cell surface receptor markers expression and soluble factors with recognized functions [241]. The mechanism underlying neuroglia polarity and morphology is not yet understood, but probably is an adaptive response to necessities of the cells [242]. In this study we investigated whether the inflammatory $A\beta_{25-35}$ challenge on microglia cells might be prevented by FAAH inhibition. To validate our experimental setting, we determine the efficacy of URB597 and the influence of $A\beta_{25-35}$ on FAAH activity. As also reported by Giacovazzo et al. (2019), URB597 was able to inhibit FAAH activity, whereas no effect was observed by $A\beta_{25-35}$ [97,243]. Moreover, we verified microglia activation driven by $A\beta_{25-35}$, valuating the enrichment of Iba1 marker. Established these parameters, the first observation concerns the cell morphology, that revealed a change after $A\beta_{25-35}$ stimulation from the resting ramified form to an amoeboid shape, with an enlarged cell body with very few extensions. This shape, typical of activated

cells towards a pro-inflammatory state M1, favored cell migration. On the contrary URB597, affecting rearrangement of microglia morphology in BV-2 cells challenged with $A\beta_{25–35}$, significantly decreased $A\beta_{25–35}$ induced migration. The ability of eCB to influence cytoskeleton plasticity might be due to an activation of CB2 receptor. Therefore, previous paper reported that JWH015 (a CBR2 agonist) significantly reduces the migration of LPS-stimulated primary microglia via mitogen-activated protein kinase-phosphatase associated to a TNF-α reduction [107]. In addition, the stimulation of CB2 receptors inhibits M1 microglia activation and promotes a neuroprotective phenotype [178]. Moreover, our data indicate that URB597 also modulates microglia phagocytosis, inducing an increased phagocytic capacity of BV-2 cells. Since URB597 inhibits FAAH that drives eCB catabolism, its administration to the cells makes available greater amounts of eCB, including 2-arachidonoylglycerol (2-AG), stimulating phagocytosis by binding to CB2 receptors, as previously described [244]. The asymmetrical organization of cytoskeleton is important for cell migration. Migrating cell is generated from extension of a lamellipodium in the direction of migration in association with new cell adhesions. Cell contractility is required to allow the body extending front [245]. All the effects depicted so far, i.e. cell shape remodeling, migration reduction and stimulation of phagocytosis, are known to depend on the rearrangements of cytoskeletal proteins.

Considering that, we evaluated the activity of Rho family small GTPases, including Rho and Cdc42 that regulate both actin cytoskeletal organization, migratory capacity and phagocytosis [246]. Rho promotes the accumulation of detyrosinated microtubules, Rac inactivates the microtubule destabilizing protein and Cdc42 regulate the orientation of the microtubule organizing centre (MTOC) [247]. RhoA, Cdc42 and Rac1 were suggested to be

involved in AD since they mediate superoxide production in microglia stimulated by Aβ [248]. Cdc42 GTPase and other Rho-type GTPases regulate the signal transduction pathways that control the generation and maintenance of cell polarity [249]. RhoA is important not only in actomyosin contractility at the cell tail, but even in the regulation of actin cytoskeleton at the leading edge by interaction with Rac1, with a mutual antagonism [250-252]. A decrease in RhoA activity fails to trigger proper actomyosin contractility inhibiting tail retraction and cellular translocation [245,253]. Our results showed an increase of Rho activity in $A\beta_{25-35}$ treated BV-2 cells favouring migration. These data are in agreement with several research works reported in the comprehensive review of Aguilar (2017). Indeed, PC12 cells treated with $A\beta_{1-42,}$ showed an increase of activated RhoA and a reduction of cell survival through inhibition of protein tyrosine phosphatase 1B (PTP1B) [254]. An increase of activated RhoA is also observed in $A\beta_{1-40}$ treated SHSY5Y cells associated to a decrease of neuronal growth [255]. The stabilization of directional movement (chemotaxis) requires input from external cues, and this is controlled by Cdc42. When Cdc42 is inhibited, the macrophage reverts to a random walk, whereas inhibition of Rac blocks all cell movement. Cdc42 directs and stabilizes Rac activity at the cell front [256]. URB597 reducing Rho activation, decreased BV-2 cells migration capacity driven by $A\beta_{25-35}$ challenge. This behaviour is confirmed by works of Kaplan (2017) and Diaz-Alonso et al. (2017), in which they showed that cannabidiol treatment reduced RhoA trough CB1 in mice brain, and that an increase of RhoA protein is related to CB1 loss in newborn pyramidal neurons, thereby disrupting the morphology of migrating cells [257,258]. The assembly and disassembly of peripheral actin filaments promote localized changes in the structure of the plasma membrane and phagocytosis [242]. Our data showed that an increase of Cdc42 activity

induced by URB597, is closely related to an enhancement of BV2 cells performing phagocytosis. Our data are in accordance with Kurihara et al. (2006) studies where they observed an increase of activated Cdc42 in neutrophil-like HL60 cells in response to CBR2 agonist JWH015 [259]. In their recent review Kelly et al. (2020) pointed out the relationship between endocannabinoids and the polarization state of microglia and how binding to cannabinoid receptors can modulate the inflammatory profile of these cells [31,260]. This ability is extremely important as the role of microglia is central in the determinism of chronic inflammation that might severely damage brain tissue and nowadays seems to be the main mechanism responsible for neuronal damage observed in AD. It is also known that low-grade chronic inflammation in absence of infection takes place in aging and it is characterized by an increased level of proinflammatory cytokines and a decreased secretion of anti-inflammatory cytokines [261]. In AD post-mortem brains, microglial activation was correlated with disease progression [262]. LPS or IFN-γ induce the M1 phenotype, which is identified by increase of iNOS expression, while the M2 phenotype is induced by the immunosuppressive cytokines, TGF-β and IL-10 [263]. Different studies have demonstrated the presence of CB1 and CB2 receptors on immune cells [264] and that eCB are able to reduce the binding NF-kB, the cell proliferation of regulatory T cells and the induction of apoptosis in these cells [265,266]. CB2 receptor activation is important for the up-regulation of Arg-1 in the M2 state, and for the phagocytic function of microglia [267]. Mecha et al (2015) demonstrated that in rat and human microglia, a stimulation with 2-AG and AEA induce an increase of Arg-1, enhancing a M2 phenotype [268]. Moreover, an LPS stimulation, that represent a pro-inflammatory stimulus associated to a M1 phenotype, showed a down regulation of the CB1, CB2, NAPE-PLD, FAAH and MAGL transcripts [268].

Therefore, the setup of treatments capable of counteracting inflammatory processes could resolve or at least delay the progression of AD. Our findings confirm that larger amounts of eCB in the microenvironment, such that induced by the addition of URB597, interfere with cytokine production. IL-1β and TNF-α were already significantly reduced after the first hour of the stimulus, IL-10 increased in the same time interval, while TGF-β increased after 24 h, according to the known cytokine kinetics. Previous reports showed that the production of TNF-α by microglia challenged with Aβ fibrillar could be inhibited by the addition of CB2 receptor agonists, reinforcing the anti-inflammatory role of the receptor [169,269]. On the other hand, ECS has been shown to activate anti-inflammatory signaling pathways that modulate immune cell functions [270]. Our results confirm this property since treatment with URB597 and consequent increase in eCB demonstrated a polarization towards the M2 phenotype of BV-2 cells with an increased release of the anti-inflammatory cytokines IL-10 and TGF-β. It was previously outlined that enhancement of eCB via inhibition of FAAH reduced iNOS in microglial cells and produced an anti-inflammatory effect after exposure to stress [271]. In addition, treatment with PF-3845, an irreversible FAAH inhibitor, down-regulated the expression of iNOS and COX-2 after traumatic brain injury [272]. In an experimental model looking at the machinery underlying neurodegeneration following ethanol exposure URB597 (0.3 mg/kg) administered for five days reduced mRNA levels of Iba-1, TNF-α, IL-6 and the monocyte chemoattractant protein-1 (MCP-1/CCL2), as well as iNOS in hippocampus microglial cells [273]. BV-2 cells incubated with $A\beta_{25-35}$ showed an increase of iNOS expression, reducing at the same time Arg-1. URB597 had an opposite trend, demonstrating the ability to counteract the pro-inflammatory

microglia phenotype induced by $A\beta_{25-35}$. The data are in agreement with Tham et al. (2007), that reported how in the LPS treatment of primary microglia cultures and BV-2 cells, URB597 might reduce the expression of iNOS [274]. Moreover, Su et al. (2017) observed a reduction in the iNOS marker after treatment with URB597 in chronic cerebral hypoperfusion mouse models (CCH) [94].

The overall data suggest that an increase of AEA, due to FAAH inhibition, induces cytoskeleton reorganization, regulates phagocytosis and cell migration processes, promoting the microglia polarization towards anti-inflammatory M2 phenotype. Therefore, URB597 might represent a promising therapeutic target in neurodegenerative disorders.

6. PROJECT II

Results

To study the cross-talk between human microglia and astrocytes cells derived from iPSC in a co-culture system to characterize the inflammatory processes. These experiments were performed at the University of Konstanz (Germany) in Marcel Leist's laboratory.

6.1. mRNA expression of microglia and astrocytes markers after stimulation with LPS and cytokines

To characterise the human cell lines used in our experiments, and to confirm their activation after pro-inflammatory stimuli, we performed qPCR on specific microglia and astrocyte markers (Fig. 28 and 29). We treated human microglia and human astrocytes with 10 ng/ml TNF-α, 100 ng/ml LPS and a complete cytokine mix (CCM) containing 10 ng/ml TNF-α, 10 ng/ml IL-1β, and 20 ng/ml IFN-γ at different time point, as characterized earlier [275,276]. The neuroglial markers represent an identity card of neuroglia both in resting and activated state.

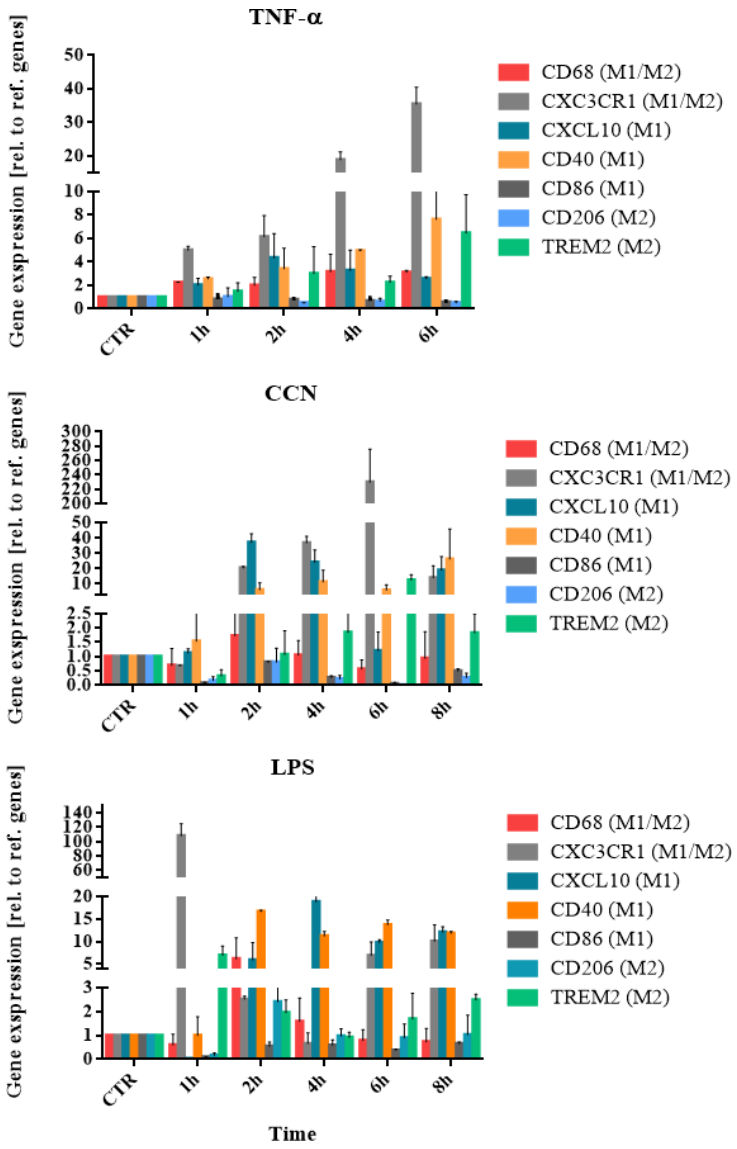

Figure 28: mRNA expression on different markers of human microglia treated with 10 ng/ml TNF-α, 100 ng/ml LPS and CCM (10 ng/ml TNF-α, 10 ng/ml IL-1β, and 20 ng/ml IFN-γ). The expression was monitored by RT-PCR and normalized to PGK and RPL13A rDNA primers. Expression profiles were determined using the 2−ΔΔCT method. Statistical analysis was performed using ANOVA analysis by Tukey's test.

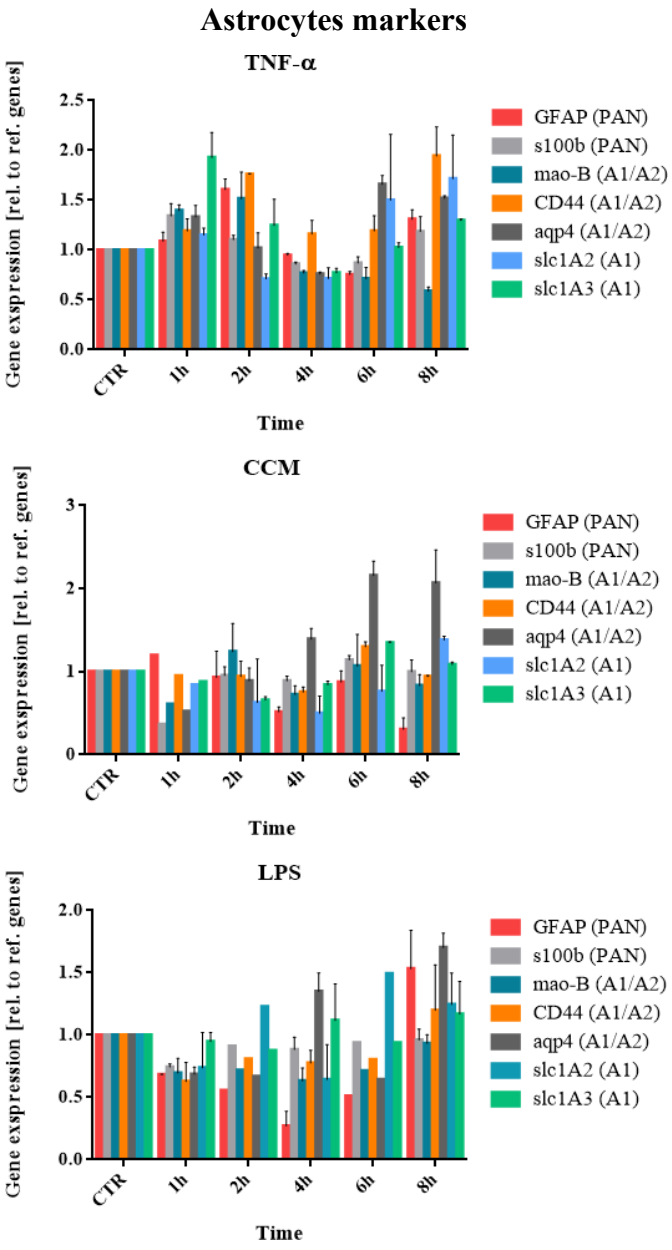

Figure 29: mRNA expression on different markers of astrocytes treated with 10 ng/ml TNF-α, 100 ng/ml LPS and CCM (10 ng/ml TNF-α, 10 ng/ml IL-1β, and 20 ng/ml IFN-γ). The expression was monitored by RT-PCR and normalized to PGK and RPL13A rDNA primers. Expression profiles were determined using the $2^{-\Delta\Delta CT}$ method. Statistical analysis was performed using ANOVA analysis by Tukey's test.

6.2. Cytokines modulations after LPS and cytokines treatment in human neuroglial cells.

To gain insight into inflammatory process modulation after treatments mentioned above, mRNA expression of pro-inflammatory cytokines was assessed on each mono-culture cell line at different time points. We analysed mRNA levels after treatment with 10 ng/ml TNF-α, 100 ng/ml LPS and a complete cytokine mix (CCM) containing 10 ng/ml TNF-α, 10 ng/ml IL-1β, and 20 ng/ml IFN-γ, as characterized earlier [275,276]. IL-10 and GFAP were used as cell line markers. The data revealed a strong cell response with the secretion of different cytokines. IL-8 and IL-6 gene expression was prominent between 1 and 2 h in presence of cytokines stimulations in both cell lines. In particular, an increase of IL-8 expression more that IL-6 was observed in astrocyte cells, whereas LPS stimulation had no effect, as reported in literature [277]. On the other hand, microglia were very responsive to LPS treatment, showing a marked increase of IL-8 and IL-6 gene expressions at all time points (Fig. 30).

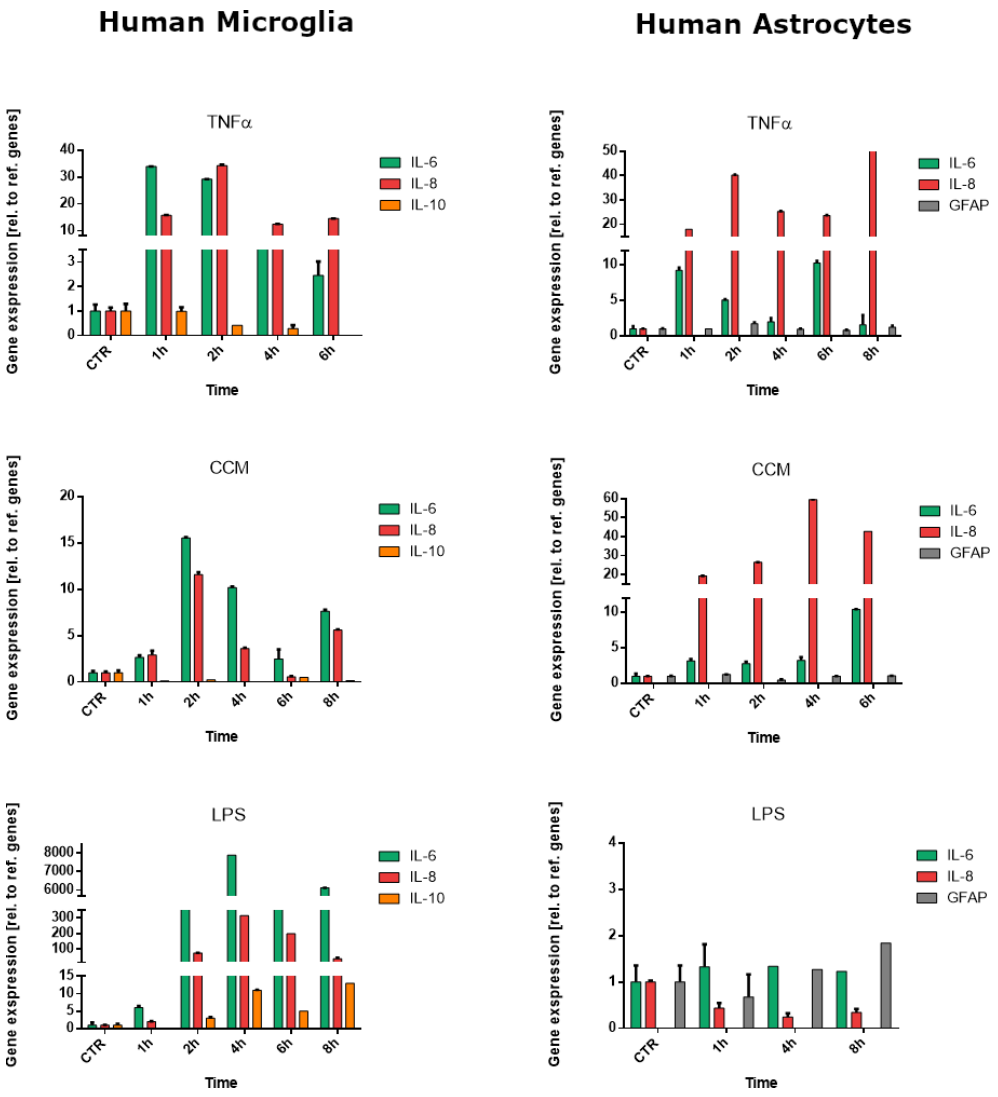

Figure 30: mRNA expression of IL-6, IL-8, IL-10, GFAP in human microglia and human astrocytes treated with 10 ng/ml TNF-α, 100 ng/ml LPS and CCM (10 ng/ml TNF-α, 10 ng/ml IL-1β, and 20 ng/ml IFN-γ) at different time points. The expression was monitored by RT-PCR and normalized to PGK and RPL13A rDNA primers. Expression profiles were determined using the 2−ΔΔCT method. Statistical analysis was performed using ANOVA analysis by Tukey's test.

6.3. NF-kB translocation after TNF-α treatment in human neuroglial stem cells.

To test the inflammatory cross-talk between microglia and astrocytes, we evaluated the translocation of the transcription factor NF-kB from the cytoplasm to the nucleus. Different important inflammatory pathways are correlated to NF-kB translocation that is a good indicator of downstream cellular responses [278,279]. The mono and co-culture cells were treated with 10 ng/ml TNF-α and 100ng/ml LPS for 1 h and 24 h. The staining analysis was performed also with the CM derived from human microglia treated for 24 h with 10 ng/ml TNF-α and 100ng/ml LPS. NF-kB staining in astrocytes showed that in a quiescent condition, most NF-kB is cytoplasmatic. After TNF-α stimulation was observed the translocation of the transcription factor into the nucleus already at 1h after stimulation. After 24 h of treatment NF-kB was founded in the cytosol. We obtained the same results after treatment with CM from human microglia both in astrocyte monoculture and in co-culture with microglia. LPS does not have any effect on the astrocytes activation, as reported in literature [277] (Fig. 31/S. 1).

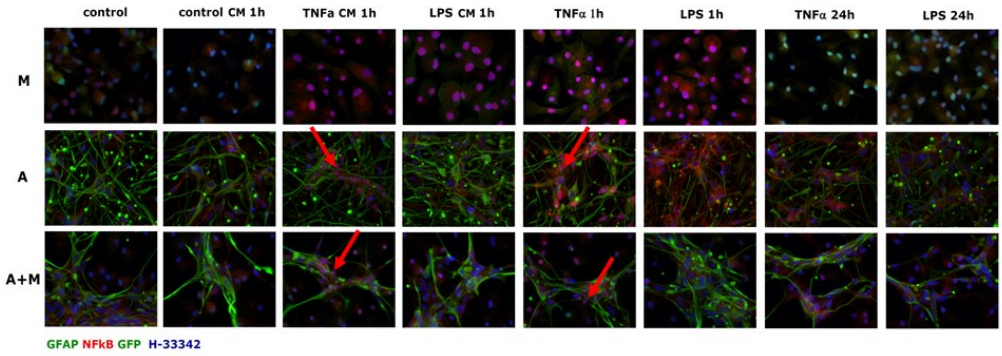

Figure 31/S 1: NF-kB nuclear translocation in activated human astrocytes. Cells were treated for 1 h and 24 h with 10 ng/mL TNF-α, 100ng/mL LPS and with CM from human microglia treated for 24 h with the same concentration of TNF-α and LPS. The cells were analysed by immunocytochemistry after 1 h and 24 h of treatment.

DISCUSSION

Several studies indicate that inflammatory processes and disturbed neuron-microglia interactions may mediate the pathogenesis of numerous neurodegenerative diseases. The causes that lead to neurodegeneration are heterogeneous, often associated with the formation and accumulation of aggregated proteins that trigger a chronic inflammatory process [280]. One of the main neuroinflammatory processes is represented by the pathogenesis of AD, in which the primary response to the amyloid β peptide (Aβ) accumulation is the production of pro-inflammatory cytokines, ILs and TNF-α, that activate glycogen synthase kinase 3 β (GSk3β) signalling pathway with the downstream activation of NF-kB [281]. During an inflammatory process, the interaction between the single cell populations in a neuroglial system, influences the cell response. At the same time microglia has a pivotal role in the cytokines secretion associated to the M1 and M2 phenotype [191,195]. Henn et al. (2011) reported that TNF-α, IL-1β and CM from activated BV-2 cells, could sensitize primary cortical astrocytes from mice and induce a TLR2 upregulation, with a consequent NF-kB translocation from cytosol to nucleus [282]. In this project we studied the cross-talk between human microglia and astrocyte cells in a co-culture system to characterize the response of a neuroglial system to inflammatory processes. To purpose we activated human astrocytes and human microglia cells with TNF-α, IL-1β and IFN-γ determining a strong cell response with the secretion of different cytokines such as IL-6 and IL-8. This data confirms what was reported by Norden et al. (2016) in microglia and astrocytes isolated from mice models [283], in which they observed an increase of pro-inflammatory cytokines, such as IL-6, IL-1β and TNF−α, in microglia at 2-4 h after LPS, while astrocytes showed a

TNF-α and TGF-β genes modulation only after 12h of treatment. Many studies indicated that activated NF-κB signal played an important role in inflammatory response cascades, triggering transcription of target genes and promoting pro-inflammatory cytokines release [284,285]. Activated microglia have a crucial role in the A1 astrocytic activation and this synergic activation was observed in the prefrontal cortex of AD patients [286,287]. Considering that, we tested whether astrocytes activation was carried out by TNFα or by the conditioned medium (CM) of activated microglia cells, analysing NF-kB nuclearization as a marker. Both TNF-α, and microglia CM induced the translocation of NF-kB from cytosol to nucleus suggesting astrocytes activation. Our data are in agreement with Liddelow et al. (2017), that demonstrated how activated microglia might induce A1 astrocytes by secreting IL-1α, TNFα, and C1q. In microglia cells the increase of pro-inflammatory cytokines, such as TNF-α, IL-1β and IL-6 is also correlated with a TLR4 and NF-kB activation, and in turn with the astrocytes activation [288,289]. Our data evidence the synergic cross-talk between microglia and astrocytes in the inflammatory processes.

7. PROJECT III

Results

To study the protective effect of the co-culture system of human astrocyte stem cells and murine microglia against proteotoxic stress induced in LUHMES neurons and to analyse the potential neuroprotective effect of URB597 against proteasome dysfunction. These experiments were performed at the University of Konstanz (Germany) in the Marcel Leist's laboratory.

Previous studies carried out in the laboratory of Prof. Marcel Leist at the University of Konstanz, using co-culture with neuronal LUHMES cells, human astrocytes and human microglia confirmed the protective effect of human neuroglial cells on LUHMES cells undergone to proteotoxic stress (unpublished data).

In this project we evaluated whether murine microglia responded to the proteotoxic insult similarly to the human one and if therefore there were any differences to be attributed to species models. Considering that, we performed the same experiments generating a co-culture with LUHMES cells, human astrocytes and BV-2 murine microglia cells treated with MG-132, a proteasome inhibitor. We also testing the potential protective effect of the FAAH inhibitor, URB597.

The ubiquitin proteasome system (UPS), a key regulator of protein catabolism in the mammalian nucleus and cytosol, is essential for the regulation of almost all vital processes including, organelles biogenesis, cell cycle, differentiation and development, immune response and inflammation, neural and muscular degeneration, as well as response to stress and extracellular modulators [290].

Inhibition of the UPS results in the accumulation of aggregated proteins and it leads to amino acid shortage [291]. As a result of proteasomal stress the integrated stress response (IRS) is being induced and causes the phosphorylation of the translation initiation factor subunit elF2α, which in turn activates the activating transcription factor 4 (ATF4), involved in the pro-apoptotic pathways. To study the effects of the proteasome impairments *in vitro*, one of the most efficient compounds is MG-132 (carbobenzoxyl-L-leucyl-L-leucyl-L-leucine) (Fig. 32). It is a natural triterpene proteasome inhibitor derived from a Chinese medicinal plant able to suppress the growth of human prostate cancer in nude mice [292,293]. MG-132 is a peptide aldehyde with an aldehyde residue as a pharmacophore acting on the catalytic threonine of the proteasome. Peptide aldehydes are inhibitors of the serine and cysteine proteases. This compound is very selective at low concentrations and therefore favourable to use. It leads to a reduced clearance of proteins by the impaired UPS and therefore to accumulations of poly-ubiquitinated proteins in the cytoplasm [294]. In dopaminergic N27 cells this compound was shown to induce cell death through an apoptotic cascade [295].

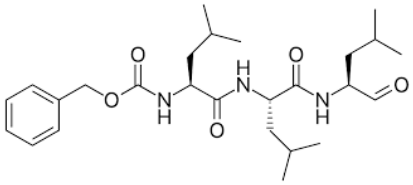

Figure 32: MG-132 structure

7.1. URB597 does not exhibit cytotoxic effects in LUHMES cells

In order to evaluate the possible URB597 cytotoxicity on LUHMES cells and to define the optimal concentration, cell viability experiments by resazurin assay and LDH assay were performed. The results showed that URB597, used at concentrations up to 25 μM, did not exert negative effects on cell viability. Therefore, according to the literature data and the previous experiments on BV-2 cells, we decided to use a concentration of URB597 of 5 μM (Fig. 33).

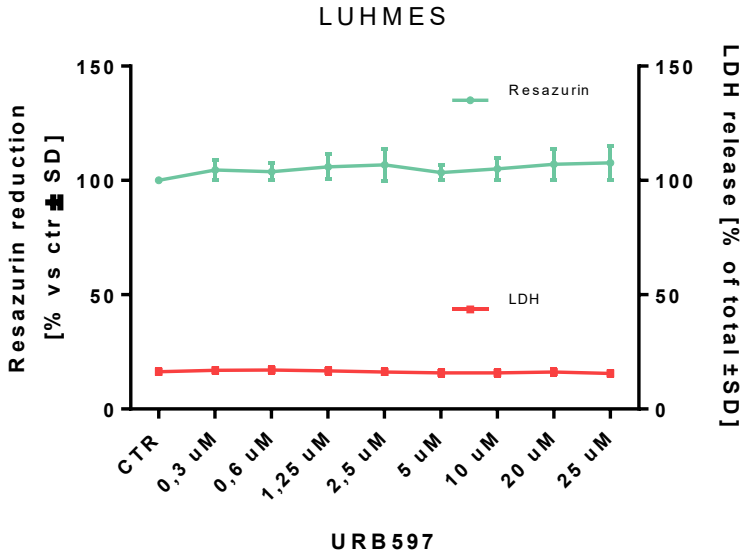

Figure 33: Resazurin and LDH assay on LUHMES cells treated in a range of concentration between 0,3 μM and 25 μM for 24 h. The data are reported as mean optical density ± SD of three independent experiments. Statistical significance was determined using ANOVA analysis by Tukey's test.

7.2. Protection of LUHMES against proteasome inhibition by neuroglial cells and endocannabinoid inhibitors.

To evaluate the response of LUHMES neuron cells to MG-132 exposure in mono- and co-culture with human astrocytes and murine microglia, we performed cell viability assays. LUHMES cells were treated on day 6 with or without MG-132 in a range of 25 nM and 200 nM in mono-culture, or together with BV-2 or astrocytes, or both cell lines (see Materials and Methods) (Fig. 34).

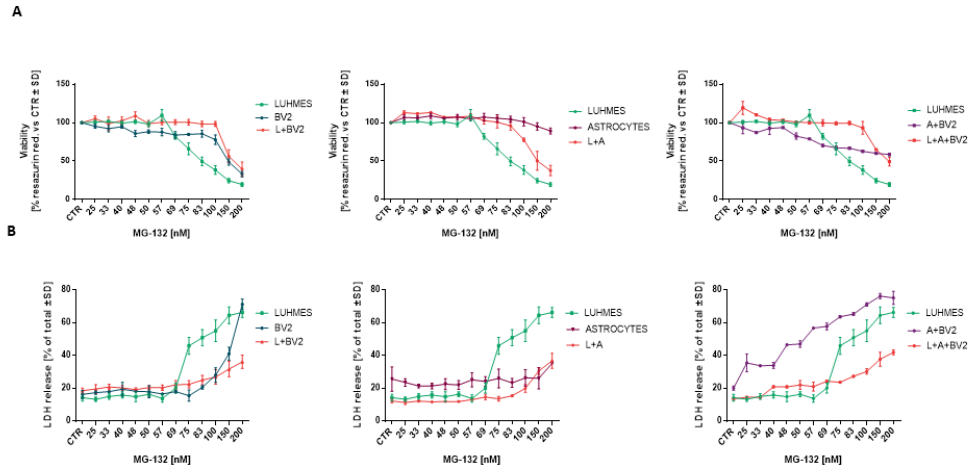

Figure 34: Cell viability analyses. Co-culture were treated on d6 with or without MG-132 in a range of 25 nM and 200 nM. After 24 h the cells were analysed by resazurin assay (A), LDH assay (B). Data were reported as percentage normalized to the untreated cells (CTR). Data were reported as mean ± SD of at least three independent experiments. Statistical significance was determined using ANOVA analysis by Tukey's test.

Cell viability tested by resazurin and LDH assays showed that LUHMES are very sensitive to cell death triggered by MG-132 (Fig. 34 A, B). We observed a decrease of LUHMES cell viability at MG-132 around 60-75 nM. BV-2 and

astrocytes alone or in combination were able to counteract LUHMES death up to 200 nM MG-132.

7.3. Co-culture effect on ATF4 proteins levels in presence of a proteasome impairment

ATF4 controls the expression of genes that are involved in amino acid import and synthesis of amino acids as well as in the expression of pro-apoptotic genes. We performed a western blot analysis at 24 h to evaluate ATF4 protein levels in LUHMES treated with a 25 nM and 200 nM MG-132 range in mono-and co-culture (Fig. 35). The results showed that ATF4 responses is attenuated in co-culture compared to LUHMES mono-culture.

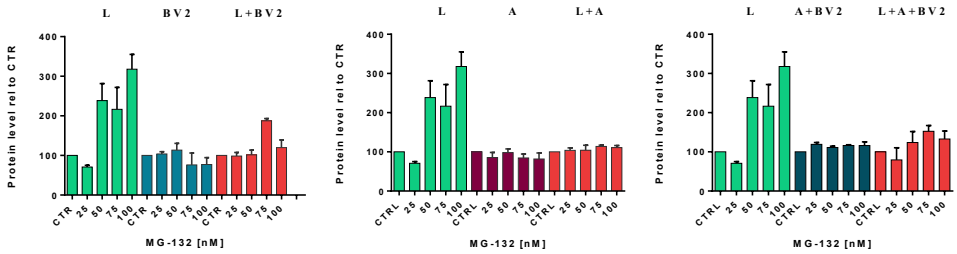

Figure 35: Expression levels of ATF4 protein analysed by western blot analysis. Overview to display the changes of ATF4 in cell cultures (as described in Results) with different concentrations of MG-132 treatment (25 nM, 50 nM, 75 nM, 100 nM). The results were normalized on the GAPDH, reported as a percentage, normalizing on the untreated cells (CTR). Data are expressed as the mean ± SD of three independent experiments. Statistical significance was determined using ANOVA analysis by Tukey's test.

We also evaluated a possible protective effect of URB597 in LUHMES cells in the presence of MG-132. LUHMES cells were pre-treated with 5µM URB597 for 1h and then we added MG-132 at two different concentrations, 25nM and 50nM (Fig. 36).

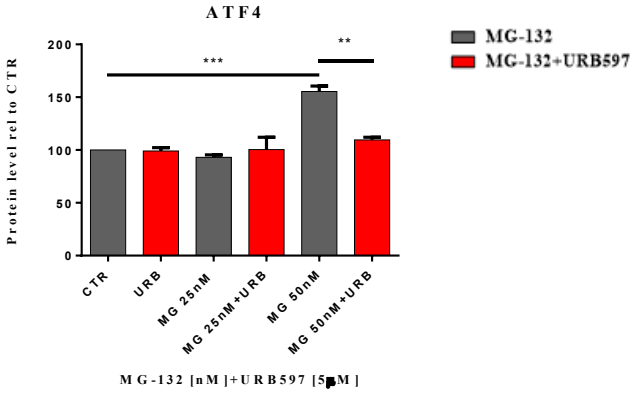

Figure 36: Expression levels of ATF4 protein levels analysed by western blot analysis. LUHMES cells were pre-treated with 5 µM URB597 for 1h and then we added to the medium MG-132 at two different concentrations, 25 nM and 50 nM. The results were normalized on the GAPDH, reported as a percentage, normalizing on the control (CTR). Data are expressed as the mean ± SD of three independent experiments.** P< 0,01 50nM MG-132 *vs* 50 nM MG-132+URB597, *** p ≤ 0.001 CTR vs 50nM MG-132.

The results showed a decrease of ATF4 protein levels in LUHMES combined treatment with respect to sample treated only with 50 nM MG-132.

7.4. GSH levels modulation in LUHMES cells in presence of proteotoxic stress and the neuroglial role

Since the proteasome impairment induces oxidative stress, we decided to evaluate the levels of GSH, for its antioxidant role.

LUHMES cells were treated on day 6 with or without MG-132 in a range of 25 nM and 200 nM in mono- and co-culture. LUHMES mono-culture showed a GSH peak between 57 nM and 69 nM MG-132, that is decreased in co-culture system (Fig. 37).

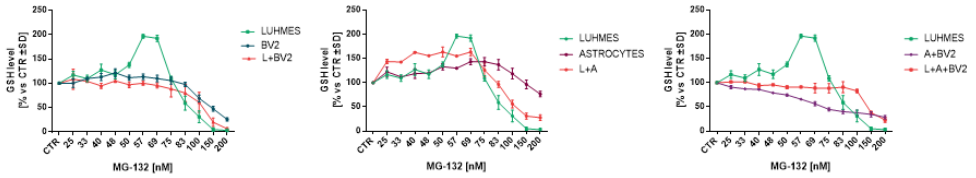

Figure 37: GSH analyses. Co-culture were treated on d6 with or without MG-132 in a range of 25 nM and 200 nM. After 24 h the cells were analysed. Data were reported as percentage normalized to the untreated cells (CTR). Data were reported as mean ± SD of at least three independent experiments. Statistical significance was determined using ANOVA analysis by Tukey's test.

7.5. Modulation of the GSH level triggered by URB597 on LUHMES cells treated with MG-132.

To characterize the potential neuroprotective effect of URB597, different cell viability assays were assessed. LUHMES cells were pre-treated on day 6 for 1 h with URB597 with or without MG-132 in a range of 25 nM and 200 nM in mono- and co-culture. No more change in the resazurin and LDH assay were observed (Data no shown). On the contrary, GSH analysis showed that URB597 is able to shift the GSH peak at 25-50 nM MG-132 in LUHMES mono-culture. Furthermore, we observed a constant maintenance of the GSH level even at 200 nM MG-132 in BV-2+LUHMES combination (Fig. 38).

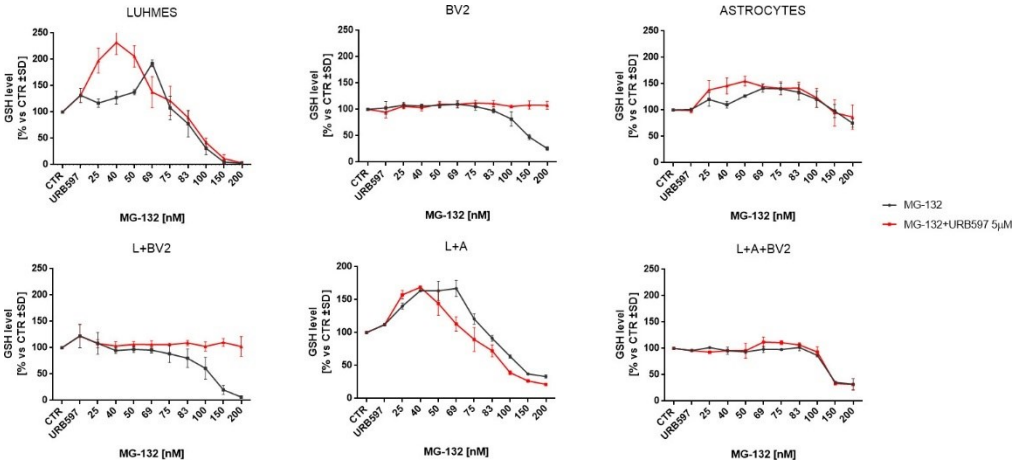

Figure 38: GSH analyses. Co-culture were pre-treated on d6 with 5µM URB597 for 1 h and then with MG-132 in a range of concentration between 25 nM and 200 nM. After 24 h the cells were analysed by GSH assay. Data were reported as percentage normalized to the untreated cells (CTR). Data were reported as mean ± SD of at least three independent experiments. Statistical significance was determined using ANOVA analysis by Tukey's test.

7.6. Modulation of mRNA levels of enzymes involve in the GSH metabolism

To investigate the relationship between the ECS and the modulation of GSH levels we analysed enzymes involved in glutathione metabolism as glutathione synthetase (GSS) and glutathione reductase (GSR). LUHMES cells treated with 25 nM and 50 nM MG-132 in presence or absence of 5 µM URB597 were analysed at 8 h and 24 h by qPCR analyses. These two concentrations overlap the GSH peak range observed above. Fig. 39 showed at 8 h and 24 h an increase of GSR gene expression in the sample treated with MG-132 alone or in presence of URB597 compared to control. A GSS gene expression was not affect by any treatment at 8 h. On the contrary, at 24 h GSS gene expression is down regulated in 25 nM MG-132 sample treated with

URB597 compared to the 25 nM MG-132 alone and to untreated cell samples, respectively (Fig. 39).

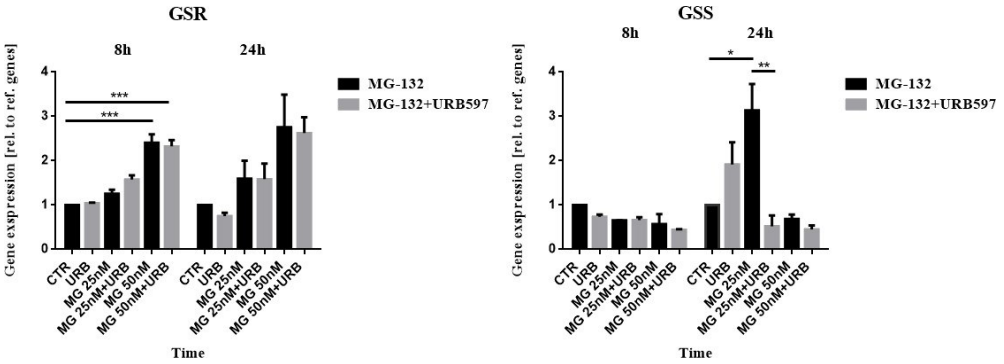

Figure 39: mRNA expression of GSS and GSR enzymes in LUHMES cells pre-treated with 5μM URB597 for 1h and after with MG-132 at 25nM and 50nM. The analyses were performed at 8 h and 24 h. The expression was monitored by RT-PCR and normalized to β-actin primer. Expression profiles were determined using the 2−ΔΔCT method. Statistical significance was determined using ANOVA analysis by Tukey's test.* *P< 0,05,* ** P< 0,01, *** p ≤ 0.001.

7.7. URB597 influences NRF2 LUHMES cells in presence of proteasome impairment

Modulation of GSH levels in LUHMES cells mono-culture in presence of URB597 compound suggests an important role of eCB in GSH biosynthesis. Since GSH production pathway is regulated by NRF2, we investigated NRF2 protein levels in LUHMES cells treated as above described. We observed at 8 h an increase of NRF2 protein level, concentration-dependent, in all samples examined with respect to untreated cells. At 24 h, an increase of NRF2 was detected in the sample treated with both 25 nM MG-132

and URB597, compared to the sample with only 25 nM MG-132. On the contrary NRF2 decrease was determined in the sample treated with both 50 nM MG-132 and 5 μM URB597, compared to 50 nM MG-132 sample (Fig. 40).

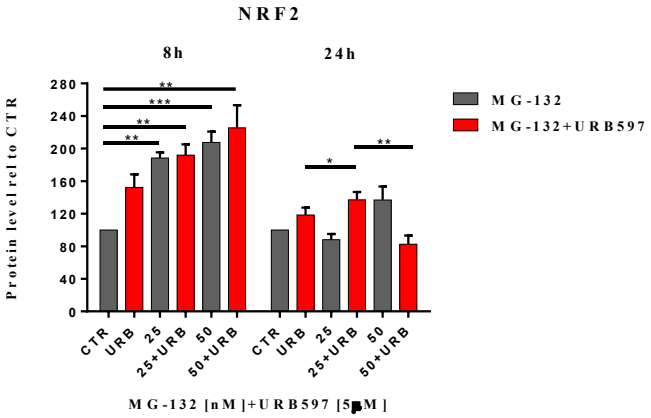

Figure 40: Expression levels of NRF2 protein levels analysed by western blot analysis. LUHMES cells were treated with 5μM URB597 for 1 h and then we added to the medium MG-132 at two different concentrations, 25nM and 50nM. The results were normalized on the GAPDH, reported as a percentage, normalizing on the untreated cells (CTR). Data are expressed as the mean ± SD of three independent experiments. Statistical significance was determined using ANOVA analysis by Tukey's test. * $P < 0,05$, ** $P< 0,01$

DISCUSSION

In many neurodegenerative diseases was observed an accumulation of proteinaceous deposits in different parts of the brain [296]. α-Synuclein, Aß and mutated huntingtin apparently share a three-dimensional structure that is able to bind and inhibit the proteasome [297]. Moreover, tau proteins directly bind and inhibit the activity of 26S proteasome in mice with tauopathy [298]. Nuclear factor κB (NF-κB), involved in the inflammatory processes, cell differentiation and cell death, can also be induced by a proteasomal inhibition [299]. In the Parkinson's disease (PD) the aggregation of proteins such as α-synuclein leads oxidative stress and mitochondrial dysfunction correlated to an alteration of the ubiquitin proteasome system (UPS) [300,301]. The proteasome is closely related to the degradation of these proteins, therefore a reduction in the proteasome activity causes adverse effects such as synaptic loss and neurons death [302]. Accumulation of poly-ubiquitinated proteins caused by a proteasome disfunction is implicated in the development of inflammatory processes that result in hemorrhagic shock, atherosclerosis and neurodegenerative disease [303-305]. The focus of this project is to characterize the neuroglial neuroprotection in presence of proteasomal impairments, evaluating whether ECS is involved in the modulation of proteotoxic stress. There are not many reports on the relationship between eCBs and proteasome Treatments with CB1 receptor agonist WIN 55.212.2 are associated with inhibition of NF-kB activity and cell death [306]. Jeon P. et al. (2011) demonstrate that WIN55.212.2 inhibits PC12 dopaminergic neuronal cell apoptosis due to proteasomal inhibition as well as NF-kB activation [307].We demonstrate that LUHMES neurons are quite susceptible to proteotoxic stress when proteasome activity was inhibited with MG-132. When human astrocytes and BV2 cells were co-cultured with LUHMES they were able to protect from

the proteotoxic stress insult. These results are in agreement with those of Gutbier et al. (2018) that reported how astrocytes generated from mouse embryonic stem cells (mAGES cells) might reduce the neuronal stress response and neurodegeneration through GSH release [308]. Tarassishin et al. (2014) showed as in human astrocytes, IL-1 induced both A1 and A2 responses, while LPS induced neither. The contrary effects were observed in mouse astrocytes, demonstrating a different interspecies response [277].Our results also underline that interspecies co-cultures as human and murine cells, are capable to exert the same protective effect against proteotoxic stress. Proteasome inhibition and persistent stress conditions activate ATF4 that promotes the induction of apoptosis [309,310]. As shown by densitometric analyses we observed a significant increase of ATF4 protein levels in LUHMES cells treated with MG-132, while ATF4 responses was attenuated in co-culture with BV2 and human astrocytes. URB597 markedly decreased the protein levels in LUHMES neurons, suggesting its involvement in countering proteasome impairment and in the apoptotic cascade. The protective effects exert by a co-culture system could be due to the release of Glutathione, as well known antioxidant molecule from neuroglial cells, thereby rescuing neurons. The proteotoxic stress response of the LUHMES might be strongly dependent on the intracellular GSH/cysteine levels. Our data showed that LUHMES mono-culture rapidly respond to proteasome induced damage with an increase of the GSH peak, that decreases in presence of BV-2 and astrocytes cells. These results are in agreement with Wang et al (2000), which reported that neurons cannot release a good amount of thiols by themselves but instead rely on astrocytes, which could deliver cysteine and/or glutathione to neurons [311]. Given these evidences, we investigate the effect of eCB on GSH release in neurons mono- and co-cultures with murine microglia and human

astrocytes treated with the proteasome inhibitor. URB597 led to an earlier increase in neuronal GSH levels that might be due to the capability of FAAH inhibitor to modulate GSS enzyme expression opening a new scenario on endocannabinoid signalling pathways. Moreover, when BV-2 cells were incubated with LUHMES in presence of FAAH inhibitor, there was a paralleled increased survival after MG-132 exposure. Altered ubiquitin-proteasome system and reduced proteasome activity are associated with oxidative stress. Eheren et al. (2013) demonstrated a correlation between ATF4 and Nrf2. In mouse hippocampal HT22 cells they observed that the induction of both ATF4 and Nrf2 is key to maintaining GSH levels under oxidative stress conditions. Accumulating evidence suggests that an age-related decline in cellular glutathione (GSH) levels may be due to a decrease of NRF2 activation [312]. Under unstressed conditions, NRF2 is bound to Keap1, and is constantly ubiquitylated and degraded by the proteasome. In response to stress, Keap1 is inactivated, resulting in NRF2 stabilization [313,314]. We analysed the NRF2 protein levels in LUHMES treated with URB597 under proteasome disfunction. We observed a decrease of NRF2 protein levels, in agreement with Biernacki et al. (2020), the authors that reported how in rats with primary hypertension, URB597 is able to increase the levels of Keap1, promoting the ubiquitination of NRF2 and in turn leading to NFR2 degradation [315]. Moreover, NFR2 protein profile levels might be correlated to that obtained from GSH, as above described, confirming URB597 in the proteotoxic stress involvement. The overall data provide a first indication of the eCB contribution in the anti-oxidant process mediate by neuroglial cells.

CONCLUSIONS

This project highlights how eCBs prevent brain inflammation through neuroglia cytoskeleton rearrangement, phagocytosis and cell migration processes and promoting the microglia polarization towards anti-inflammatory M2 phenotype.

Neuroglial co-culture system represents an excellent model to reproduce physiological environment confirming how neuroglial cells represent the first brain defense playing a pivotal role in the neuron protection. Moreover, neuroglia is able to prevent proteotoxic insult and ECS contributes to recovery of proteasome impairment through the modulation of GSH metabolism.

SUPPLEMENTARY DATA

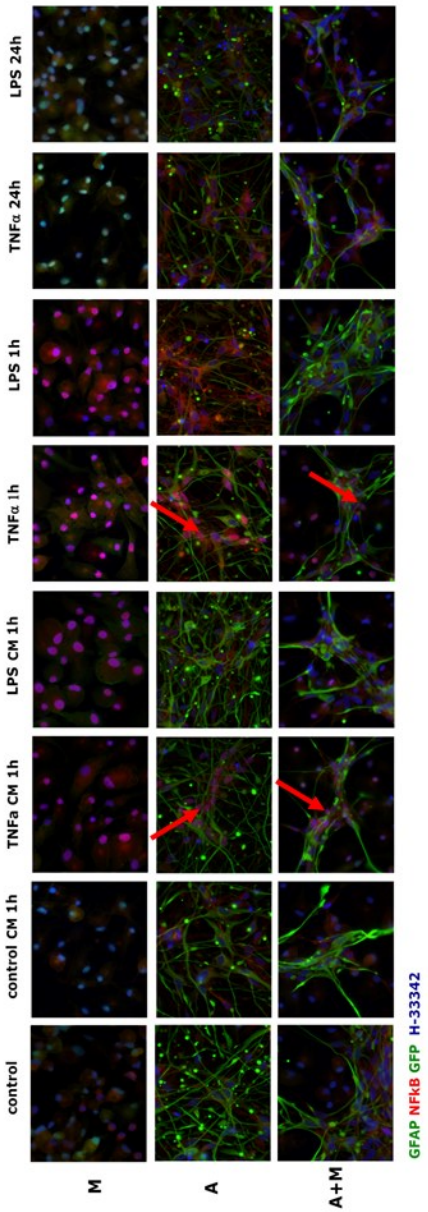

Figure 31/S 1: NF-kB nuclear translocation in activated human astrocytes. Cells were treated for 1 h and 24 h with 10 ng/mL TNF-α and with CM from human microglia treated for 24 h with the same concentration of TNF-α. The cells were analysed by immunocytochemistry after 1 h and 24 h of treatment.

REFERENCES

1. Kaur, D.; Sharma, V.; Deshmukh, R. Activation of microglia and astrocytes: a roadway to neuroinflammation and Alzheimer's disease. *Inflammopharmacology* **2019**, *27*, 663-677.
2. Labzin, L.I.; Heneka, M.T.; Latz, E. Innate Immunity and Neurodegeneration. *Annu Rev Med* **2018**, *69*, 437-449.
3. Wang, D.D.; Bordey, A. The astrocyte odyssey. *Prog Neurobiol* **2008**, *86*, 342-367.
4. Colombo, E.; Farina, C. Astrocytes: Key Regulators of Neuroinflammation. *Trends Immunol* **2016**, *37*, 608-620.
5. Sofroniew, M.V.; Vinters, H.V. Astrocytes: biology and pathology. *Acta Neuropathol* **2010**, *119*, 7-35.
6. Li, T.; Chen, X.; Zhang, C.; Zhang, Y.; Yao, W. An update on reactive astrocytes in chronic pain. *J Neuroinflammation* **2019**, *16*, 140.
7. Boche, D.; Perry, V.H.; Nicoll, J.A. Review: activation patterns of microglia and their identification in the human brain. *Neuropathol Appl Neurobiol* **2013**, *39*, 3-18.
8. Ginhoux, F.; Greter, M.; Leboeuf, M.; Nandi, S.; See, P.; Gokhan, S.; Mehler, M.F.; Conway, S.J.; Ng, L.G.; Stanley, E.R., et al. Fate mapping analysis reveals that adult microglia derive from primitive macrophages. *Science* **2010**, *330*, 841-845.
9. Borst, K.; Schwabenland, M.; Prinz, M. Microglia metabolism in health and disease. *Neurochem Int* **2019**, *130*, 104331.
10. Walter, L.; Stella, N. Cannabinoids and neuroinflammation. *Br J Pharmacol* **2004**, *141*, 775-785.
11. Grieco, M.; Giorgi, A.; Gentile, M.C.; d'Erme, M.; Morano, S.; Maras, B.; Filardi, T. Glucagon-Like Peptide-1: A Focus on Neurodegenerative Diseases. *Front Neurosci* **2019**, *13*, 1112.
12. Galimberti, D.; Fenoglio, C.; Scarpini, E. Inflammation in neurodegenerative disorders: friend or foe? *Curr Aging Sci* **2008**, *1*, 30-41.
13. Cristino, L.; Bisogno, T.; Di Marzo, V. Cannabinoids and the expanded endocannabinoid system in neurological disorders. *Nat Rev Neurol* **2020**, *16*, 9-29.
14. Mechoulam, R.; Shvo, Y. Hashish. I. The structure of cannabidiol. *Tetrahedron* **1963**, *19*, 2073-2078.
15. Mechoulam, R.; Gaoni, Y. A Total Synthesis of Dl-Delta-1-Tetrahydrocannabinol, the Active Constituent of Hashish. *J Am Chem Soc* **1965**, *87*, 3273-3275.

16. Alexander, S.P. Therapeutic potential of cannabis-related drugs. *Prog Neuropsychopharmacol Biol Psychiatry* **2016**, *64*, 157-166.
17. Novotna, A.; Mares, J.; Ratcliffe, S.; Novakova, I.; Vachova, M.; Zapletalova, O.; Gasperini, C.; Pozzilli, C.; Cefaro, L.; Comi, G., et al. A randomized, double-blind, placebo-controlled, parallel-group, enriched-design study of nabiximols* (Sativex((R))), as add-on therapy, in subjects with refractory spasticity caused by multiple sclerosis. *Eur J Neurol* **2011**, *18*, 1122-1131.
18. Little, P.J.; Compton, D.R.; Johnson, M.R.; Melvin, L.S.; Martin, B.R. Pharmacology and stereoselectivity of structurally novel cannabinoids in mice. *J Pharmacol Exp Ther* **1988**, *247*, 1046-1051.
19. Beardsley, P.M.; Scimeca, J.A.; Martin, B.R. Studies on the agonistic activity of delta 9-11-tetrahydrocannabinol in mice, dogs and rhesus monkeys and its interactions with delta 9-tetrahydrocannabinol. *J Pharmacol Exp Ther* **1987**, *241*, 521-526.
20. Devinsky, O.; Marsh, E.; Friedman, D.; Thiele, E.; Laux, L.; Sullivan, J.; Miller, I.; Flamini, R.; Wilfong, A.; Filloux, F., et al. Cannabidiol in patients with treatment-resistant epilepsy: an open-label interventional trial. *Lancet Neurol* **2016**, *15*, 270-278.
21. Devinsky, O.; Cross, J.H.; Laux, L.; Marsh, E.; Miller, I.; Nabbout, R.; Scheffer, I.E.; Thiele, E.A.; Wright, S.; Cannabidiol in Dravet Syndrome Study, G. Trial of Cannabidiol for Drug-Resistant Seizures in the Dravet Syndrome. *N Engl J Med* **2017**, *376*, 2011-2020.
22. Devane, W.A.; Dysarz, F.A., 3rd; Johnson, M.R.; Melvin, L.S.; Howlett, A.C. Determination and characterization of a cannabinoid receptor in rat brain. *Mol Pharmacol* **1988**, *34*, 605-613.
23. Matsuda, L.A.; Lolait, S.J.; Brownstein, M.J.; Young, A.C.; Bonner, T.I. Structure of a cannabinoid receptor and functional expression of the cloned cDNA. *Nature* **1990**, *346*, 561-564.
24. Munro, S.; Thomas, K.L.; Abu-Shaar, M. Molecular characterization of a peripheral receptor for cannabinoids. *Nature* **1993**, *365*, 61-65.
25. Wilson, R.I.; Nicoll, R.A. Endogenous cannabinoids mediate retrograde signalling at hippocampal synapses. *Nature* **2001**, *410*, 588-592.
26. Koch, M.; Varela, L.; Kim, J.G.; Kim, J.D.; Hernandez-Nuno, F.; Simonds, S.E.; Castorena, C.M.; Vianna, C.R.; Elmquist, J.K.; Morozov, Y.M., et al. Hypothalamic POMC neurons promote cannabinoid-induced feeding. *Nature* **2015**, *519*, 45-50.
27. Benard, G.; Massa, F.; Puente, N.; Lourenco, J.; Bellocchio, L.; Soria-Gomez, E.; Matias, I.; Delamarre, A.; Metna-Laurent, M.; Cannich, A., et al. Mitochondrial CB(1) receptors regulate neuronal energy metabolism. *Nat Neurosci* **2012**, *15*, 558-564.

28. Mendizabal-Zubiaga, J.; Melser, S.; Benard, G.; Ramos, A.; Reguero, L.; Arrabal, S.; Elezgarai, I.; Gerrikagoitia, I.; Suarez, J.; Rodriguez De Fonseca, F., et al. Cannabinoid CB1 Receptors Are Localized in Striated Muscle Mitochondria and Regulate Mitochondrial Respiration. *Front Physiol* **2016**, *7*, 476.
29. Bosier, B.; Bellocchio, L.; Metna-Laurent, M.; Soria-Gomez, E.; Matias, I.; Hebert-Chatelain, E.; Cannich, A.; Maitre, M.; Leste-Lasserre, T.; Cardinal, P., et al. Astroglial CB1 cannabinoid receptors regulate leptin signaling in mouse brain astrocytes. *Mol Metab* **2013**, *2*, 393-404.
30. Prenderville, J.A.; Kelly, A.M.; Downer, E.J. The role of cannabinoids in adult neurogenesis. *Br J Pharmacol* **2015**, *172*, 3950-3963.
31. Kelly, R.; Joers, V.; Tansey, M.G.; McKernan, D.P.; Dowd, E. Microglial Phenotypes and Their Relationship to the Cannabinoid System: Therapeutic Implications for Parkinson's Disease. *Molecules* **2020**, *25*.
32. Li, X.; Hua, T.; Vemuri, K.; Ho, J.H.; Wu, Y.; Wu, L.; Popov, P.; Benchama, O.; Zvonok, N.; Locke, K., et al. Crystal Structure of the Human Cannabinoid Receptor CB2. *Cell* **2019**, *176*, 459-467 e413.
33. Cassano, T.; Calcagnini, S.; Pace, L.; De Marco, F.; Romano, A.; Gaetani, S. Cannabinoid Receptor 2 Signaling in Neurodegenerative Disorders: From Pathogenesis to a Promising Therapeutic Target. *Front Neurosci* **2017**, *11*, 30.
34. Cristino, L.; de Petrocellis, L.; Pryce, G.; Baker, D.; Guglielmotti, V.; Di Marzo, V. Immunohistochemical localization of cannabinoid type 1 and vanilloid transient receptor potential vanilloid type 1 receptors in the mouse brain. *Neuroscience* **2006**, *139*, 1405-1415.
35. Cristino, L.; Starowicz, K.; De Petrocellis, L.; Morishita, J.; Ueda, N.; Guglielmotti, V.; Di Marzo, V. Immunohistochemical localization of anabolic and catabolic enzymes for anandamide and other putative endovanilloids in the hippocampus and cerebellar cortex of the mouse brain. *Neuroscience* **2008**, *151*, 955-968.
36. Edwards, J.G. TRPV1 in the central nervous system: synaptic plasticity, function, and pharmacological implications. *Prog Drug Res* **2014**, *68*, 77-104.
37. Stampanoni Bassi, M.; Gentile, A.; Iezzi, E.; Zagaglia, S.; Musella, A.; Simonelli, I.; Gilio, L.; Furlan, R.; Finardi, A.; Marfia, G.A., et al. Transient Receptor Potential Vanilloid 1 Modulates Central Inflammation in Multiple Sclerosis. *Front Neurol* **2019**, *10*, 30.
38. Villapol, S. Roles of Peroxisome Proliferator-Activated Receptor Gamma on Brain and Peripheral Inflammation. *Cell Mol Neurobiol* **2018**, *38*, 121-132.
39. Laleh, P.; Yaser, K.; Abolfazl, B.; Shahriar, A.; Mohammad, A.J.; Nazila, F.; Alireza, O. Oleoylethanolamide increases the expression of PPAR-Alpha and reduces appetite and body weight in obese people: A clinical trial. *Appetite* **2018**, *128*, 44-49.

40. Quintanilla, R.A.; Utreras, E.; Cabezas-Opazo, F.A. Role of PPAR gamma in the Differentiation and Function of Neurons. *PPAR Res* **2014**, *2014*, 768594.
41. Sylantyev, S.; Jensen, T.P.; Ross, R.A.; Rusakov, D.A. Cannabinoid- and lysophosphatidylinositol-sensitive receptor GPR55 boosts neurotransmitter release at central synapses. *Proc Natl Acad Sci U S A* **2013**, *110*, 5193-5198.
42. McHugh, D.; Wager-Miller, J.; Page, J.; Bradshaw, H.B. siRNA knockdown of GPR18 receptors in BV-2 microglia attenuates N-arachidonoyl glycine-induced cell migration. *J Mol Signal* **2012**, *7*, 10.
43. Penumarti, A.; Abdel-Rahman, A.A. The novel endocannabinoid receptor GPR18 is expressed in the rostral ventrolateral medulla and exerts tonic restraining influence on blood pressure. *J Pharmacol Exp Ther* **2014**, *349*, 29-38.
44. Devane, W.A.; Hanus, L.; Breuer, A.; Pertwee, R.G.; Stevenson, L.A.; Griffin, G.; Gibson, D.; Mandelbaum, A.; Etinger, A.; Mechoulam, R. Isolation and structure of a brain constituent that binds to the cannabinoid receptor. *Science* **1992**, *258*, 1946-1949.
45. Mechoulam, R.; Ben-Shabat, S.; Hanus, L.; Ligumsky, M.; Kaminski, N.E.; Schatz, A.R.; Gopher, A.; Almog, S.; Martin, B.R.; Compton, D.R., et al. Identification of an endogenous 2-monoglyceride, present in canine gut, that binds to cannabinoid receptors. *Biochem Pharmacol* **1995**, *50*, 83-90.
46. Bisogno, T. Endogenous cannabinoids: structure and metabolism. *J Neuroendocrinol* **2008**, *20 Suppl 1*, 1-9.
47. Lu, H.C.; Mackie, K. Review of the Endocannabinoid System. *Biol Psychiatry Cogn Neurosci Neuroimaging* **2020**, 10.1016/j.bpsc.2020.07.016.
48. Burkey, T.H.; Quock, R.M.; Consroe, P.; Ehlert, F.J.; Hosohata, Y.; Roeske, W.R.; Yamamura, H.I. Relative efficacies of cannabinoid CB1 receptor agonists in the mouse brain. *Eur J Pharmacol* **1997**, *336*, 295-298.
49. Glass, M.; Northup, J.K. Agonist selective regulation of G proteins by cannabinoid CB(1) and CB(2) receptors. *Mol Pharmacol* **1999**, *56*, 1362-1369.
50. Di Marzo, V. New approaches and challenges to targeting the endocannabinoid system. *Nat Rev Drug Discov* **2018**, *17*, 623-639.
51. Cravatt, B.F.; Giang, D.K.; Mayfield, S.P.; Boger, D.L.; Lerner, R.A.; Gilula, N.B. Molecular characterization of an enzyme that degrades neuromodulatory fatty-acid amides. *Nature* **1996**, *384*, 83-87.
52. Dinh, T.P.; Carpenter, D.; Leslie, F.M.; Freund, T.F.; Katona, I.; Sensi, S.L.; Kathuria, S.; Piomelli, D. Brain monoglyceride lipase participating in endocannabinoid inactivation. *Proc Natl Acad Sci U S A* **2002**, *99*, 10819-10824.
53. Bisogno, T.; Howell, F.; Williams, G.; Minassi, A.; Cascio, M.G.; Ligresti, A.; Matias, I.; Schiano-Moriello, A.; Paul, P.; Williams, E.J., et al. Cloning of the

first sn1-DAG lipases points to the spatial and temporal regulation of endocannabinoid signaling in the brain. *J Cell Biol* **2003**, *163*, 463-468.
54. Okamoto, Y.; Morishita, J.; Tsuboi, K.; Tonai, T.; Ueda, N. Molecular characterization of a phospholipase D generating anandamide and its congeners. *J Biol Chem* **2004**, *279*, 5298-5305.
55. Kozak, K.R.; Prusakiewicz, J.J.; Marnett, L.J. Oxidative metabolism of endocannabinoids by COX-2. *Curr Pharm Des* **2004**, *10*, 659-667.
56. Blankman, J.L.; Simon, G.M.; Cravatt, B.F. A comprehensive profile of brain enzymes that hydrolyze the endocannabinoid 2-arachidonoylglycerol. *Chem Biol* **2007**, *14*, 1347-1356.
57. Tsuboi, K.; Zhao, L.Y.; Okamoto, Y.; Araki, N.; Ueno, M.; Sakamoto, H.; Ueda, N. Predominant expression of lysosomal N-acylethanolamine-hydrolyzing acid amidase in macrophages revealed by immunochemical studies. *Biochim Biophys Acta* **2007**, *1771*, 623-632.
58. Navia-Paldanius, D.; Aaltonen, N.; Lehtonen, M.; Savinainen, J.R.; Taschler, U.; Radner, F.P.; Zimmermann, R.; Laitinen, J.T. Increased tonic cannabinoid CB1R activity and brain region-specific desensitization of CB1R Gi/o signaling axis in mice with global genetic knockout of monoacylglycerol lipase. *Eur J Pharm Sci* **2015**, *77*, 180-188.
59. Imperatore, R.; Morello, G.; Luongo, L.; Taschler, U.; Romano, R.; De Gregorio, D.; Belardo, C.; Maione, S.; Di Marzo, V.; Cristino, L. Genetic deletion of monoacylglycerol lipase leads to impaired cannabinoid receptor CB(1)R signaling and anxiety-like behavior. *J Neurochem* **2015**, *135*, 799-813.
60. Nomura, D.K.; Lombardi, D.P.; Chang, J.W.; Niessen, S.; Ward, A.M.; Long, J.Z.; Hoover, H.H.; Cravatt, B.F. Monoacylglycerol lipase exerts dual control over endocannabinoid and fatty acid pathways to support prostate cancer. *Chem Biol* **2011**, *18*, 846-856.
61. Piro, J.R.; Benjamin, D.I.; Duerr, J.M.; Pi, Y.; Gonzales, C.; Wood, K.M.; Schwartz, J.W.; Nomura, D.K.; Samad, T.A. A dysregulated endocannabinoid-eicosanoid network supports pathogenesis in a mouse model of Alzheimer's disease. *Cell Rep* **2012**, *1*, 617-623.
62. Fezza, F.; Bari, M.; Florio, R.; Talamonti, E.; Feole, M.; Maccarrone, M. Endocannabinoids, related compounds and their metabolic routes. *Molecules* **2014**, *19*, 17078-17106.
63. Castillo, P.E.; Younts, T.J.; Chavez, A.E.; Hashimotodani, Y. Endocannabinoid signaling and synaptic function. *Neuron* **2012**, *76*, 70-81.
64. Araque, A.; Castillo, P.E.; Manzoni, O.J.; Tonini, R. Synaptic functions of endocannabinoid signaling in health and disease. *Neuropharmacology* **2017**, *124*, 13-24.
65. Regehr, W.G.; Carey, M.R.; Best, A.R. Activity-dependent regulation of synapses by retrograde messengers. *Neuron* **2009**, *63*, 154-170.

66. Deutsch, D.G.; Chin, S.A. Enzymatic synthesis and degradation of anandamide, a cannabinoid receptor agonist. *Biochem Pharmacol* **1993**, *46*, 791-796.
67. Bachur, N.R.; Udenfriend, S. Microsomal synthesis of fatty acid amides. *J Biol Chem* **1966**, *241*, 1308-1313.
68. Patricelli, M.P.; Lashuel, H.A.; Giang, D.K.; Kelly, J.W.; Cravatt, B.F. Comparative characterization of a wild type and transmembrane domain-deleted fatty acid amide hydrolase: identification of the transmembrane domain as a site for oligomerization. *Biochemistry* **1998**, *37*, 15177-15187.
69. Hillard, C.J.; Wilkison, D.M.; Edgemond, W.S.; Campbell, W.B. Characterization of the kinetics and distribution of N-arachidonylethanolamine (anandamide) hydrolysis by rat brain. *Biochim Biophys Acta* **1995**, *1257*, 249-256.
70. Desarnaud, F.; Cadas, H.; Piomelli, D. Anandamide amidohydrolase activity in rat brain microsomes. Identification and partial characterization. *J Biol Chem* **1995**, *270*, 6030-6035.
71. Lever, I.J.; Robinson, M.; Cibelli, M.; Paule, C.; Santha, P.; Yee, L.; Hunt, S.P.; Cravatt, B.F.; Elphick, M.R.; Nagy, I., et al. Localization of the endocannabinoid-degrading enzyme fatty acid amide hydrolase in rat dorsal root ganglion cells and its regulation after peripheral nerve injury. *J Neurosci* **2009**, *29*, 3766-3780.
72. Ueda, N.; Puffenbarger, R.A.; Yamamoto, S.; Deutsch, D.G. The fatty acid amide hydrolase (FAAH). *Chem Phys Lipids* **2000**, *108*, 107-121.
73. Bracey, M.H.; Hanson, M.A.; Masuda, K.R.; Stevens, R.C.; Cravatt, B.F. Structural adaptations in a membrane enzyme that terminates endocannabinoid signaling. *Science* **2002**, *298*, 1793-1796.
74. Patricelli, M.P.; Lovato, M.A.; Cravatt, B.F. Chemical and mutagenic investigations of fatty acid amide hydrolase: evidence for a family of serine hydrolases with distinct catalytic properties. *Biochemistry* **1999**, *38*, 9804-9812.
75. Palermo, G.; Rothlisberger, U.; Cavalli, A.; De Vivo, M. Computational insights into function and inhibition of fatty acid amide hydrolase. *Eur J Med Chem* **2015**, *91*, 15-26.
76. Schlosburg, J.E.; Kinsey, S.G.; Lichtman, A.H. Targeting fatty acid amide hydrolase (FAAH) to treat pain and inflammation. *AAPS J* **2009**, *11*, 39-44.
77. Su, S.H.; Wu, Y.F.; Lin, Q.; Yu, F.; Hai, J. Cannabinoid receptor agonist WIN55,212-2 and fatty acid amide hydrolase inhibitor URB597 suppress chronic cerebral hypoperfusion-induced neuronal apoptosis by inhibiting c-Jun N-terminal kinase signaling. *Neuroscience* **2015**, *301*, 563-575.

78. Su, M.K.; Seely, K.A.; Moran, J.H.; Hoffman, R.S. Metabolism of classical cannabinoids and the synthetic cannabinoid JWH-018. *Clin Pharmacol Ther* **2015**, *97*, 562-564.
79. Su, S.H.; Wang, Y.Q.; Wu, Y.F.; Wang, D.P.; Lin, Q.; Hai, J. Cannabinoid receptor agonist WIN55,212-2 and fatty acid amide hydrolase inhibitor URB597 may protect against cognitive impairment in rats of chronic cerebral hypoperfusion via PI3K/AKT signaling. *Behav Brain Res* **2016**, *313*, 334-344.
80. Fowler, C.J.; Rojo, M.L.; Rodriguez-Gaztelumendi, A. Modulation of the endocannabinoid system: neuroprotection or neurotoxicity? *Exp Neurol* **2010**, *224*, 37-47.
81. Cadas, H.; di Tomaso, E.; Piomelli, D. Occurrence and biosynthesis of endogenous cannabinoid precursor, N-arachidonoyl phosphatidylethanolamine, in rat brain. *J Neurosci* **1997**, *17*, 1226-1242.
82. Bisogno, T.; Cascio, M.G.; Saha, B.; Mahadevan, A.; Urbani, P.; Minassi, A.; Appendino, G.; Saturnino, C.; Martin, B.; Razdan, R., et al. Development of the first potent and specific inhibitors of endocannabinoid biosynthesis. *Biochim Biophys Acta* **2006**, *1761*, 205-212.
83. Moore, S.A.; Nomikos, G.G.; Dickason-Chesterfield, A.K.; Schober, D.A.; Schaus, J.M.; Ying, B.P.; Xu, Y.C.; Phebus, L.; Simmons, R.M.; Li, D., et al. Identification of a high-affinity binding site involved in the transport of endocannabinoids. *Proc Natl Acad Sci U S A* **2005**, *102*, 17852-17857.
84. Ortar, G.; Cascio, M.G.; Moriello, A.S.; Camalli, M.; Morera, E.; Nalli, M.; Di Marzo, V. Carbamoyl tetrazoles as inhibitors of endocannabinoid inactivation: a critical revisitation. *Eur J Med Chem* **2008**, *43*, 62-72.
85. Zhang, D.; Saraf, A.; Kolasa, T.; Bhatia, P.; Zheng, G.Z.; Patel, M.; Lannoye, G.S.; Richardson, P.; Stewart, A.; Rogers, J.C., et al. Fatty acid amide hydrolase inhibitors display broad selectivity and inhibit multiple carboxylesterases as off-targets. *Neuropharmacology* **2007**, *52*, 1095-1105.
86. Rodrigues da Silva, N.; Gomes, F.V.; Sonego, A.B.; Silva, N.R.D.; Guimaraes, F.S. Cannabidiol attenuates behavioral changes in a rodent model of schizophrenia through 5-HT1A, but not CB1 and CB2 receptors. *Pharmacol Res* **2020**, *156*, 104749.
87. Echeverry, C.; Prunell, G.; Narbondo, C.; de Medina, V.S.; Nadal, X.; Reyes-Parada, M.; Scorza, C. A Comparative In Vitro Study of the Neuroprotective Effect Induced by Cannabidiol, Cannabigerol, and Their Respective Acid Forms: Relevance of the 5-HT1A Receptors. *Neurotox Res* **2020**, 10.1007/s12640-020-00277-y.
88. LoVerme, J.; Duranti, A.; Tontini, A.; Spadoni, G.; Mor, M.; Rivara, S.; Stella, N.; Xu, C.; Tarzia, G.; Piomelli, D. Synthesis and characterization of a peripherally restricted CB1 cannabinoid antagonist, URB447, that reduces

feeding and body-weight gain in mice. *Bioorg Med Chem Lett* **2009**, *19*, 639-643.
89. Zhao, Y.Z.; Yang, H.B.; Tang, X.Y.; Shi, M. Rh(II)-catalyzed [3+2] cycloaddition of 2 H-azirines with N-sulfonyl-1,2,3-triazoles. *Chemistry* **2015**, *21*, 3562-3566.
90. Bridges, D.; Ahmad, K.; Rice, A.S. The synthetic cannabinoid WIN55,212-2 attenuates hyperalgesia and allodynia in a rat model of neuropathic pain. *Br J Pharmacol* **2001**, *133*, 586-594.
91. Cinar, R.; Iyer, M.R.; Kunos, G. The therapeutic potential of second and third generation CB1R antagonists. *Pharmacol Ther* **2020**, *208*, 107477.
92. Lou, Z.Y.; Zhao, C.B.; Xiao, B.G. Immunoregulation of experimental autoimmune encephalomyelitis by the selective CB1 receptor antagonist. *J Neurosci Res* **2012**, *90*, 84-95.
93. Carloni, S.; Crinelli, R.; Palma, L.; Alvarez, F.J.; Piomelli, D.; Duranti, A.; Balduini, W.; Alonso-Alconada, D. The Synthetic Cannabinoid URB447 Reduces Brain Injury and the Associated White Matter Demyelination after Hypoxia-Ischemia in Neonatal Rats. *ACS Chem Neurosci* **2020**, *11*, 1291-1299.
94. Su, S.H.; Wu, Y.F.; Lin, Q.; Hai, J. Cannabinoid receptor agonist WIN55,212-2 and fatty acid amide hydrolase inhibitor URB597 ameliorate neuroinflammatory responses in chronic cerebral hypoperfusion model by blocking NF-kappaB pathways. *Naunyn Schmiedebergs Arch Pharmacol* **2017**, *390*, 1189-1200.
95. Calapai, F.; Cardia, L.; Sorbara, E.E.; Navarra, M.; Gangemi, S.; Calapai, G.; Mannucci, C. Cannabinoids, Blood-Brain Barrier, and Brain Disposition. *Pharmaceutics* **2020**, *12*.
96. Piomelli, D.; Tarzia, G.; Duranti, A.; Tontini, A.; Mor, M.; Compton, T.R.; Dasse, O.; Monaghan, E.P.; Parrott, J.A.; Putman, D. Pharmacological profile of the selective FAAH inhibitor KDS-4103 (URB597). *CNS Drug Rev* **2006**, *12*, 21-38.
97. Mor, M.; Rivara, S.; Lodola, A.; Plazzi, P.V.; Tarzia, G.; Duranti, A.; Tontini, A.; Piersanti, G.; Kathuria, S.; Piomelli, D. Cyclohexylcarbamic acid 3'- or 4'-substituted biphenyl-3-yl esters as fatty acid amide hydrolase inhibitors: synthesis, quantitative structure-activity relationships, and molecular modeling studies. *J Med Chem* **2004**, *47*, 4998-5008.
98. Karwad, M.A.; Couch, D.G.; Theophilidou, E.; Sarmad, S.; Barrett, D.A.; Larvin, M.; Wright, K.L.; Lund, J.N.; O'Sullivan, S.E. The role of CB1 in intestinal permeability and inflammation. *FASEB J* **2017**, *31*, 3267-3277.
99. Fegley, D.; Gaetani, S.; Duranti, A.; Tontini, A.; Mor, M.; Tarzia, G.; Piomelli, D. Characterization of the fatty acid amide hydrolase inhibitor cyclohexyl carbamic acid 3'-carbamoyl-biphenyl-3-yl ester (URB597): effects on

anandamide and oleoylethanolamide deactivation. *J Pharmacol Exp Ther* **2005**, *313*, 352-358.
100. Makara, J.K.; Mor, M.; Fegley, D.; Szabo, S.I.; Kathuria, S.; Astarita, G.; Duranti, A.; Tontini, A.; Tarzia, G.; Rivara, S., et al. Selective inhibition of 2-AG hydrolysis enhances endocannabinoid signaling in hippocampus. *Nat Neurosci* **2005**, *8*, 1139-1141.
101. Alexander, J.P.; Cravatt, B.F. Mechanism of carbamate inactivation of FAAH: implications for the design of covalent inhibitors and in vivo functional probes for enzymes. *Chem Biol* **2005**, *12*, 1179-1187.
102. Mileni, M.; Kamtekar, S.; Wood, D.C.; Benson, T.E.; Cravatt, B.F.; Stevens, R.C. Crystal structure of fatty acid amide hydrolase bound to the carbamate inhibitor URB597: discovery of a deacylating water molecule and insight into enzyme inactivation. *J Mol Biol* **2010**, *400*, 743-754.
103. Russo, R.; Loverme, J.; La Rana, G.; Compton, T.R.; Parrott, J.; Duranti, A.; Tontini, A.; Mor, M.; Tarzia, G.; Calignano, A., et al. The fatty acid amide hydrolase inhibitor URB597 (cyclohexylcarbamic acid 3'-carbamoylbiphenyl-3-yl ester) reduces neuropathic pain after oral administration in mice. *J Pharmacol Exp Ther* **2007**, *322*, 236-242.
104. Gobbi, G.; Bambico, F.R.; Mangieri, R.; Bortolato, M.; Campolongo, P.; Solinas, M.; Cassano, T.; Morgese, M.G.; Debonnel, G.; Duranti, A., et al. Antidepressant-like activity and modulation of brain monoaminergic transmission by blockade of anandamide hydrolysis. *Proc Natl Acad Sci U S A* **2005**, *102*, 18620-18625.
105. Naidu, P.S.; Kinsey, S.G.; Guo, T.L.; Cravatt, B.F.; Lichtman, A.H. Regulation of inflammatory pain by inhibition of fatty acid amide hydrolase. *J Pharmacol Exp Ther* **2010**, *334*, 182-190.
106. Fernandez-Ruiz, J.; Romero, J.; Ramos, J.A. Endocannabinoids and Neurodegenerative Disorders: Parkinson's Disease, Huntington's Chorea, Alzheimer's Disease, and Others. *Handb Exp Pharmacol* **2015**, *231*, 233-259.
107. Romero-Sandoval, E.A.; Horvath, R.; Landry, R.P.; DeLeo, J.A. Cannabinoid receptor type 2 activation induces a microglial anti-inflammatory phenotype and reduces migration via MKP induction and ERK dephosphorylation. *Mol Pain* **2009**, *5*, 25.
108. Maresz, K.; Pryce, G.; Ponomarev, E.D.; Marsicano, G.; Croxford, J.L.; Shriver, L.P.; Ledent, C.; Cheng, X.; Carrier, E.J.; Mann, M.K., et al. Direct suppression of CNS autoimmune inflammation via the cannabinoid receptor CB1 on neurons and CB2 on autoreactive T cells. *Nat Med* **2007**, *13*, 492-497.
109. Centonze, D.; Finazzi-Agro, A.; Bernardi, G.; Maccarrone, M. The endocannabinoid system in targeting inflammatory neurodegenerative diseases. *Trends Pharmacol Sci* **2007**, *28*, 180-187.

110. Garcia-Arencibia, M.; Garcia, C.; Kurz, A.; Rodriguez-Navarro, J.A.; Gispert-Sachez, S.; Mena, M.A.; Auburger, G.; de Yebenes, J.G.; Fernandez-Ruiz, J. Cannabinoid CB1 receptors are early downregulated followed by a further upregulation in the basal ganglia of mice with deletion of specific park genes. *J Neural Transm Suppl* **2009**, 10.1007/978-3-211-92660-4_22, 269-275.
111. Van Laere, K.; Casteels, C.; Lunskens, S.; Goffin, K.; Grachev, I.D.; Bormans, G.; Vandenberghe, W. Regional changes in type 1 cannabinoid receptor availability in Parkinson's disease in vivo. *Neurobiol Aging* **2012**, *33*, 620 e621-628.
112. Navarrete, F.; Garcia-Gutierrez, M.S.; Aracil-Fernandez, A.; Lanciego, J.L.; Manzanares, J. Cannabinoid CB1 and CB2 Receptors, and Monoacylglycerol Lipase Gene Expression Alterations in the Basal Ganglia of Patients with Parkinson's Disease. *Neurotherapeutics* **2018**, *15*, 459-469.
113. Chung, Y.C.; Shin, W.H.; Baek, J.Y.; Cho, E.J.; Baik, H.H.; Kim, S.R.; Won, S.Y.; Jin, B.K. CB2 receptor activation prevents glial-derived neurotoxic mediator production, BBB leakage and peripheral immune cell infiltration and rescues dopamine neurons in the MPTP model of Parkinson's disease. *Exp Mol Med* **2016**, *48*, e205.
114. Shi, J.; Cai, Q.; Zhang, J.; He, X.; Liu, Y.; Zhu, R.; Jin, L. AM1241 alleviates MPTP-induced Parkinson's disease and promotes the regeneration of DA neurons in PD mice. *Oncotarget* **2017**, *8*, 67837-67850.
115. Gomez-Galvez, Y.; Palomo-Garo, C.; Fernandez-Ruiz, J.; Garcia, C. Potential of the cannabinoid CB(2) receptor as a pharmacological target against inflammation in Parkinson's disease. *Prog Neuropsychopharmacol Biol Psychiatry* **2016**, *64*, 200-208.
116. van der Stelt, M.; Fox, S.H.; Hill, M.; Crossman, A.R.; Petrosino, S.; Di Marzo, V.; Brotchie, J.M. A role for endocannabinoids in the generation of parkinsonism and levodopa-induced dyskinesia in MPTP-lesioned non-human primate models of Parkinson's disease. *FASEB J* **2005**, *19*, 1140-1142.
117. Pisani, A.; Fezza, F.; Galati, S.; Battista, N.; Napolitano, S.; Finazzi-Agro, A.; Bernardi, G.; Brusa, L.; Pierantozzi, M.; Stanzione, P., et al. High endogenous cannabinoid levels in the cerebrospinal fluid of untreated Parkinson's disease patients. *Ann Neurol* **2005**, *57*, 777-779.
118. Pisani, V.; Moschella, V.; Bari, M.; Fezza, F.; Galati, S.; Bernardi, G.; Stanzione, P.; Pisani, A.; Maccarrone, M. Dynamic changes of anandamide in the cerebrospinal fluid of Parkinson's disease patients. *Mov Disord* **2010**, *25*, 920-924.
119. Fernandez-Suarez, D.; Celorrio, M.; Riezu-Boj, J.I.; Ugarte, A.; Pacheco, R.; Gonzalez, H.; Oyarzabal, J.; Hillard, C.J.; Franco, R.; Aymerich, M.S. Monoacylglycerol lipase inhibitor JZL184 is neuroprotective and alters glial

cell phenotype in the chronic MPTP mouse model. *Neurobiol Aging* **2014**, *35*, 2603-2616.
120. Celorrio, M.; Fernandez-Suarez, D.; Rojo-Bustamante, E.; Echeverry-Alzate, V.; Ramirez, M.J.; Hillard, C.J.; Lopez-Moreno, J.A.; Maldonado, R.; Oyarzabal, J.; Franco, R., et al. Fatty acid amide hydrolase inhibition for the symptomatic relief of Parkinson's disease. *Brain Behav Immun* **2016**, *57*, 94-105.
121. Glass, M.; Faull, R.L.; Dragunow, M. Loss of cannabinoid receptors in the substantia nigra in Huntington's disease. *Neuroscience* **1993**, *56*, 523-527.
122. Dowie, M.J.; Bradshaw, H.B.; Howard, M.L.; Nicholson, L.F.; Faull, R.L.; Hannan, A.J.; Glass, M. Altered CB1 receptor and endocannabinoid levels precede motor symptom onset in a transgenic mouse model of Huntington's disease. *Neuroscience* **2009**, *163*, 456-465.
123. Denovan-Wright, E.M.; Robertson, H.A. Cannabinoid receptor messenger RNA levels decrease in a subset of neurons of the lateral striatum, cortex and hippocampus of transgenic Huntington's disease mice. *Neuroscience* **2000**, *98*, 705-713.
124. Chiarlone, A.; Bellocchio, L.; Blazquez, C.; Resel, E.; Soria-Gomez, E.; Cannich, A.; Ferrero, J.J.; Sagredo, O.; Benito, C.; Romero, J., et al. A restricted population of CB1 cannabinoid receptors with neuroprotective activity. *Proc Natl Acad Sci U S A* **2014**, *111*, 8257-8262.
125. Ruiz-Calvo, A.; Maroto, I.B.; Bajo-Graneras, R.; Chiarlone, A.; Gaudioso, A.; Ferrero, J.J.; Resel, E.; Sanchez-Prieto, J.; Rodriguez-Navarro, J.A.; Marsicano, G., et al. Pathway-Specific Control of Striatal Neuron Vulnerability by Corticostriatal Cannabinoid CB1 Receptors. *Cereb Cortex* **2018**, *28*, 307-322.
126. Pietropaolo, S.; Bellocchio, L.; Ruiz-Calvo, A.; Cabanas, M.; Du, Z.; Guzman, M.; Garret, M.; Cho, Y.H. Chronic cannabinoid receptor stimulation selectively prevents motor impairments in a mouse model of Huntington's disease. *Neuropharmacology* **2015**, *89*, 368-374.
127. Bisogno, T.; Martire, A.; Petrosino, S.; Popoli, P.; Di Marzo, V. Symptom-related changes of endocannabinoid and palmitoylethanolamide levels in brain areas of R6/2 mice, a transgenic model of Huntington's disease. *Neurochem Int* **2008**, *52*, 307-313.
128. Bari, M.; Battista, N.; Valenza, M.; Mastrangelo, N.; Malaponti, M.; Catanzaro, G.; Centonze, D.; Finazzi-Agro, A.; Cattaneo, E.; Maccarrone, M. In vitro and in vivo models of Huntington's disease show alterations in the endocannabinoid system. *FEBS J* **2013**, *280*, 3376-3388.
129. Battista, N.; Bari, M.; Tarditi, A.; Mariotti, C.; Bachoud-Levi, A.C.; Zuccato, C.; Finazzi-Agro, A.; Genitrini, S.; Peschanski, M.; Di Donato, S., et al. Severe deficiency of the fatty acid amide hydrolase (FAAH) activity segregates with

the Huntington's disease mutation in peripheral lymphocytes. *Neurobiol Dis* **2007**, *27*, 108-116.
130. Baker, D.; Pryce, G.; Croxford, J.L.; Brown, P.; Pertwee, R.G.; Huffman, J.W.; Layward, L. Cannabinoids control spasticity and tremor in a multiple sclerosis model. *Nature* **2000**, *404*, 84-87.
131. Baker, D.; Pryce, G.; Croxford, J.L.; Brown, P.; Pertwee, R.G.; Makriyannis, A.; Khanolkar, A.; Layward, L.; Fezza, F.; Bisogno, T., et al. Endocannabinoids control spasticity in a multiple sclerosis model. *FASEB J* **2001**, *15*, 300-302.
132. Arevalo-Martin, A.; Molina-Holgado, E.; Guaza, C. A CB(1)/CB(2) receptor agonist, WIN 55,212-2, exerts its therapeutic effect in a viral autoimmune model of multiple sclerosis by restoring self-tolerance to myelin. *Neuropharmacology* **2012**, *63*, 385-393.
133. Sanchez Lopez, A.J.; Roman-Vega, L.; Ramil Tojeiro, E.; Giuffrida, A.; Garcia-Merino, A. Regulation of cannabinoid receptor gene expression and endocannabinoid levels in lymphocyte subsets by interferon-beta: a longitudinal study in multiple sclerosis patients. *Clin Exp Immunol* **2015**, *179*, 119-127.
134. Centonze, D.; Bari, M.; Rossi, S.; Prosperetti, C.; Furlan, R.; Fezza, F.; De Chiara, V.; Battistini, L.; Bernardi, G.; Bernardini, S., et al. The endocannabinoid system is dysregulated in multiple sclerosis and in experimental autoimmune encephalomyelitis. *Brain* **2007**, *130*, 2543-2553.
135. Rosen, D.R.; Siddique, T.; Patterson, D.; Figlewicz, D.A.; Sapp, P.; Hentati, A.; Donaldson, D.; Goto, J.; O'Regan, J.P.; Deng, H.X., et al. Mutations in Cu/Zn superoxide dismutase gene are associated with familial amyotrophic lateral sclerosis. *Nature* **1993**, *362*, 59-62.
136. Moreno-Martet, M.; Espejo-Porras, F.; Fernandez-Ruiz, J.; de Lago, E. Changes in endocannabinoid receptors and enzymes in the spinal cord of SOD1(G93A) transgenic mice and evaluation of a Sativex((R)) -like combination of phytocannabinoids: interest for future therapies in amyotrophic lateral sclerosis. *CNS Neurosci Ther* **2014**, *20*, 809-815.
137. Espejo-Porras, F.; Fernandez-Ruiz, J.; de Lago, E. Analysis of endocannabinoid receptors and enzymes in the post-mortem motor cortex and spinal cord of amyotrophic lateral sclerosis patients. *Amyotroph Lateral Scler Frontotemporal Degener* **2018**, *19*, 377-386.
138. Bilsland, L.G.; Dick, J.R.; Pryce, G.; Petrosino, S.; Di Marzo, V.; Baker, D.; Greensmith, L. Increasing cannabinoid levels by pharmacological and genetic manipulation delay disease progression in SOD1 mice. *FASEB J* **2006**, *20*, 1003-1005.
139. Elliott, M.B.; Tuma, R.F.; Amenta, P.S.; Barbe, M.F.; Jallo, J.I. Acute effects of a selective cannabinoid-2 receptor agonist on neuroinflammation in a model of traumatic brain injury. *J Neurotrauma* **2011**, *28*, 973-981.

140. Witting, A.; Weydt, P.; Hong, S.; Kliot, M.; Moller, T.; Stella, N. Endocannabinoids accumulate in spinal cord of SOD1 G93A transgenic mice. *J Neurochem* **2004**, *89*, 1555-1557.
141. Clay, E.; Zhou, J.; Yi, Z.M.; Zhai, S.; Toumi, M. Economic burden for Alzheimer's disease in China from 2010 to 2050: a modelling study. *J Mark Access Health Policy* **2019**, *7*, 1667195.
142. Galimberti, D.; Scarpini, E. Progress in Alzheimer's disease. *J Neurol* **2012**, *259*, 201-211.
143. Bertram, L.; Lill, C.M.; Tanzi, R.E. The genetics of Alzheimer disease: back to the future. *Neuron* **2010**, *68*, 270-281.
144. Selkoe, D.J. Alzheimer's disease: genes, proteins, and therapy. *Physiol Rev* **2001**, *81*, 741-766.
145. Selkoe, D.J. Alzheimer's disease. *Cold Spring Harb Perspect Biol* **2011**, *3*.
146. Priller, C.; Bauer, T.; Mitteregger, G.; Krebs, B.; Kretzschmar, H.A.; Herms, J. Synapse formation and function is modulated by the amyloid precursor protein. *J Neurosci* **2006**, *26*, 7212-7221.
147. Turner, P.R.; O'Connor, K.; Tate, W.P.; Abraham, W.C. Roles of amyloid precursor protein and its fragments in regulating neural activity, plasticity and memory. *Prog Neurobiol* **2003**, *70*, 1-32.
148. Moir, R.D.; Lathe, R.; Tanzi, R.E. The antimicrobial protection hypothesis of Alzheimer's disease. *Alzheimers Dement* **2018**, *14*, 1602-1614.
149. Mattson, M.P.; Barger, S.W.; Cheng, B.; Lieberburg, I.; Smith-Swintosky, V.L.; Rydel, R.E. beta-Amyloid precursor protein metabolites and loss of neuronal Ca2+ homeostasis in Alzheimer's disease. *Trends Neurosci* **1993**, *16*, 409-414.
150. Goate, A.; Chartier-Harlin, M.C.; Mullan, M.; Brown, J.; Crawford, F.; Fidani, L.; Giuffra, L.; Haynes, A.; Irving, N.; James, L., et al. Segregation of a missense mutation in the amyloid precursor protein gene with familial Alzheimer's disease. *Nature* **1991**, *349*, 704-706.
151. Esch, F.S.; Keim, P.S.; Beattie, E.C.; Blacher, R.W.; Culwell, A.R.; Oltersdorf, T.; McClure, D.; Ward, P.J. Cleavage of amyloid beta peptide during constitutive processing of its precursor. *Science* **1990**, *248*, 1122-1124.
152. Sisodia, S.S.; Koo, E.H.; Beyreuther, K.; Unterbeck, A.; Price, D.L. Evidence that beta-amyloid protein in Alzheimer's disease is not derived by normal processing. *Science* **1990**, *248*, 492-495.
153. Haass, C.; Hung, A.Y.; Schlossmacher, M.G.; Oltersdorf, T.; Teplow, D.B.; Selkoe, D.J. Normal cellular processing of the beta-amyloid precursor protein results in the secretion of the amyloid beta peptide and related molecules. *Ann N Y Acad Sci* **1993**, *695*, 109-116.
154. Holtzman, D.M.; Morris, J.C.; Goate, A.M. Alzheimer's disease: the challenge of the second century. *Sci Transl Med* **2011**, *3*, 77sr71.

155. Munoz-Torrero, D. Acetylcholinesterase inhibitors as disease-modifying therapies for Alzheimer's disease. *Curr Med Chem* **2008**, *15*, 2433-2455.
156. Tricco, A.C.; Ashoor, H.M.; Soobiah, C.; Rios, P.; Veroniki, A.A.; Hamid, J.S.; Ivory, J.D.; Khan, P.A.; Yazdi, F.; Ghassemi, M., et al. Comparative Effectiveness and Safety of Cognitive Enhancers for Treating Alzheimer's Disease: Systematic Review and Network Metaanalysis. *J Am Geriatr Soc* **2018**, *66*, 170-178.
157. McShane, R.; Westby, M.J.; Roberts, E.; Minakaran, N.; Schneider, L.; Farrimond, L.E.; Maayan, N.; Ware, J.; Debarros, J. Memantine for dementia. *Cochrane Database Syst Rev* **2019**, *3*, CD003154.
158. Chen, R.; Chan, P.T.; Chu, H.; Lin, Y.C.; Chang, P.C.; Chen, C.Y.; Chou, K.R. Treatment effects between monotherapy of donepezil versus combination with memantine for Alzheimer disease: A meta-analysis. *PLoS One* **2017**, *12*, e0183586.
159. Ali, M.M.; Ghouri, R.G.; Ans, A.H.; Akbar, A.; Toheed, A. Recommendations for Anti-inflammatory Treatments in Alzheimer's Disease: A Comprehensive Review of the Literature. *Cureus* **2019**, *11*, e4620.
160. Kennedy, M.E.; Stamford, A.W.; Chen, X.; Cox, K.; Cumming, J.N.; Dockendorf, M.F.; Egan, M.; Ereshefsky, L.; Hodgson, R.A.; Hyde, L.A., et al. The BACE1 inhibitor verubecestat (MK-8931) reduces CNS beta-amyloid in animal models and in Alzheimer's disease patients. *Sci Transl Med* **2016**, *8*, 363ra150.
161. Panza, F.; Lozupone, M.; Solfrizzi, V.; Sardone, R.; Piccininni, C.; Dibello, V.; Stallone, R.; Giannelli, G.; Bellomo, A.; Greco, A., et al. BACE inhibitors in clinical development for the treatment of Alzheimer's disease. *Expert Rev Neurother* **2018**, *18*, 847-857.
162. Aisen, P.S.; Gauthier, S.; Ferris, S.H.; Saumier, D.; Haine, D.; Garceau, D.; Duong, A.; Suhy, J.; Oh, J.; Lau, W.C., et al. Tramiprosate in mild-to-moderate Alzheimer's disease - a randomized, double-blind, placebo-controlled, multi-centre study (the Alphase Study). *Arch Med Sci* **2011**, *7*, 102-111.
163. Salloway, S.; Sperling, R.; Keren, R.; Porsteinsson, A.P.; van Dyck, C.H.; Tariot, P.N.; Gilman, S.; Arnold, D.; Abushakra, S.; Hernandez, C., et al. A phase 2 randomized trial of ELND005, scyllo-inositol, in mild to moderate Alzheimer disease. *Neurology* **2011**, *77*, 1253-1262.
164. Dalakas, M.C.; Alexopoulos, H.; Spaeth, P.J. Complement in neurological disorders and emerging complement-targeted therapeutics. *Nat Rev Neurol* **2020**, 10.1038/s41582-020-0400-0.
165. Vaz, M.; Silvestre, S. Alzheimer's disease: Recent treatment strategies. *Eur J Pharmacol* **2020**, *887*, 173554.

166. Matsunaga, S.; Fujishiro, H.; Takechi, H. Efficacy and Safety of Glycogen Synthase Kinase 3 Inhibitors for Alzheimer's Disease: A Systematic Review and Meta-Analysis. *J Alzheimers Dis* **2019**, *69*, 1031-1039.
167. Wischik, C.M.; Edwards, P.C.; Lai, R.Y.; Roth, M.; Harrington, C.R. Selective inhibition of Alzheimer disease-like tau aggregation by phenothiazines. *Proc Natl Acad Sci U S A* **1996**, *93*, 11213-11218.
168. Wischik, C.M.; Staff, R.T.; Wischik, D.J.; Bentham, P.; Murray, A.D.; Storey, J.M.; Kook, K.A.; Harrington, C.R. Tau aggregation inhibitor therapy: an exploratory phase 2 study in mild or moderate Alzheimer's disease. *J Alzheimers Dis* **2015**, *44*, 705-720.
169. Ramirez, B.G.; Blazquez, C.; Gomez del Pulgar, T.; Guzman, M.; de Ceballos, M.L. Prevention of Alzheimer's disease pathology by cannabinoids: neuroprotection mediated by blockade of microglial activation. *J Neurosci* **2005**, *25*, 1904-1913.
170. Benito, C.; Nunez, E.; Tolon, R.M.; Carrier, E.J.; Rabano, A.; Hillard, C.J.; Romero, J. Cannabinoid CB2 receptors and fatty acid amide hydrolase are selectively overexpressed in neuritic plaque-associated glia in Alzheimer's disease brains. *J Neurosci* **2003**, *23*, 11136-11141.
171. Jackson, S.J.; Diemel, L.T.; Pryce, G.; Baker, D. Cannabinoids and neuroprotection in CNS inflammatory disease. *J Neurol Sci* **2005**, *233*, 21-25.
172. Pazos, M.R.; Nunez, E.; Benito, C.; Tolon, R.M.; Romero, J. Role of the endocannabinoid system in Alzheimer's disease: new perspectives. *Life Sci* **2004**, *75*, 1907-1915.
173. Karkkaine, E.; Tanila, H.; Laitinen, J.T. Functional autoradiography shows unaltered cannabinoid CB1 receptor signalling in hippocampus and cortex of APP/PS1 transgenic mice. *CNS Neurol Disord Drug Targets* **2012**, *11*, 1038-1044.
174. Maccarrone, M.; Totaro, A.; Leuti, A.; Giacovazzo, G.; Scipioni, L.; Mango, D.; Coccurello, R.; Nistico, R.; Oddi, S. Early alteration of distribution and activity of hippocampal type-1 cannabinoid receptor in Alzheimer's disease-like mice overexpressing the human mutant amyloid precursor protein. *Pharmacol Res* **2018**, *130*, 366-373.
175. Aso, E.; Juves, S.; Maldonado, R.; Ferrer, I. CB2 cannabinoid receptor agonist ameliorates Alzheimer-like phenotype in AbetaPP/PS1 mice. *J Alzheimers Dis* **2013**, *35*, 847-858.
176. Mazzola, C.; Micale, V.; Drago, F. Amnesia induced by beta-amyloid fragments is counteracted by cannabinoid CB1 receptor blockade. *Eur J Pharmacol* **2003**, *477*, 219-225.
177. Esposito, G.; Iuvone, T.; Savani, C.; Scuderi, C.; De Filippis, D.; Papa, M.; Di Marzo, V.; Steardo, L. Opposing control of cannabinoid receptor stimulation

on amyloid-beta-induced reactive gliosis: in vitro and in vivo evidence. *J Pharmacol Exp Ther* **2007**, *322*, 1144-1152.
178. Ehrhart, J.; Obregon, D.; Mori, T.; Hou, H.; Sun, N.; Bai, Y.; Klein, T.; Fernandez, F.; Tan, J.; Shytle, R.D. Stimulation of cannabinoid receptor 2 (CB2) suppresses microglial activation. *J Neuroinflammation* **2005**, *2*, 29.
179. Lopez, A.; Aparicio, N.; Pazos, M.R.; Grande, M.T.; Barreda-Manso, M.A.; Benito-Cuesta, I.; Vazquez, C.; Amores, M.; Ruiz-Perez, G.; Garcia-Garcia, E., et al. Cannabinoid CB2 receptors in the mouse brain: relevance for Alzheimer's disease. *J Neuroinflammation* **2018**, *15*, 158.
180. van der Stelt, M.; Mazzola, C.; Esposito, G.; Matias, I.; Petrosino, S.; De Filippis, D.; Micale, V.; Steardo, L.; Drago, F.; Iuvone, T., et al. Endocannabinoids and beta-amyloid-induced neurotoxicity in vivo: effect of pharmacological elevation of endocannabinoid levels. *Cell Mol Life Sci* **2006**, *63*, 1410-1424.
181. Mulder, J.; Zilberter, M.; Pasquare, S.J.; Alpar, A.; Schulte, G.; Ferreira, S.G.; Kofalvi, A.; Martin-Moreno, A.M.; Keimpema, E.; Tanila, H., et al. Molecular reorganization of endocannabinoid signalling in Alzheimer's disease. *Brain* **2011**, *134*, 1041-1060.
182. Jung, K.M.; Astarita, G.; Yasar, S.; Vasilevko, V.; Cribbs, D.H.; Head, E.; Cotman, C.W.; Piomelli, D. An amyloid beta42-dependent deficit in anandamide mobilization is associated with cognitive dysfunction in Alzheimer's disease. *Neurobiol Aging* **2012**, *33*, 1522-1532.
183. Milton, N.G. Anandamide and noladin ether prevent neurotoxicity of the human amyloid-beta peptide. *Neurosci Lett* **2002**, *332*, 127-130.
184. Waksman, Y.; Olson, J.M.; Carlisle, S.J.; Cabral, G.A. The central cannabinoid receptor (CB1) mediates inhibition of nitric oxide production by rat microglial cells. *J Pharmacol Exp Ther* **1999**, *288*, 1357-1366.
185. Bisogno, T.; Di Marzo, V. The role of the endocannabinoid system in Alzheimer's disease: facts and hypotheses. *Curr Pharm Des* **2008**, *14*, 2299-3305.
186. Pardon, M.C.; Sarmad, S.; Rattray, I.; Bates, T.E.; Scullion, G.A.; Marsden, C.A.; Barrett, D.A.; Lowe, J.; Kendall, D.A. Repeated novel cage exposure-induced improvement of early Alzheimer's-like cognitive and amyloid changes in TASTPM mice is unrelated to changes in brain endocannabinoids levels. *Neurobiol Aging* **2009**, *30*, 1099-1113.
187. Hill, M.N.; Patel, S.; Carrier, E.J.; Rademacher, D.J.; Ormerod, B.K.; Hillard, C.J.; Gorzalka, B.B. Downregulation of endocannabinoid signaling in the hippocampus following chronic unpredictable stress. *Neuropsychopharmacology* **2005**, *30*, 508-515.
188. Abu-Rumeileh, S.; Oeckl, P.; Baiardi, S.; Halbgebauer, S.; Steinacker, P.; Capellari, S.; Otto, M.; Parchi, P. CSF Ubiquitin Levels Are Higher in

Alzheimer's Disease than in Frontotemporal Dementia and Reflect the Molecular Subtype in Prion Disease. *Biomolecules* **2020**, *10*.
189. Cores, A.; Piquero, M.; Villacampa, M.; Leon, R.; Menendez, J.C. NRF2 Regulation Processes as a Source of Potential Drug Targets against Neurodegenerative Diseases. *Biomolecules* **2020**, *10*.
190. Colombo, R.; Atherton, E.; Sheppard, R.C.; Woolley, V. 4-Chloromethylphenoxyacetyl polystyrene and polyamide supports for solid-phase peptide synthesis. *Int J Pept Protein Res* **1983**, *21*, 118-126.
191. Block, M.L.; Hong, J.S. Chronic microglial activation and progressive dopaminergic neurotoxicity. *Biochem Soc Trans* **2007**, *35*, 1127-1132.
192. Davalos, D.; Grutzendler, J.; Yang, G.; Kim, J.V.; Zuo, Y.; Jung, S.; Littman, D.R.; Dustin, M.L.; Gan, W.B. ATP mediates rapid microglial response to local brain injury in vivo. *Nat Neurosci* **2005**, *8*, 752-758.
193. De Caris, M.G.; Grieco, M.; Maggi, E.; Francioso, A.; Armeli, F.; Mosca, L.; Pinto, A.; D'Erme, M.; Mancini, P.; Businaro, R. Blueberry Counteracts BV-2 Microglia Morphological and Functional Switch after LPS Challenge. *Nutrients* **2020**, *12*.
194. Bao, Y.; Zhu, Y.; He, G.; Ni, H.; Liu, C.; Ma, L.; Zhang, L.; Shi, D. Dexmedetomidine Attenuates Neuroinflammation In LPS-Stimulated BV2 Microglia Cells Through Upregulation Of miR-340. *Drug Des Devel Ther* **2019**, *13*, 3465-3475.
195. Orihuela, R.; McPherson, C.A.; Harry, G.J. Microglial M1/M2 polarization and metabolic states. *Br J Pharmacol* **2016**, *173*, 649-665.
196. Kettenmann, H.; Kirchhoff, F.; Verkhratsky, A. Microglia: new roles for the synaptic stripper. *Neuron* **2013**, *77*, 10-18.
197. Soulet, D.; Rivest, S. Microglia. *Curr Biol* **2008**, *18*, R506-508.
198. ElAli, A.; Rivest, S. Microglia in Alzheimer's disease: A multifaceted relationship. *Brain Behav Immun* **2016**, *55*, 138-150.
199. Pocock, J.M.; Kettenmann, H. Neurotransmitter receptors on microglia. *Trends Neurosci* **2007**, *30*, 527-535.
200. Colonna, M.; Butovsky, O. Microglia Function in the Central Nervous System During Health and Neurodegeneration. *Annu Rev Immunol* **2017**, *35*, 441-468.
201. Njie, E.G.; Boelen, E.; Stassen, F.R.; Steinbusch, H.W.; Borchelt, D.R.; Streit, W.J. Ex vivo cultures of microglia from young and aged rodent brain reveal age-related changes in microglial function. *Neurobiol Aging* **2012**, *33*, 195 e191-112.
202. Heithoff, B.P.; George, K.K.; Phares, A.N.; Zuidhoek, I.A.; Munoz-Ballester, C.; Robel, S. Astrocytes are necessary for blood-brain barrier maintenance in the adult mouse brain. *Glia* **2020**, 10.1002/glia.23908.

203. Sofroniew, M.V. Astrocyte barriers to neurotoxic inflammation. *Nat Rev Neurosci* **2015**, *16*, 249-263.
204. Abbott, N.J. Astrocyte-endothelial interactions and blood-brain barrier permeability. *J Anat* **2002**, *200*, 629-638.
205. Saint-Pol, J.; Gosselet, F.; Duban-Deweer, S.; Pottiez, G.; Karamanos, Y. Targeting and Crossing the Blood-Brain Barrier with Extracellular Vesicles. *Cells* **2020**, *9*.
206. Daneman, R.; Zhou, L.; Kebede, A.A.; Barres, B.A. Pericytes are required for blood-brain barrier integrity during embryogenesis. *Nature* **2010**, *468*, 562-566.
207. Gosselet, F.; Saint-Pol, J.; Candela, P.; Fenart, L. Amyloid-beta peptides, Alzheimer's disease and the blood-brain barrier. *Curr Alzheimer Res* **2013**, *10*, 1015-1033.
208. Cabezas, R.; Avila, M.; Gonzalez, J.; El-Bacha, R.S.; Baez, E.; Garcia-Segura, L.M.; Jurado Coronel, J.C.; Capani, F.; Cardona-Gomez, G.P.; Barreto, G.E. Astrocytic modulation of blood brain barrier: perspectives on Parkinson's disease. *Front Cell Neurosci* **2014**, *8*, 211.
209. Chiarini, A.; Armato, U.; Gardenal, E.; Gui, L.; Dal Pra, I. Amyloid beta-Exposed Human Astrocytes Overproduce Phospho-Tau and Overrelease It within Exosomes, Effects Suppressed by Calcilytic NPS 2143-Further Implications for Alzheimer's Therapy. *Front Neurosci* **2017**, *11*, 217.
210. Lotharius, J.; Barg, S.; Wiekop, P.; Lundberg, C.; Raymon, H.K.; Brundin, P. Effect of mutant alpha-synuclein on dopamine homeostasis in a new human mesencephalic cell line. *J Biol Chem* **2002**, *277*, 38884-38894.
211. Hoshimaru, M.; Ray, J.; Sah, D.W.; Gage, F.H. Differentiation of the immortalized adult neuronal progenitor cell line HC2S2 into neurons by regulatable suppression of the v-myc oncogene. *Proc Natl Acad Sci U S A* **1996**, *93*, 1518-1523.
212. Yin, M.; Liu, S.; Yin, Y.; Li, S.; Li, Z.; Wu, X.; Zhang, B.; Ang, S.L.; Ding, Y.; Zhou, J. Ventral mesencephalon-enriched genes that regulate the development of dopaminergic neurons in vivo. *J Neurosci* **2009**, *29*, 5170-5182.
213. Scholz, D.; Poltl, D.; Genewsky, A.; Weng, M.; Waldmann, T.; Schildknecht, S.; Leist, M. Rapid, complete and large-scale generation of post-mitotic neurons from the human LUHMES cell line. *J Neurochem* **2011**, *119*, 957-971.
214. Thomson, J.A.; Itskovitz-Eldor, J.; Shapiro, S.S.; Waknitz, M.A.; Swiergiel, J.J.; Marshall, V.S.; Jones, J.M. Embryonic stem cell lines derived from human blastocysts. *Science* **1998**, *282*, 1145-1147.
215. Palm, T.; Bolognin, S.; Meiser, J.; Nickels, S.; Trager, C.; Meilenbrock, R.L.; Brockhaus, J.; Schreitmuller, M.; Missler, M.; Schwamborn, J.C. Rapid and robust generation of long-term self-renewing human neural stem cells with the ability to generate mature astroglia. *Sci Rep* **2015**, *5*, 16321.

216. van Wilgenburg, B.; Browne, C.; Vowles, J.; Cowley, S.A. Efficient, long term production of monocyte-derived macrophages from human pluripotent stem cells under partly-defined and fully-defined conditions. *PLoS One* **2013**, *8*, e71098.
217. Haenseler, W.; Sansom, S.N.; Buchrieser, J.; Newey, S.E.; Moore, C.S.; Nicholls, F.J.; Chintawar, S.; Schnell, C.; Antel, J.P.; Allen, N.D., et al. A Highly Efficient Human Pluripotent Stem Cell Microglia Model Displays a Neuronal-Co-culture-Specific Expression Profile and Inflammatory Response. *Stem Cell Reports* **2017**, *8*, 1727-1742.
218. Blasi, E.; Barluzzi, R.; Bocchini, V.; Mazzolla, R.; Bistoni, F. Immortalization of murine microglial cells by a v-raf/v-myc carrying retrovirus. *J Neuroimmunol* **1990**, *27*, 229-237.
219. Rodriguez-Corrales, J.A.; Josan, J.S. Resazurin Live Cell Assay: Setup and Fine-Tuning for Reliable Cytotoxicity Results. *Methods Mol Biol* **2017**, *1647*, 207-219.
220. Kumar, P.; Nagarajan, A.; Uchil, P.D. Analysis of Cell Viability by the Lactate Dehydrogenase Assay. *Cold Spring Harb Protoc* **2018**, *2018*.
221. Livak, K.J.; Schmittgen, T.D. Analysis of relative gene expression data using real-time quantitative PCR and the 2(-Delta Delta C(T)) Method. *Methods* **2001**, *25*, 402-408.
222. Bisogno, T.; Maccarrone, M. Latest advances in the discovery of fatty acid amide hydrolase inhibitors. *Expert Opin Drug Discov* **2013**, *8*, 509-522.
223. Frozza, R.L.; Horn, A.P.; Hoppe, J.B.; Simao, F.; Gerhardt, D.; Comiran, R.A.; Salbego, C.G. A comparative study of beta-amyloid peptides Abeta1-42 and Abeta25-35 toxicity in organotypic hippocampal slice cultures. *Neurochem Res* **2009**, *34*, 295-303.
224. Harry, G.J. Microglia during development and aging. *Pharmacol Ther* **2013**, *139*, 313-326.
225. Ito, D.; Imai, Y.; Ohsawa, K.; Nakajima, K.; Fukuuchi, Y.; Kohsaka, S. Microglia-specific localisation of a novel calcium binding protein, Iba1. *Brain Res Mol Brain Res* **1998**, *57*, 1-9.
226. Ito, D.; Tanaka, K.; Suzuki, S.; Dembo, T.; Fukuuchi, Y. Enhanced expression of Iba1, ionized calcium-binding adapter molecule 1, after transient focal cerebral ischemia in rat brain. *Stroke* **2001**, *32*, 1208-1215.
227. Mori, I.; Imai, Y.; Kohsaka, S.; Kimura, Y. Upregulated expression of Iba1 molecules in the central nervous system of mice in response to neurovirulent influenza A virus infection. *Microbiol Immunol* **2000**, *44*, 729-735.
228. Imai, Y.; Ibata, I.; Ito, D.; Ohsawa, K.; Kohsaka, S. A novel gene iba1 in the major histocompatibility complex class III region encoding an EF hand protein expressed in a monocytic lineage. *Biochem Biophys Res Commun* **1996**, *224*, 855-862.

229. Sasaki, Y.; Ohsawa, K.; Kanazawa, H.; Kohsaka, S.; Imai, Y. Iba1 is an actin-cross-linking protein in macrophages/microglia. *Biochem Biophys Res Commun* **2001**, *286*, 292-297.
230. Kirik, O.V.; Sukhorukova, E.G.; Korzhevskii, D.E. [Calcium-binding Iba-1/AIF-1 protein in rat brain cells]. *Morfologiia* **2010**, *137*, 5-8.
231. Lucin, K.M.; Wyss-Coray, T. Immune activation in brain aging and neurodegeneration: too much or too little? *Neuron* **2009**, *64*, 110-122.
232. Sacerdote, P.; Massi, P.; Panerai, A.E.; Parolaro, D. In vivo and in vitro treatment with the synthetic cannabinoid CP55, 940 decreases the in vitro migration of macrophages in the rat: involvement of both CB1 and CB2 receptors. *J Neuroimmunol* **2000**, *109*, 155-163.
233. Ridley, A.J. Rho GTPases and actin dynamics in membrane protrusions and vesicle trafficking. *Trends Cell Biol* **2006**, *16*, 522-529.
234. Stankiewicz, T.R.; Linseman, D.A. Rho family GTPases: key players in neuronal development, neuronal survival, and neurodegeneration. *Front Cell Neurosci* **2014**, *8*, 314.
235. Bos, J.L.; Rehmann, H.; Wittinghofer, A. GEFs and GAPs: critical elements in the control of small G proteins. *Cell* **2007**, *129*, 865-877.
236. Garcia-Mata, R.; Boulter, E.; Burridge, K. The 'invisible hand': regulation of RHO GTPases by RHOGDIs. *Nat Rev Mol Cell Biol* **2011**, *12*, 493-504.
237. Nobes, C.D.; Hall, A. Rho, rac, and cdc42 GTPases regulate the assembly of multimolecular focal complexes associated with actin stress fibers, lamellipodia, and filopodia. *Cell* **1995**, *81*, 53-62.
238. Das, R.; Chinnathambi, S. Actin-mediated Microglial Chemotaxis via G-Protein Coupled Purinergic Receptor in Alzheimer's Disease. *Neuroscience* **2020**, *448*, 325-336.
239. Sferra, A.; Nicita, F.; Bertini, E. Microtubule Dysfunction: A Common Feature of Neurodegenerative Diseases. *Int J Mol Sci* **2020**, *21*.
240. Gordon, S. Alternative activation of macrophages. *Nat Rev Immunol* **2003**, *3*, 23-35.
241. Chhor, V.; Le Charpentier, T.; Lebon, S.; Ore, M.V.; Celador, I.L.; Josserand, J.; Degos, V.; Jacotot, E.; Hagberg, H.; Savman, K., et al. Characterization of phenotype markers and neuronotoxic potential of polarised primary microglia in vitro. *Brain Behav Immun* **2013**, *32*, 70-85.
242. Etienne-Manneville, S.; Hall, A. Rho GTPases in cell biology. *Nature* **2002**, *420*, 629-635.
243. Giacovazzo, G.; Bisogno, T.; Piscitelli, F.; Verde, R.; Oddi, S.; Maccarrone, M.; Coccurello, R. Different Routes to Inhibit Fatty Acid Amide Hydrolase: Do All Roads Lead to the Same Place? *Int J Mol Sci* **2019**, *20*.
244. Guida, F.; Luongo, L.; Boccella, S.; Giordano, M.E.; Romano, R.; Bellini, G.; Manzo, I.; Furiano, A.; Rizzo, A.; Imperatore, R., et al. Palmitoylethanolamide

induces microglia changes associated with increased migration and phagocytic activity: involvement of the CB2 receptor. *Sci Rep* **2017**, *7*, 375.
245. Ridley, A.J. Rho GTPases and cell migration. *J Cell Sci* **2001**, *114*, 2713-2722.
246. Luo, L. Rho GTPases in neuronal morphogenesis. *Nat Rev Neurosci* **2000**, *1*, 173-180.
247. Wittmann, T.; Waterman-Storer, C.M. Cell motility: can Rho GTPases and microtubules point the way? *J Cell Sci* **2001**, *114*, 3795-3803.
248. Moon, M.Y.; Kim, H.J.; Li, Y.; Kim, J.G.; Jeon, Y.J.; Won, H.Y.; Kim, J.S.; Kwon, H.Y.; Choi, I.G.; Ro, E., et al. Involvement of small GTPase RhoA in the regulation of superoxide production in BV2 cells in response to fibrillar Abeta peptides. *Cell Signal* **2013**, *25*, 1861-1869.
249. Johnson, D.I. Cdc42: An essential Rho-type GTPase controlling eukaryotic cell polarity. *Microbiol Mol Biol Rev* **1999**, *63*, 54-105.
250. El Atat, O.; Fakih, A.; El-Sibai, M. RHOG Activates RAC1 through CDC42 Leading to Tube Formation in Vascular Endothelial Cells. *Cells* **2019**, *8*.
251. El-Sibai, M.; Pertz, O.; Pang, H.; Yip, S.C.; Lorenz, M.; Symons, M.; Condeelis, J.S.; Hahn, K.M.; Backer, J.M. RhoA/ROCK-mediated switching between Cdc42- and Rac1-dependent protrusion in MTLn3 carcinoma cells. *Exp Cell Res* **2008**, *314*, 1540-1552.
252. Heasman, S.J.; Carlin, L.M.; Cox, S.; Ng, T.; Ridley, A.J. Coordinated RhoA signaling at the leading edge and uropod is required for T cell transendothelial migration. *J Cell Biol* **2010**, *190*, 553-563.
253. Worthylake, R.A.; Lemoine, S.; Watson, J.M.; Burridge, K. RhoA is required for monocyte tail retraction during transendothelial migration. *J Cell Biol* **2001**, *154*, 147-160.
254. Aguilar, B.J.; Zhu, Y.; Lu, Q. Rho GTPases as therapeutic targets in Alzheimer's disease. *Alzheimers Res Ther* **2017**, *9*, 97.
255. Petratos, S.; Li, Q.X.; George, A.J.; Hou, X.; Kerr, M.L.; Unabia, S.E.; Hatzinisiriou, I.; Maksel, D.; Aguilar, M.I.; Small, D.H. The beta-amyloid protein of Alzheimer's disease increases neuronal CRMP-2 phosphorylation by a Rho-GTP mechanism. *Brain* **2008**, *131*, 90-108.
256. Allen, W.E.; Zicha, D.; Ridley, A.J.; Jones, G.E. A role for Cdc42 in macrophage chemotaxis. *J Cell Biol* **1998**, *141*, 1147-1157.
257. Diaz-Alonso, J.; de Salas-Quiroga, A.; Paraiso-Luna, J.; Garcia-Rincon, D.; Garcez, P.P.; Parsons, M.; Andradas, C.; Sanchez, C.; Guillemot, F.; Guzman, M., et al. Loss of Cannabinoid CB1 Receptors Induces Cortical Migration Malformations and Increases Seizure Susceptibility. *Cereb Cortex* **2017**, *27*, 5303-5317.
258. Kaplan, H.M.; Pazarci, P. Effects of chronic Delta(9)-tetrahydrocannabinol treatment on Rho/Rho-kinase signalization pathway in mouse brain. *Saudi Pharm J* **2017**, *25*, 1078-1081.

259. Kurihara, R.; Tohyama, Y.; Matsusaka, S.; Naruse, H.; Kinoshita, E.; Tsujioka, T.; Katsumata, Y.; Yamamura, H. Effects of peripheral cannabinoid receptor ligands on motility and polarization in neutrophil-like HL60 cells and human neutrophils. *J Biol Chem* **2006**, *281*, 12908-12918.
260. Rom, S.; Persidsky, Y. Cannabinoid receptor 2: potential role in immunomodulation and neuroinflammation. *J Neuroimmune Pharmacol* **2013**, *8*, 608-620.
261. Franceschi, C.; Garagnani, P.; Parini, P.; Giuliani, C.; Santoro, A. Inflammaging: a new immune-metabolic viewpoint for age-related diseases. *Nat Rev Endocrinol* **2018**, *14*, 576-590.
262. Xiang, Z.; Haroutunian, V.; Ho, L.; Purohit, D.; Pasinetti, G.M. Microglia activation in the brain as inflammatory biomarker of Alzheimer's disease neuropathology and clinical dementia. *Dis Markers* **2006**, *22*, 95-102.
263. Yao, Y.; Xu, X.H.; Jin, L. Macrophage Polarization in Physiological and Pathological Pregnancy. *Front Immunol* **2019**, *10*, 792.
264. Kendall, D.A.; Yudowski, G.A. Cannabinoid Receptors in the Central Nervous System: Their Signaling and Roles in Disease. *Front Cell Neurosci* **2016**, *10*, 294.
265. Holt, S.; Comelli, F.; Costa, B.; Fowler, C.J. Inhibitors of fatty acid amide hydrolase reduce carrageenan-induced hind paw inflammation in pentobarbital-treated mice: comparison with indomethacin and possible involvement of cannabinoid receptors. *Br J Pharmacol* **2005**, *146*, 467-476.
266. Rivera, P.; Bindila, L.; Pastor, A.; Perez-Martin, M.; Pavon, F.J.; Serrano, A.; de la Torre, R.; Lutz, B.; Rodriguez de Fonseca, F.; Suarez, J. Pharmacological blockade of the fatty acid amide hydrolase (FAAH) alters neural proliferation, apoptosis and gliosis in the rat hippocampus, hypothalamus and striatum in a negative energy context. *Front Cell Neurosci* **2015**, *9*, 98.
267. Carlisle, S.J.; Marciano-Cabral, F.; Staab, A.; Ludwick, C.; Cabral, G.A. Differential expression of the CB2 cannabinoid receptor by rodent macrophages and macrophage-like cells in relation to cell activation. *Int Immunopharmacol* **2002**, *2*, 69-82.
268. Mecha, M.; Feliu, A.; Carrillo-Salinas, F.J.; Rueda-Zubiaurre, A.; Ortega-Gutierrez, S.; de Sola, R.G.; Guaza, C. Endocannabinoids drive the acquisition of an alternative phenotype in microglia. *Brain Behav Immun* **2015**, *49*, 233-245.
269. Luo, X.Q.; Li, A.; Yang, X.; Xiao, X.; Hu, R.; Wang, T.W.; Dou, X.Y.; Yang, D.J.; Dong, Z. Paeoniflorin exerts neuroprotective effects by modulating the M1/M2 subset polarization of microglia/macrophages in the hippocampal CA1 region of vascular dementia rats via cannabinoid receptor 2. *Chin Med* **2018**, *13*, 14.

270. Tanaka, M.; Yagyu, K.; Sackett, S.; Zhang, Y. Anti-Inflammatory Effects by Pharmacological Inhibition or Knockdown of Fatty Acid Amide Hydrolase in BV2 Microglial Cells. *Cells* **2019**, *8*.
271. Chen, H.C.; Spiers, J.G.; Sernia, C.; Lavidis, N.A. Inhibition of Fatty Acid Amide Hydrolase by PF-3845 Alleviates the Nitrergic and Proinflammatory Response in Rat Hippocampus Following Acute Stress. *Int J Neuropsychopharmacol* **2018**, *21*, 786-795.
272. Tchantchou, F.; Tucker, L.B.; Fu, A.H.; Bluett, R.J.; McCabe, J.T.; Patel, S.; Zhang, Y. The fatty acid amide hydrolase inhibitor PF-3845 promotes neuronal survival, attenuates inflammation and improves functional recovery in mice with traumatic brain injury. *Neuropharmacology* **2014**, *85*, 427-439.
273. Rivera, P.; Fernandez-Arjona, M.D.M.; Silva-Pena, D.; Blanco, E.; Vargas, A.; Lopez-Avalos, M.D.; Grondona, J.M.; Serrano, A.; Pavon, F.J.; Rodriguez de Fonseca, F., et al. Pharmacological blockade of fatty acid amide hydrolase (FAAH) by URB597 improves memory and changes the phenotype of hippocampal microglia despite ethanol exposure. *Biochem Pharmacol* **2018**, *157*, 244-257.
274. Tham, C.S.; Whitaker, J.; Luo, L.; Webb, M. Inhibition of microglial fatty acid amide hydrolase modulates LPS stimulated release of inflammatory mediators. *FEBS Lett* **2007**, *581*, 2899-2904.
275. Henn, A.; Lund, S.; Hedtjarn, M.; Schrattenholz, A.; Porzgen, P.; Leist, M. The suitability of BV2 cells as alternative model system for primary microglia cultures or for animal experiments examining brain inflammation. *ALTEX* **2009**, *26*, 83-94.
276. Falsig, J.; Latta, M.; Leist, M. Defined inflammatory states in astrocyte cultures: correlation with susceptibility towards CD95-driven apoptosis. *J Neurochem* **2004**, *88*, 181-193.
277. Tarassishin, L.; Suh, H.S.; Lee, S.C. LPS and IL-1 differentially activate mouse and human astrocytes: role of CD14. *Glia* **2014**, *62*, 999-1013.
278. Mitchell, J.P.; Carmody, R.J. NF-kappaB and the Transcriptional Control of Inflammation. *Int Rev Cell Mol Biol* **2018**, *335*, 41-84.
279. Wardyn, J.D.; Ponsford, A.H.; Sanderson, C.M. Dissecting molecular cross-talk between Nrf2 and NF-kappaB response pathways. *Biochem Soc Trans* **2015**, *43*, 621-626.
280. Currais, A.; Fischer, W.; Maher, P.; Schubert, D. Intraneuronal protein aggregation as a trigger for inflammation and neurodegeneration in the aging brain. *FASEB J* **2017**, *31*, 5-10.
281. Kim, E.A.; Cho, C.H.; Kim, D.W.; Choi, S.Y.; Huh, J.W.; Cho, S.W. Antioxidative effects of ethyl 2-(3-(benzo[d]thiazol-2-yl)ureido)acetate against amyloid beta-induced oxidative cell death via NF-kappaB, GSK-3beta and beta-

catenin signaling pathways in cultured cortical neurons. *Free Radic Res* **2015**, *49*, 411-421.
282. Henn, A.; Kirner, S.; Leist, M. TLR2 hypersensitivity of astrocytes as functional consequence of previous inflammatory episodes. *J Immunol* **2011**, *186*, 3237-3247.
283. Norden, D.M.; Trojanowski, P.J.; Villanueva, E.; Navarro, E.; Godbout, J.P. Sequential activation of microglia and astrocyte cytokine expression precedes increased Iba-1 or GFAP immunoreactivity following systemic immune challenge. *Glia* **2016**, *64*, 300-316.
284. Meffert, M.K.; Baltimore, D. Physiological functions for brain NF-kappaB. *Trends Neurosci* **2005**, *28*, 37-43.
285. Yuan, H.; Ma, J.; Li, T.; Han, X. MiR-29b aggravates lipopolysaccharide-induced endothelial cells inflammatory damage by regulation of NF-kappaB and JNK signaling pathways. *Biomed Pharmacother* **2018**, *99*, 451-461.
286. Zamanian, J.L.; Xu, L.; Foo, L.C.; Nouri, N.; Zhou, L.; Giffard, R.G.; Barres, B.A. Genomic analysis of reactive astrogliosis. *J Neurosci* **2012**, *32*, 6391-6410.
287. Liddelow, S.A.; Guttenplan, K.A.; Clarke, L.E.; Bennett, F.C.; Bohlen, C.J.; Schirmer, L.; Bennett, M.L.; Munch, A.E.; Chung, W.S.; Peterson, T.C., et al. Neurotoxic reactive astrocytes are induced by activated microglia. *Nature* **2017**, *541*, 481-487.
288. Azam, S.; Jakaria, M.; Kim, I.S.; Kim, J.; Haque, M.E.; Choi, D.K. Regulation of Toll-Like Receptor (TLR) Signaling Pathway by Polyphenols in the Treatment of Age-Linked Neurodegenerative Diseases: Focus on TLR4 Signaling. *Front Immunol* **2019**, *10*, 1000.
289. Rahimifard, M.; Maqbool, F.; Moeini-Nodeh, S.; Niaz, K.; Abdollahi, M.; Braidy, N.; Nabavi, S.M.; Nabavi, S.F. Targeting the TLR4 signaling pathway by polyphenols: A novel therapeutic strategy for neuroinflammation. *Ageing Res Rev* **2017**, *36*, 11-19.
290. Coux, O.; Zieba, B.A.; Meiners, S. The Proteasome System in Health and Disease. *Adv Exp Med Biol* **2020**, *1233*, 55-100.
291. Suraweera, A.; Munch, C.; Hanssum, A.; Bertolotti, A. Failure of amino acid homeostasis causes cell death following proteasome inhibition. *Mol Cell* **2012**, *48*, 242-253.
292. Guo, N.; Peng, Z. MG132, a proteasome inhibitor, induces apoptosis in tumor cells. *Asia Pac J Clin Oncol* **2013**, *9*, 6-11.
293. Kisselev, A.F.; Goldberg, A.L. Proteasome inhibitors: from research tools to drug candidates. *Chem Biol* **2001**, *8*, 739-758.
294. Rideout, H.J.; Stefanis, L. Proteasomal inhibition-induced inclusion formation and death in cortical neurons require transcription and ubiquitination. *Mol Cell Neurosci* **2002**, *21*, 223-238.

295. Sun, F.; Anantharam, V.; Zhang, D.; Latchoumycandane, C.; Kanthasamy, A.; Kanthasamy, A.G. Proteasome inhibitor MG-132 induces dopaminergic degeneration in cell culture and animal models. *Neurotoxicology* **2006**, *27*, 807-815.
296. Boland, B.; Yu, W.H.; Corti, O.; Mollereau, B.; Henriques, A.; Bezard, E.; Pastores, G.M.; Rubinsztein, D.C.; Nixon, R.A.; Duchen, M.R., et al. Promoting the clearance of neurotoxic proteins in neurodegenerative disorders of ageing. *Nat Rev Drug Discov* **2018**, *17*, 660-688.
297. Thibaudeau, T.A.; Anderson, R.T.; Smith, D.M. A common mechanism of proteasome impairment by neurodegenerative disease-associated oligomers. *Nat Commun* **2018**, *9*, 1097.
298. Myeku, N.; Clelland, C.L.; Emrani, S.; Kukushkin, N.V.; Yu, W.H.; Goldberg, A.L.; Duff, K.E. Tau-driven 26S proteasome impairment and cognitive dysfunction can be prevented early in disease by activating cAMP-PKA signaling. *Nat Med* **2016**, *22*, 46-53.
299. Cullen, S.J.; Ponnappan, S.; Ponnappan, U. Proteasome inhibition up-regulates inflammatory gene transcription induced by an atypical pathway of NF-kappaB activation. *Biochem Pharmacol* **2010**, *79*, 706-714.
300. Terron, A.; Bal-Price, A.; Paini, A.; Monnet-Tschudi, F.; Bennekou, S.H.; Members, E.W.E.; Leist, M.; Schildknecht, S. An adverse outcome pathway for parkinsonian motor deficits associated with mitochondrial complex I inhibition. *Arch Toxicol* **2018**, *92*, 41-82.
301. Poewe, W.; Seppi, K.; Tanner, C.M.; Halliday, G.M.; Brundin, P.; Volkmann, J.; Schrag, A.E.; Lang, A.E. Parkinson disease. *Nat Rev Dis Primers* **2017**, *3*, 17013.
302. Hegde, A.N. Ubiquitin-proteasome-mediated local protein degradation and synaptic plasticity. *Prog Neurobiol* **2004**, *73*, 311-357.
303. Versari, D.; Herrmann, J.; Gossl, M.; Mannheim, D.; Sattler, K.; Meyer, F.B.; Lerman, L.O.; Lerman, A. Dysregulation of the ubiquitin-proteasome system in human carotid atherosclerosis. *Arterioscler Thromb Vasc Biol* **2006**, *26*, 2132-2139.
304. Layfield, R.; Lowe, J.; Bedford, L. The ubiquitin-proteasome system and neurodegenerative disorders. *Essays Biochem* **2005**, *41*, 157-171.
305. Wang, J.; Maldonado, M.A. The ubiquitin-proteasome system and its role in inflammatory and autoimmune diseases. *Cell Mol Immunol* **2006**, *3*, 255-261.
306. Juttler, E.; Potrovita, I.; Tarabin, V.; Prinz, S.; Dong-Si, T.; Fink, G.; Schwaninger, M. The cannabinoid dexanabinol is an inhibitor of the nuclear factor-kappa B (NF-kappa B). *Neuropharmacology* **2004**, *47*, 580-592.

307. Jeon, P.; Yang, S.; Jeong, H.; Kim, H. Cannabinoid receptor agonist protects cultured dopaminergic neurons from the death by the proteasomal dysfunction. *Anat Cell Biol* **2011**, *44*, 135-142.
308. Gutbier, S.; Spreng, A.S.; Delp, J.; Schildknecht, S.; Karreman, C.; Suciu, I.; Brunner, T.; Groettrup, M.; Leist, M. Prevention of neuronal apoptosis by astrocytes through thiol-mediated stress response modulation and accelerated recovery from proteotoxic stress. *Cell Death Differ* **2018**, *25*, 2101-2117.
309. Zong, Z.H.; Du, Z.X.; Li, N.; Li, C.; Zhang, Q.; Liu, B.Q.; Guan, Y.; Wang, H.Q. Implication of Nrf2 and ATF4 in differential induction of CHOP by proteasome inhibition in thyroid cancer cells. *Biochim Biophys Acta* **2012**, *1823*, 1395-1404.
310. Wortel, I.M.N.; van der Meer, L.T.; Kilberg, M.S.; van Leeuwen, F.N. Surviving Stress: Modulation of ATF4-Mediated Stress Responses in Normal and Malignant Cells. *Trends Endocrinol Metab* **2017**, *28*, 794-806.
311. Wang, X.F.; Cynader, M.S. Astrocytes provide cysteine to neurons by releasing glutathione. *J Neurochem* **2000**, *74*, 1434-1442.
312. Suh, J.H.; Shenvi, S.V.; Dixon, B.M.; Liu, H.; Jaiswal, A.K.; Liu, R.M.; Hagen, T.M. Decline in transcriptional activity of Nrf2 causes age-related loss of glutathione synthesis, which is reversible with lipoic acid. *Proc Natl Acad Sci U S A* **2004**, *101*, 3381-3386.
313. Tonelli, C.; Chio, I.I.C.; Tuveson, D.A. Transcriptional Regulation by Nrf2. *Antioxid Redox Signal* **2018**, *29*, 1727-1745.
314. Vargas, M.R.; Johnson, D.A.; Sirkis, D.W.; Messing, A.; Johnson, J.A. Nrf2 activation in astrocytes protects against neurodegeneration in mouse models of familial amyotrophic lateral sclerosis. *J Neurosci* **2008**, *28*, 13574-13581.
315. Biernacki, M.; Baranowska-Kuczko, M.; Niklinska, G.N.; Skrzydlewska, E. The FAAH Inhibitor URB597 Modulates Lipid Mediators in the Brain of Rats with Spontaneous Hypertension. *Biomolecules* **2020**, *10*.

APPENDIX

SCIENTIFIC PUBBLICATIONS DURING THE PhD COURSE

(2017-2020)

Biochemical Pharmacology 167 (2019) 50–57

Contents lists available at ScienceDirect

Biochemical Pharmacology

journal homepage: www.elsevier.com/locate/biochempharm

Poly(ADP-ribosylated) proteins in β-amyloid peptide-stimulated microglial cells

Virginia Correani[a,1], Sara Martire[a,1,2], Giuseppina Mignogna[a], Lisa Beatrice Caruso[b], Italo Tempera[b], Alessandra Giorgi[a], Maddalena Grieco[a], Luciana Mosca[a], M.Eugenia Schininà[a], Bruno Maras[a], Maria d'Erme[a,*]

[a] Department of Biochemical Sciences, Sapienza University Roma, Italy
[b] Wistar Institute for Cancer Research & Molecular Biology, Lewis Katz School of Medicine-Temple University, Philadelphia, USA

ARTICLE INFO

Keywords:
Alzheimer disease
Microglia
PARP-1
Proteomics
β-Amyloid peptide

ABSTRACT

Amyloid-treated microglia prime and sustain neuroinflammatory processes in the central nervous system activating different signalling pathways inside the cells. Since a key role for PARP-1 has been demonstrated in inflammation and in neurodegeneration, we investigated PARylated proteins in resting and in β-amyloid peptide treated BV2 microglial cells. A total of 1158 proteins were identified by mass spectrometry with 117 specifically modified in the amyloid-treated cells. Intervention of PARylation on the proteome of microglia showed to be widespread in different cellular districts and to affect various cellular pathways, highlighting the role of this dynamic post-translational modification in cellular regulation. Ubiquitination is one of the more enriched pathways, encompassing PARylated proteins like NEDD4, an E3 ubiquitine ligase and USP10, a de-ubiquitinase, both associated with intracellular responses induced by β-amyloid peptide challenge. PARylation of NEDD4 may be involved in the recruiting of this protein to the plasma membrane where it regulates the endocytosis of AMPA receptors, whereas USP10 may be responsible for the increase of p53 levels in amyloid stimulated microglia. Unfolded protein response and Endoplasmic Reticulum Stress pathways, strictly correlated with the Ubiquitination process, also showed enrichment in PARylated proteins. PARylation may thus represent one of the molecular switches responsible for the transition of microglia towards the inflammatory microglia phenotype, a pivotal player in brain diseases including neurodegenerative processes. The establishment of trials with PARP inhibitors to test their efficacy in the containment of neurodegenerative diseases may be envisaged.

1. Introduction

Alzheimer's disease (AD) is a growing public health concern due to the rapid increase in life expectancy. In developed countries, it already affects a large percentage of people and it is stably increasing towards epidemic proportions [1]. Although the aetiology of this neurodegenerative pathology remains elusive, inflammatory processes are recognized as the main culprit of its development. In the Central Nervous System (CNS), microglia cells are the major actors in the production of inflammatory mediators such as cytokines, chemokines and pro-oxidative molecules [2]. Microglia are macrophagic-like cells that play a pivotal role in maintenance of brain homeostasis, in detection of invading pathogens, and in tissue repair of the neuronal compartment [3]. Microglia activation in AD is induced by a 40-42 amino acids peptide (β-amyloid peptide, Aβ), arising from the sequential proteolytic processing of the Amyloid Precursor Protein (APP) by beta- and gamma-secretases [4,5]. When an imbalance between Aβ production and clearance occurs, oligomerization takes place [6]. Whereas a part of the oligomeric assemblies converge towards the formation of insoluble fibrils, some species of these soluble oligomers are able to interact with different receptors on the microglia plasma membrane, particularly with Toll-like receptors, eliciting an inflammatory response via NF-kB pathway [7]. Furthermore, Aβ oligomers prime the activation of NADPH oxidase, responsible for superoxide production and for the consequent oxidative stress increase [8]. Both these events mark the settlement of an inflammatory phenotype that sustains and speeds up

* Corresponding author.
E-mail address: Smaria.derme@uniroma1.it (M. d'Erme).
[1] Both authors equally contributed to this work.
[2] Present address: Green Center for Reproductive Biology Sciences, Department of Obstetrics and Gynecology, University of Texas Southwestern Medical Center, Dallas, TX 75390, USA.

https://doi.org/10.1016/j.bcp.2018.10.026
Received 20 September 2018; Accepted 23 October 2018
Available online 09 November 2018
0006-2952/

frontiers in Neuroscience

MINI REVIEW
published: 18 October 2019
doi: 10.3389/fnins.2019.01112

Glucagon-Like Peptide-1: A Focus on Neurodegenerative Diseases

*Maddalena Grieco[1], Alessandra Giorgi[1], Maria Cristina Gentile[2], Maria d'Erme[1], Susanna Morano[2], Bruno Maras[1] and Tiziana Filardi[2]**

[1] Department of Biochemical Sciences, Faculty of Pharmacy and Medicine, Sapienza University of Rome, Rome, Italy,
[2] Department of Experimental Medicine, Faculty of Medicine and Dentistry, Sapienza University of Rome, Rome, Italy

Diabetes mellitus is one of the major risk factors for cognitive dysfunction. The pathogenesis of brain impairment caused by chronic hyperglycemia is complex and includes mitochondrial dysfunction, neuroinflammation, neurotransmitters' alteration, and vascular disease, which lead to cognitive impairment, neurodegeneration, loss of synaptic plasticity, brain aging, and dementia. Glucagon-like peptide-1 (GLP-1), a gut released hormone, is attracting attention as a possible link between metabolic and brain impairment. Several studies have shown the influence of GPL-1 on neuronal functions such as thermogenesis, blood pressure control, neurogenesis, neurodegeneration, retinal repair, and energy homeostasis. Moreover, modulation of GLP-1 activity can influence amyloid β peptide aggregation in Alzheimer's disease (AD) and dopamine (DA) levels in Parkinson's disease (PD). GLP-1 receptor agonists (GLP-1RAs) showed beneficial actions on brain ischemia in animal models, such as the reduction of cerebral infarct area and the improvement of neurological deficit, acting mainly through inhibition of oxidative stress, inflammation, and apoptosis. They might also exert a beneficial effect on the cognitive impairment induced by diabetes or obesity improving learning and memory by modulating synaptic plasticity. Moreover, GLP-1RAs reduced hippocampal neurodegeneration. Besides this, there are growing evidences on neuroprotective effects of these agonists in animal models of neurodegenerative diseases, regardless of diabetes. In PD animal models, GPL-1RAs were able to protect motor activity and dopaminergic neurons whereas in AD models, they seemed to improve nearly all neuropathological features and cognitive functions. Although further clinical studies of GPL-1RAs in humans are needed, they seem to be a promising therapy for diabetes-associated cognitive decline.

Keywords: glucagon-like peptide-1, GLP-1 receptor agonists, Parkinson's disease, Alzheimer's disease, neurodegenerative diseases, type 2 diabetes

OPEN ACCESS

Edited by:
Mats Ljungman,
Centro for Genomic Regulation (CRG), Spain

Reviewed by:
Alberto Granzotto,
Center for Research on Aging Sciences and Translational Medicine Center (CeSI-MeT), Italy
Christian Hölscher,
Lancaster University, United Kingdom

****Correspondence:***
Tiziana Filardi
tiziana.filardi@uniroma1.it

Specialty section:
This article was submitted to Neurodegeneration, a section of the journal Frontiers in Neuroscience

Received: *14 June 2019*
Accepted: *02 October 2019*
Published: *18 October 2019*

Citation:
Grieco M, Giorgi A, Gentile MC, d'Erme M, Morano S, Maras B and Filardi T (2019) Glucagon-Like Peptide-1: A Focus on Neurodegenerative Diseases. Front. Neurosci. 13:1112. doi: 10.3389/fnins.2019.01112

INTRODUCTION

The concern for neurodegeneration, a worldwide expanding set of diseases, stimulated the research on risk factors related to the lifestyle of the population, leading to interesting findings on the association between dysmetabolism and brain impairment. In this perspective, gut/brain axis and altered insulin release and response seem to be the main actors in establishing the pathological metabolic set up for the development of neurodegenerative diseases. Indeed, insulin works as pro-survival neurotrophic factor with its receptor widespread in cognitive areas as hippocampus and in dopaminergic system (Haas et al., 2016; Fiory et al., 2019).

nutrients

MDPI

Article

Blueberry Counteracts BV-2 Microglia Morphological and Functional Switch after LPS Challenge

Maria Giovanna De Caris [1], Maddalena Grieco [2], Elisa Maggi [3], Antonio Francioso [2], Federica Armeli [3], Luciana Mosca [2], Alessandro Pinto [1], Maria D'Erme [2], Patrizia Mancini [1,*] and Rita Businaro [3]

1 Department of Experimental Medicine, Sapienza University of Rome, Viale Regina Elena 324, 00161 Rome, Italy; mariagiovanna.decaris@uniroma1.it (M.G.D.C.); alessandro.pinto@uniroma1.it (A.P.)
2 Department of Biochemical Sciences, Sapienza University of Rome, Piazzale Aldo Moro 5, 00185 Rome, Italy; maddalena.grieco@uniroma1.it (M.G.); antonio.francioso@uniroma1.it (A.F.); luciana.mosca@uniroma1.it (L.M.); maria.derme@uniroma1.it (M.D.)
3 Department of Medico-Surgical Sciences and Biotechnologies, Sapienza University of Rome, Corso della Repubblica 79, 04100 Latina, Italy; elisa.maggi@uniroma1.it (E.M.); federica.armeli@uniroma1.it (F.A.); rita.businaro@uniroma1.it (R.B.)
* Correspondence: patrizia.mancini@uniroma1.it; Tel.: +39-064461526

Received: 29 April 2020; Accepted: 16 June 2020; Published: 19 June 2020

Abstract: Microglia, the innate immune cells of the CNS, respond to brain injury by activating and modifying their morphology. Our study arises from the great interest that has been focused on blueberry (BB) for the antioxidant and pharmacological properties displayed by its components. We analyzed the influence of hydroalcoholic BB extract in resting or lipopolysaccharide (LPS)-stimulated microglia BV-2 cells. BB exerted a protective effect against LPS-induced cytotoxicity, as indicated by cell viability. BB was also able to influence the actin cytoskeleton organization, to recover the control phenotype after LPS insult, and also to reduce LPS-driven migration. We evaluated the activity of Rho and Rac1 GTPases, which regulate both actin cytoskeletal organization and migratory capacity. LPS caused an increase in Rac1 activity, which was counteracted by BB extract. Furthermore, we demonstrated that, in the presence of BB, mRNA expression of pro-inflammatory cytokines IL-1β, IL-6 and TNF-α decreased, as did the immunofluorescence signal of iNOS, whereas that of Arg-1 was increased. Taken together, our results show that, during the inflammatory response, BB extract shifts the M1 polarization towards the M2 phenotype through an actin cytoskeletal rearrangement. Based on that, we might consider BB as a nutraceutical with anti-inflammatory activities.

Keywords: blueberry; BV-2 cells; actin cytoskeleton; cell migration; Rho; Rac1; M1/M2 phenotypes; inflammatory cytokines

1. Introduction

Great interest has been focused on blueberry (BB) for the nutraceutical and pharmacological properties displayed by polyphenolic compounds isolated from its extracts. The cultivation of BB is spreading in many countries, not only because its taste is particularly pleasant to consumers, but also because there are increasing reports that demonstrate its health benefits through a wide range of mechanisms: antioxidant, anti-inflammatory, anti-bacterial [1,2]. Experimental evidence pointed out that a prolonged intake of fruit-derived polyphenols can provide an important support for the prevention and treatment of chronic multifactorial diseases such as diabetes, cardiovascular diseases, neurodegenerative diseases and cancer [1–5]. BB is part of the Ericaceae family, which includes

In press

Journal of Neuropathology and Experimental Neurology
Stimulation of the serotonin receptor 7 restores brain histone H3 acetylation and MeCP2 co-repressor protein levels in a female mouse model of Rett syndrome

Stimulation of the serotonin receptor 7 restores histone H3 acetylation levels and MeCP2 co-repressor protein levels in the brain of a female mouse model of Rett syndrome

Giorgia Napoletani[1*], Daniele Vigli[1,2*], Livia Cosentino[2], Maddalena Grieco[2], Maria Cristina Talamo[1], Enza Lacivita[3], Marcello Leopoldo[3], Giovanni Laviola[2], Andrea Fuso[4], Maria d'Erme[1], Bianca De Filippis[2]

[1]Department of Biochemical Sciences, Sapienza University of Roma, Italy; [2]Center for Behavioral Sciences and Mental Health, Istituto Superiore di Sanità, Roma, Italy; [3]Department of Pharmacy, University of Bari "Aldo Moro", Bari, Italy; [4]Department of Experimental Medicine, Sapienza University of Roma, Italy

equally contributed

Correspondence to:

Bianca De Filippis, Center for Behavioral Sciences and Mental Health, Istituto Superiore di Sanità, Viale Regina Elena, 299, 00161 Roma, Italy. Tel: +390649902107, Fax: +39064957821, e-mail: bianca.defilippis@iss.it.

Da: em.jnen.0.6f2407.1a1c7c02@editorialmanager.com <em.jnen.0.6f2407.1a1c7c02@editorialmanager.com> per conto di JNEN <em@editorialmanager.com>
Inviato: Venerdì 6 Novembre 2020, 18:49
A: De Filippis Bianca
Oggetto: JNEN Decision

Nov 06, 2020

RE: JNEN 20-266, entitled "Stimulation of the Serotonin Receptor 7 Restores Brain Histone H3 Acetylation and MeCP2 Corepressor Protein Levels in a Female Mouse Model of Rett Syndrome"

Dear Dr. De Filippis,

I am pleased to inform you that your revisions are satisfactory. I am pleased to accept the revised paper for publication in Journal of Neuropathology and Experimental Neurology.

Thank you for considering our journal for your paper.

With Kind Regards,

John M. Lee, MD, PhD
Editor-in-Chief
Journal of Neuropathology and Experimental Neurology

Undergoing submission

Actin cytoskeletal organization underlines microglia polarization regulated by FAAH inhibition

Maddalena Grieco[1], Maria Giovanna De Caris[2], Elisa Maggi[3], Federica Armeli[3], Roberto Coccurello[4,5], Mauro Maccarron[6], Tiziana Bisogno[7], Maria D'Erme[1], Patrizia Mancini[2], Rita Businaro*[3].

[1] Department of Biochemical Sciences, Sapienza University of Rome, Piazzale Aldo Moro 5, 00185 Rome, Italy; [2] Department of Experimental Medicine, Sapienza University of Rome, Viale Regina Elena 324, 00161 Rome, Italy; [3] Department of Medico-Surgical Sciences and Biotechnologies, Sapienza University of Rome, Corso della Repubblica 79, 04100 Latina, Italy; [4] Fondazione Santa Lucia IRCCS, Preclinical Neuroscience, Via del Fosso di Fiorano 64, 00143 Rome, Italy; [5] Institute for Complex Systems (ISC), C.N.R., Via dei Taurini 19, 00185 Rome, Italy; [6] Department of Applied Clinical and Biotechnological Sciences, University of L'Aquila, L'Aquila, Italy; [7] Endocannabinoid Research Group, Institute of Translational Pharmacology, CNR,Via Fosso del Cavaliere 100, 00133 Rome, Italy

Correspondence: rita.businaro@uniroma1.it

ABSTRACT

Endocannabinoids modulating the behaviour of microglia and astrocytes might act as possible targets for therapeutic intervention. Recent studies have indicated that endocannabinoid levels and metabolic enzymes change during the progression of Alzheimer's disease (AD) and that the inhibition of fatty acid amide hydrolase (FAAH), the main catabolic enzyme of anandamide (AEA), has beneficial effects in mice with AD. The aim of this study was to determine whether URB597, a FAAH inhibitor, targets microglia polarization by altering the cytoskeleton reorganization induced by amyloid-β peptide (Aβ) in BV-2 microglial cells. Evaluation of actin cytoskeleton showed that Aβ treatment increased the surface area of BV-2 cells, which acquired a flat and polygonal morphology. Although URB597 did not affect cell morphology only, it partially rescued the control phenotype in BV-2 cells incubated with the combined treatment. Rho family proteins have a critical role in the plasticity of the actin cytoskeleton, influencing morphological changes, migration and phagocytic activity of cells. We observed an increase of Rho protein activation in Aβ samples and a decrease in samples treated with URB597 alone or in combination with Aβ compared to controls, while an increase of Cdc42 protein activation was observed in all samples with respect to control. Aβ induced the migration of BV-2 cells up to 2 h after stimulation. We also found that by reducing Rho protein activity, URB597 was able to reduce the migration rate. URB597 also increased the number of BV-2 cells performing phagocytosis. Taken together, these data suggest that an increase of AEA, due to FAAH inhibition, may induce cytoskeleton reorganization, regulating phagocytosis and cell migration processes, and promote microglial polarization towards an anti-inflammatory phenotype.